

PROCEEDINGS



7th

MpCCI

USER FORUM

FEBRUARY 21st AND 22nd, 2006

7th

MpCCI

USER FORUM

PROCEEDINGS

WELCOME

7TH MPCCI USER FORUM 2006 AT SCHLOSS BIRLINGHOVEN

Multi-Physics Analysis generally means the combination of experts and experiences made in the field of various simulation disciplines, with the objective of obtaining the solution to a complex problem.

To this end, several experts from the various application areas, branches and disciplines, again have presented their way to define the necessity and the value of multi-physics analysis.

We would like to give sincere thanks to all these presenters; their contributions greatly contributed to the 7th MpCCI User Forum and demonstrated the diversity and capability of multi-physics applications.

Software partners:

- ABAQUS,
- CD adapco Group and
- CDAJ,
- CEDRAT S.A.,
- FlowMaster,
- FLUENT,
- Genias Graphics,

• MSC Software

and end-users from

- BA Mosbach together with University of Frankfurt,
- Fraunhofer EMI,
- JAEA Japan,
- Schneider Electric US,
- TU Braunschweig together with DLR Sistec,
- TU Cottbus and
- University Erlangen

showed impressive results and solutions around MpCCI.

The Proceedings of the 7th MpCCI User Forum 2006 provides the reader with lots of information around MpCCI. This book will show short and medium term potentials for using coupled multi-physics simulation environments in your own application area.

On behalf of the MpCCI Team



Klaus Wolf

CONTACT

Klaus Wolf

Fraunhofer Institute SCAI

Schloss Birlinghoven

53754 Sankt Augustin,

Germany

Phone: +49 (0) 2241 / 14 - 2557

klaus.wolf@scai.fraunhofer.de

MPCCI NEWS

MpCCI Development and Business Issues Klaus Wolf, Fraunhofer Institute SCAI	10-21
--	-------

MPCCI DEVELOPMENT AND MPCCI COOPERATIONS

Fluid-Structure Interaction Simulation using ABAQUS and FLUENT Albert Kurkchubasche, ABAQUS Inc. US	22-33
Coupled Solutions with StarCD Katsushi Moriyama, CD-adapco JAPAN Co., LTD.	34-39
Multiphysics with FLUENT and MpCCI Mark Pelzer, FLUENT Deutschland	40-47
Fluid-Structure Interaction Simulations with MSC.Marc and STAR-CD or FLUENT Pieter Vosbeck, MSC.Software	48-55
1D and 3D Co-Simulation between Flowmaster and CFD packages Abdul Ludhi, Flowmaster LTD	56-65
Multidisciplinary Simulation and Visualisation with MpCCI and EnSight Johannes Grawe, Genias Graphics; Klaus Wolf, Fraunhofer Institute SCAI	66-75
Approaches to Industrial FSI – An overview with case studies Fred Mendonça, CD-adapco, United Kingdom	76-87

FLUID-STRUCTURE-INTERACTIONS

Simulation of Blast-Structure-Interaction with Coupled Explicit Hydro-Codes Arno Klomfass, Fraunhofer Institute EMI	88-97
Computational Aeroacoustics using MpCCI as Coupling Interface between Fluid Mechanics, Structural Mechanics and Acoustics F. Schäfer, I. Ali, S. Becker, Institute of Fluid Mechanics University of Erlangen; M. Kaltenbacher, M. Escobar, G. Link, Department of Sensor Technology, University of Erlangen	98-111
Simulation of Fluid Damped Structural Vibrations Sven Schrape, Brandenburgisch Technische Universität Cottbus	112-121
An MpCCI-based Software Integration Environment for Hypersonic Fluid-Structure Problems R. Niesner, M. Haupt, P. Horst, Institute of Aircraft Design and Lightweight Structures, Technische Universität Braun- schweig; F. Dannemann, A. Schreiber, German Aerospace Center DLR, Simulation and Software Technology	122-131
Towards Construction of a Numerical Testbed for Nuclear Power Plants Yoshio Suzuki, Osamu Hazama, Hitoshi Matsubara, Rong Tian, Akemi Nishida, Masayuki Tani and Norihiro Nakajima Center of Computational Science Systems, Japan Atomic Energy Agency JAERI	132-137
Fluid-structure interaction in abdominal aortic aneurysms Uwe Janoske, University of Cooperative Education Mosbach; FH Frankfurt/Main; FLUENT Deutschland; Klinikum der Johann Wolfgang Goethe-Universität Frankfurt/Main; Klinikum der Philipps-Universität Marburg	138-145

COUPLING OF FLUID AND ELECTRO-MAGNETICS

FLUX for Electromagnetic design, extended to multiphysics using MPCCI 146-149

Ian Lyttle, Benjamin Pulido, Ali Zolfaghari, Kevin Parker,
Schneider Electric

FLUX for Electromagnetic design, extended to multiphysics using MPCCI 150-153

Sebastien Cadeau Belliard, CEDRAT Group

Electro-Thermal Analyses of Gas Insulated Switchgear to Predict The Temperature Rising 154

J. S. Ryu, H. Y. Kang, B. B. Hyun, S. W. Lee, Y. G. Kim, Y. J. Shin, LS Industrial System, Korea

Use of MpCCI to Perform Electro-Thermal Analyses for Air Circuit Breaker 155

J. S. Ryu, H. Y. Kang, B. B. Hyun, S. W. Lee, Y. G. Kim, Y. J. Shin, LS Industrial System, Korea



PARTICIPANTS OF THE 7th MPCCI USERFORUM 2006

MPCCI DEVELOPMENT AND BUSINESS ISSUES

Klaus Wolf, Fraunhofer Institute SCAI

There is an increasing need for multidisciplinary simulations in various research and engineering fields. Fluid-structure interaction, magneto-hydro dynamics, thermal coupling, plasma computations or coupled manufacturing processes define only a subset of recent multi-physics activities. There is a common feeling in the community that in most cases not a single (proprietary) simulation system can provide all necessary features but that coupling the best codes of each discipline will enable more flexibility and simulation quality to the end user.

The MpCCI interface has been accepted as a »de-facto« standard for simulation code coupling. MpCCI is developed at Fraunhofer Institute for Algorithms and Scientific Computing SCAI.

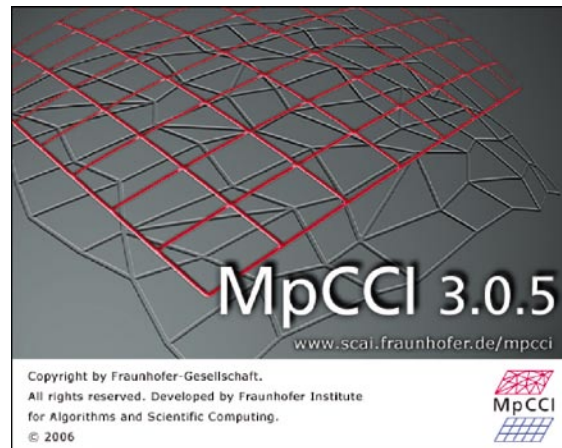
MPCCI 3.0.5 – NEW FEATURES AND IMPROVEMENTS

A new and improved version of MpCCI will be released in June 2006. MpCCI 3.0.5 installation and usage on distributed systems has been simplified. Different coordinate and unit system can now be used in one coupled application. New interpolation schemes are available. Further codes have been adapted to the MpCCI interface.

Installation on distributed heterogeneous platforms

The file system structure of the MpCCI installation has been reorganized:

- for simplification of the handling of various platforms and
- for simplification of the handling of various application codes.



Different platforms for Unix, Linux and the Microsoft Windows XP version of MpCCI may be installed on a file server in parallel. In MpCCI 3.0.5 there is no need to go through any further configuration after having unpacked and copied the MpCCI delivery package to a user defined directory.

To guarantee full compatibility with 3rd party software the user may download and install pre-selected but standard versions of

- Java Runtime Environment JRE,
 - MPICH for Windows XP, and
 - OpenSSH for Windows
- together with MpCCI 3.0.5.

Command interface

The command environment was completely rewritten and reorganized to account for an easy integration of further commercial or in-house codes. All code relates files are now located in one code-specific directory. Adding a new code thus only means to add and copy a further MpCCI code directory into the local MpCCI installation.

The MpCCI command environment is now a generic command tree where each command is realised by a separate Perl Module. The interfaces used within that command tree are specified such that any extension for new commands and code environments is straight forward. This new command environment now provides a unique look and feel for all commands and MpCCI supported codes.

CONTACT

Klaus Wolf
 Fraunhofer Institute SCAI
 Schloss Birlinghoven
 53754 Sankt Augustin,
 Germany
 Phone: +49 (0) 2241 / 14 - 2557
klaus.wolf@scai.fraunhofer.de

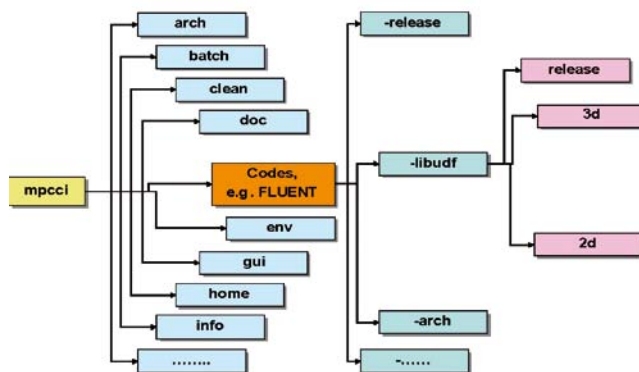


Figure 1: MpCCI command tree

MpCCI 3.0.5-27, Build (Fri Apr 7 17:41:09 2006)

Usage:

```
mpcci SUBCMD [OPTIONS] [ARGS] [HELPKEY] ...
```

Synopsis:

»mpcci« is the root for all MpCCI related commands.
 You need to specify at least one subcommand (SUBCMD) on
 the commandline.

Please type either

»mpcci SUBCMD HELPKEY« or

»mpcci HELPKEY SUBCMD«

to get more detailed help on the subcommands.

Subcommands:

ABAQUS	Tools related to ABAQUS.
ANSYS	Tools related to ANSYS.
FLUENT	Tools related to FLUENT.
FLUX	Tools related to FLUX.
IcePak	Tools related to IcePak.
MSC.Marc	Tools related to MSC.Marc.
PERMAS	Tools related to PERMAS.
RadTherm	Tools related to RadTherm.
StarCD	Tools related to StarCD.
arch [-n]	Print the MpCCI architecture without a newline or with a newline [-n] at the end and exit. This is in fact a shortcut for »mpcci info arch«.
batch <project>	Start an MpCCI batch job with project file <project>.
clean	Remove all files from the temporary MpCCI directory »/home/user/.mpcci/ tmp«.
doc	View the MpCCI documentation.
env	Print out the environment used by MpCCI in various formats for further processing.
gui	Launch the MpCCI GUI.
help	This screen.

home	[-n]	Print the MpCCI home directory without a newline or with a newline [-n] at the end and exit. This is in fact a shortcut for »mpcci info home«.
info		Print general information about MpCCI.
kill		Platform independent process kill based on commandline pattern matching.
license		Manage the license server and print license related information.
list		List information about the MpCCI installation and the supported codes.
lmutil		Run the FlexLM »lmutil [OPTIONS]« command delivered with MpCCI. Avoid running the lmutil command installed by codes other than MpCCI.
observe		Start the MpCCI file observer.
playback		Create a C source from an MpCCI debuglevel-3 logfile.
pm		Launch the MpCCI project manager.
ps		Unix »ps-ef« compatible ps for all platforms.
ptoi		Convert an MpCCI project file into an MpCCI input file.
server		Start the MpCCI server and control processes.
ssh		Check/fix your ssh installation.
test		Run some install/communication tests.
vis		Launch the MpCCI visualizer.
where	<CMD>	Find all locations of the executable <CMD> in the PATH.
xterm		Start a process inside an xterm.

THE MPCCI GRAPHICAL USER INTERFACE

Tools and Commands

To ease practical use of MpCCI most of the commands now can be invoked also from the GUI menu bar:

- information about the codes,
 - license status and management,
 - some test suites, and
 - details about the environment
- can now be accessed by a few clicks in the GUI.

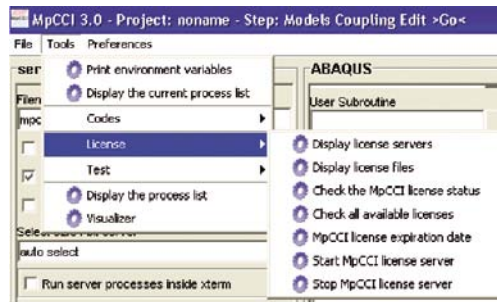


Figure 2: MpCCI Menu Bar/
Tools Menu

Unit Systems and Coordinate Length Units

One major improvement in 3.0.5 is the possibility to couple models with different grid length units and with different unit systems. When reading the model files MpCCI 3.0.5 now checks for the metrics and unit system and shows the parameters in the model panel of the GUI. During coupling definition the GUI presents for each quantity the specified unit system.



Figure 3 (ahead): Selection of Unit
System

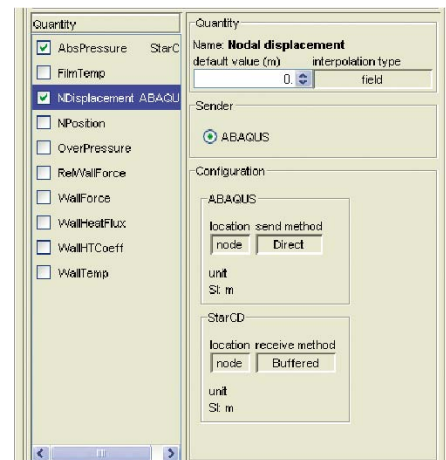


Figure 4 (right): Unit
System used per
Quantity

Running Codes in parallel

Most codes supported by MpCCI offer different ways to start them as parallel system:

- using MPI for a message passing approach,
- using shared memory techniques, or
- spawning parallel threads.

MpCCI 3.0.5 supports these different modes of parallelisms by adequate parameters in the GO-panel of its GUI. The parallel options of the codes have been integrated into the selection menus.

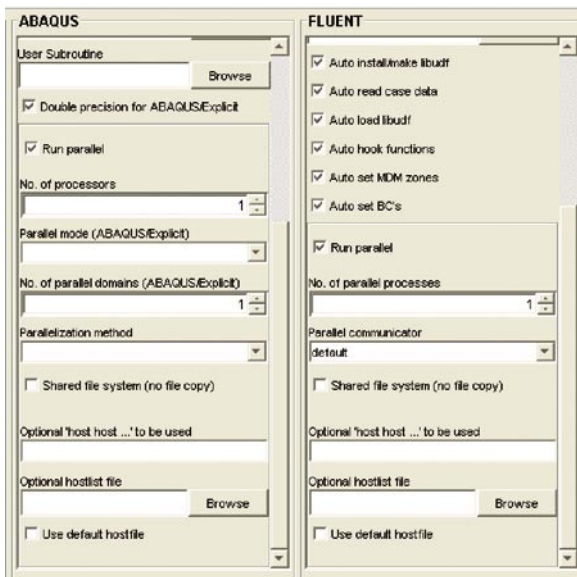


Figure 5: Starting parallel Codes

ASSOCIATION AND INTERPOLATION SCHEMES

Alignment of Coordinate Systems

If the two coupled models are not based on the same coordinate system the user may use the MpCCI command »mpcci <code> align« to transform the given input model into an aligned position with the other code's model. The transformed result is written into the modified input deck – which is identical to the original one except the nodal point coordinates. The homogeneous 4x4 transformation matrix respectively the reference coordinate systems used are indirectly defined via two planes. Each plane is defined via three non co-linear points p1, p2 and p3.

Association and Data transfer

If the meshes are located in the same reference system, the coupling/neighbour computation can be set up. The method for associating meshes and the physical quantities to be transferred need to be chosen. The association method determines which entities are associated. There are two different association methods available:

- Point Element (PE): A node of one mesh is associated with the element of the other mesh containing the node. The location of the node is given by the local coordinates.
- Element Element (EE): Elements of one mesh are associated with all intersecting elements of the other. The intersection figure is used as associative link. It is used for element based data.

All physical quantities are assigned to an interpolation type characterizing the data transfer. There are two types of data transfer schemes:

- Flux: The data is treated as a flux, which means that it is transferred in a conservative way.
- Field: The data is treated as field data, where the transfer need not be conservative.

Improvements on Element-Element-Association

The Element-Element Association is based on intersections of elements. In a two step neighbourhood search, intersecting elements are aligned.

First for each element of one mesh, those elements of another mesh are selected that are close. Then the candidates are tested for intersection.

The results of the neighborhood search are pairs of intersecting elements together with the size of their overlap. For reducing the complexity of calculating and representing the intersection we split all elements into simplexes, neglecting the error due to warping effects.

Volume Coupling with EE

With the EE-association, flux and field based data transfer is an interpolation over the size of intersection areas. As the problem of calculating intersections can be badly conditioned a robust algorithm must be used, that can handle problems resulting from floating point arithmetic. We have implemented two different algorithms. The current algorithm transforms intersecting elements to local (bary-centric) coordinates of an intersecting element. Then volumes of trapezoids are calculated and summed up.

The weakness of this algorithm is the transformation to local coordinates for elements with bad aspect ratio. We have improved the concept so that even aspect ratios smaller than $10e-6$ do not lead to bad results.

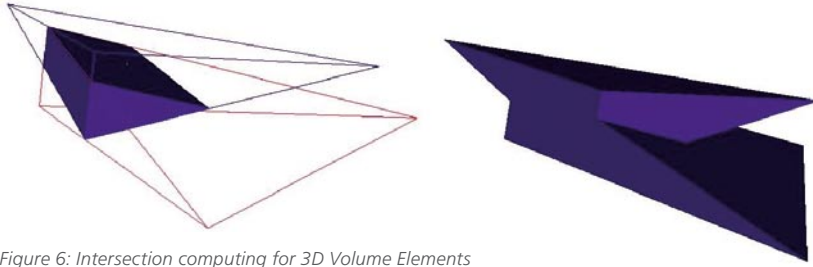


Figure 6: Intersection computing for 3D Volume Elements

The second one is a topology aware clipping algorithm. Given two simplexes or other convex manifolds we choose one to be the clipping simplex. For each face (or edge in 2D) we determine the plane it lies in, and cut off the part of the other simplex lying beyond it. This is done successively for each face of the clipping simplex. Then the volume of the resulting intersection figure is calculated. No coordinate transformation is needed.

The necessary Face-Face intersection tests can be reduced to two inner products and a simple sign comparison, so that the topology of the intersection figure can be determined in a robust and consistent way, without depending on the exact position of the intersection line.

Surface Coupling with EE

For EE based surface coupling a projection must be carried out as the surfaces do not necessarily share the same space. Hence MpCCI projects the elements of one mesh in an orthogonal way onto the other mesh.

Then the intersection is calculated with the projection image instead of the mesh itself. The problem with this projection method is that it does neither define a bijective nor a steady mapping between the meshes. There are element parts of the target mesh that keeps unrecognised (left part of figure).

The solution is to give up the strict orthogonal projection using a more complex one instead. Therefore unique projection directions are determined for all nodes. The projection directions for the rest of the mesh are interpolated such that a steady and bijective projection between the meshes is defined. But as this projection is longer linear over one element, the intersection figure of a target face and the projection image of a source face becomes more

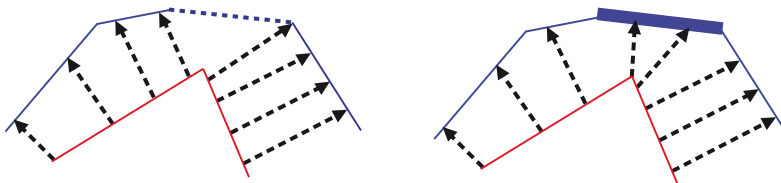


Figure 7: orthogonal projection (left)

adapted interpolation

difficult to handle. Therefore we calculate the intersection of edges and curved projected edges and linearise the part of the projected edges between the intersection points. Thus the presentation gets more easy to handle and the projection keeps steady and bijective.

Improved Point-Element based Flux Data Transfer (PE)

If coupling meshes are different there is no node-node correspondence. Thus for each node the physically corresponding point on the other mesh is searched for. The corresponding point is described by local coordinates related to the element containing the node.

The neighborhood search is performed in two steps: First a number of elements is computed, that are most likely to contain the nodes. In the second step the best match is chosen among the results. The best match is the element containing the node, or with surface coupling the one containing the closest point. The problem arises when trying to transfer data conservatively between a coarse source mesh and a fine target mesh. Nodes of a source mesh are transferring their data to the nodes of the associated element of the target mesh. The data is portioned by means of the local coordinates and distributed to the assigned target element nodes. The problem occurs when there are target nodes whose incident elements are not associated with a source node. Then no data is transported to the so called orphaned nodes. One way to solve this problem is to do a post processing step including a relaxation. This method preserves the data to be transferred but it is expensive concerning time complexity. It also smoothes strong data contrasts. Therefore we introduce another transfer algorithm based on EE.

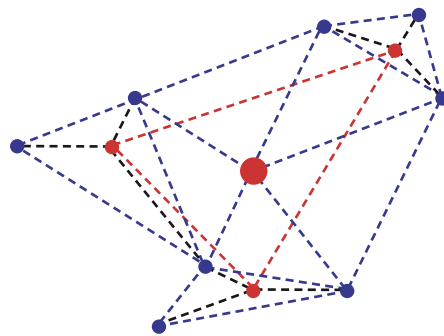


Figure 8: The red nodes contribute to the data of all blue nodes (black lines) except the one in the centre.

Node based Data transfer with EE

EE-Association is used for accurate and conservative Data transfer with element based data. This method can be adapted to node based data. The difference to the element based data is that the data can not be easily portioned by the intersection sizes to be then transported to the target mesh. Instead values are integrated over the intersection area of the source element. Then the data is transported to the intersecting area of the target element. There the data is portioned and distributed back to the nodes. As the association is bijective for volume and with the new EE-surface association for surfaces too, this method no longer results in orphaned nodes.

CODE ADAPTER

MpCCI version 3.0.5 of the MpCCI coupling environment supports:

- ABAQUS 6.5 and 6.6
- Ansys 7.1 to 10.0
- FLUENT 6.2 and 6.3
- Flux3D 9.2
- ICEPAK 4.1, 4.2
- MSC.Marc 2005R3
- Permas 10
- StarCD 3.2x
- RadTherm 7.1

Fraunhofer SCAI has established long term cooperations with most of the software vendors. Joint development plans, combined marketing activities and cooperative support for end users ensure solution quality and success in application.

MPCCI BUSINESS DEVELOPMENT

The first commercial version MpCCI 3.0.x was released in autumn 2004; MpCCI 3.0.4 was published in April 2005 and provided full functional interfaces and graphical user interface.

In March 2006 there are around 90 licensed installation of MpCCI world-wide. Around 30 of them are for research and academic – more than 50 licenses are installed at industrial sites. Additionally more than 50 MpCCI installations are used for demonstration and teaching purposes at the headquarters and local offices of our CAE partners

The following numbers may act as a snapshot of the geographic distribution of MpCCI usage worldwide (March 2006):

Germany:	25
Europe:	27
USA:	26
Japan, Korea, Asia:	12

A more detailed statistics on the code distribution is given in the following list (Note: the total number is bigger than 90 as each user needs more than 1 code adapter):

ABAQUS:	55
ANSYS:	12
FLUENT:	58
Flux3d (prototype):	1
Icepak (prototype):	1
MSC.Marc (prototype)	2
Permas:	2
StarCD:	15
RadTherm:	2
Inhouse Codes / SDK:	20

FLUID-STRUCTURE INTERACTION USING ABAQUS-FLUENT

Albert Kurkchubasche; ABAQUS, Inc.

INTRODUCTION TO ABAQUS

Company Profile

- Founded in 1978 – consistent, stable growth throughout our history
- The acknowledged leader in advanced finite element analysis software
- Key supplier to world-class product development companies
- Focused on Realistic Simulation
- Acquired by Dassault Systèmes in 2005

Technology Leadership

- More than 220 people in R&D
- One of the largest and most talented structural mechanics teams in the world
- Track record of inventing significant new FEA functionality
- Driven to maintain leadership in key, customer-driven technology areas

ABAQUS Products

Analysis Products (finite element solution)

- ABAQUS/Standard
- ABAQUS/Explicit

Interactive Products (modeling and visualization)

- ABAQUS/CAE
 - Process Automation Toolkit
- ABAQUS for CATIA V5

MULTIDISCIPLINARY SIMULATION

An analysis is multidisciplinary when it includes two or more distinct and coupled physical fields that all require a solution to solve the problem

One field may affect the response of another field through:

- The constitutive behavior, such as yield stress defined as a function of temperature
- Surface tractions, such as fluid exerting pressure on a structure
- Body forces/fluxes, such as heat generation due to joule heating
- Geometric changes, such as fluid in contact with a deforming body

ABAQUS provides fully coupled and sequentially coupled methods to solve multidisciplinary simulation.

Fully Coupled Methods

For the fully coupled method ABAQUS solves all the physics field degrees of freedom with a single solver.

Unified solver

$$\begin{bmatrix} K_s & K_{sf} \\ K_{fs} & K_f \end{bmatrix} \begin{Bmatrix} U_s \\ U_f \end{Bmatrix} = \begin{Bmatrix} F_s \\ F_f \end{Bmatrix}$$

ABAQUS provides variety built-in procedures using the fully coupled approach:

- Coupled thermal-stress analysis
- Coupled thermal-electrical analysis
- Coupled pore fluid diffusion and stress analysis
- Acoustic, shock, and coupled acoustic-structural analysis.

Sequentially Coupled Method

In a sequential coupled method each of the physics fields is solved by a different solver.

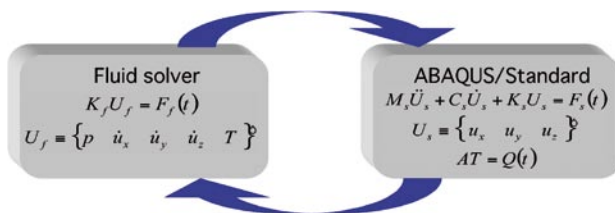
ABAQUS provides:

- an open-systems approach for general co-simulations through MpCCI
 - any third-party analysis software compatible with MpCCI can couple to ABAQUS
- direct interfaces for co-simulation for specific »niche« applications
 - ABAQUS/Explicit-MADYMO coupling.

Example of Open-Product Approach

One application of the co-simulation using MpCCI is fluid-structure interaction. Any CFD code using MpCCI can couple with ABAQUS/Standard and ABAQUS/Explicit.

- Implicit solver is suitable for most problems
- Explicit solver is suitable for strongly nonlinear interactions, where the critical stable time increment for fluid-structure interaction is small



CONTACT

Albert Kurkchubasche
 ABAQUS, Inc.
 39221 Paseo Padre Parkway
 Fremont, CA 94538-1611
 USA
 Phone: +1 510 7945891
 albert.kurkchubasche@
 ABAQUS.com

Example of Direct Co-simulation

ABAQUS/Explicit – MADYMO Coupling

- Crash safety simulation performed with the occupant simulation program MADYMO



FLUID-STRUCTURE INTERACTION USING MPCCI

Benefits of using MpCCI for FSI

This strategy offers the following advantages to our customers:

- Both, unidirectional and bidirectional coupling between ABAQUS and CFD code
- Both, ABAQUS/Standard and ABAQUS/Explicit are supported
- Relatively independent setup of fluid and structural subproblems using familiar tools
- Use of familiar, dedicated algorithms to solve each domain independently
- Industry-standard code coupling based on MpCCI – a widely used, scalable, interprocess communication and mapping tool
- Open-systems approach to co-simulation with other codes that use MpCCI

INDUSTRIAL APPLICATION

FSI Applications

Automotive

- Thermal-stress analysis of engine, exhaust manifold, cooling jackets
- Design of Formula 1 race cars
- Hydraulic engine mounts, disc brake system, ABS, shock absorbers

Aerospace/defense

- Airflow around wing
- Combustion-driven propellant ablation

Power/gas

- Sloshing in gas tank
- Pipelines, risers
- Heat exchangers (nuclear power)

Equipment design

- Pumps

Electronics

- Cooling of electronic components
- Manufacturing of integrated circuits

Rubber

- Flow limiters, seals
- Tire hydroplaning

Consumer products

- Airflow and high-speed manufacturing
- Application of adhesives
- Air-driven media (copiers)

MEMS

- Inkjet nozzles

Medical

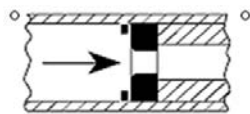
- Heart valves, blood flow

Example: Vernay-VernaFlo® Fluid Flow Limiter

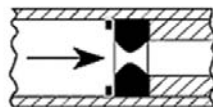
Custom-engineered valves to provide a constant volume output with a varying range of inlet pressures.

Simulation objectives:

- Determine bulk flow for an inlet pressure range 0-40 psi
- Maintain constant flow in valve over a range of operating pressures
- Experimental validation



Under low pressure



Under high pressure

Cross-section of typical flow control valve

Flow control valve cross-section

Model Specifications

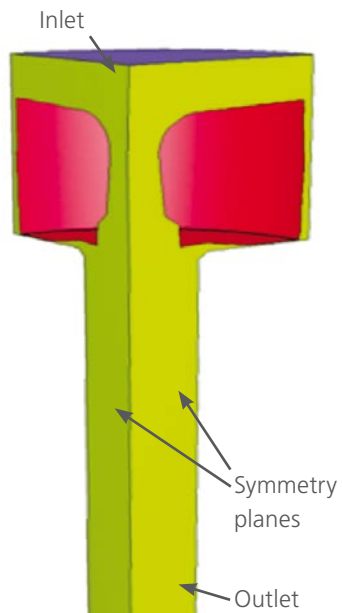
ABAQUS model

- ~22,000 C3D8RH elements
- Finite-sliding frictional contact between compound rubber ring and rigid seat
- Hyperelastic material behavior
 - Calibrated using uniaxial and biaxial test data provided by Vernay Laboratories

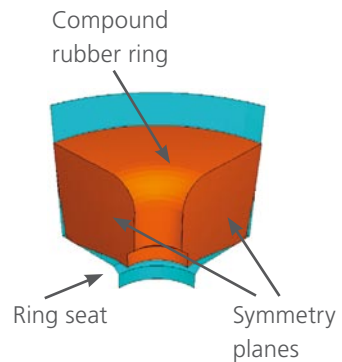
FLUENT model

- 233,000 tetrahedral cells
- Standard turbulence model
 - $k-\epsilon$ model with standard parameters

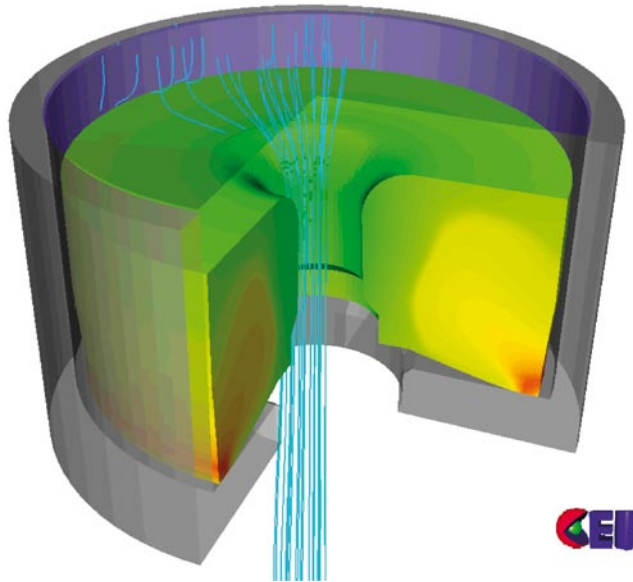
FLUENT model



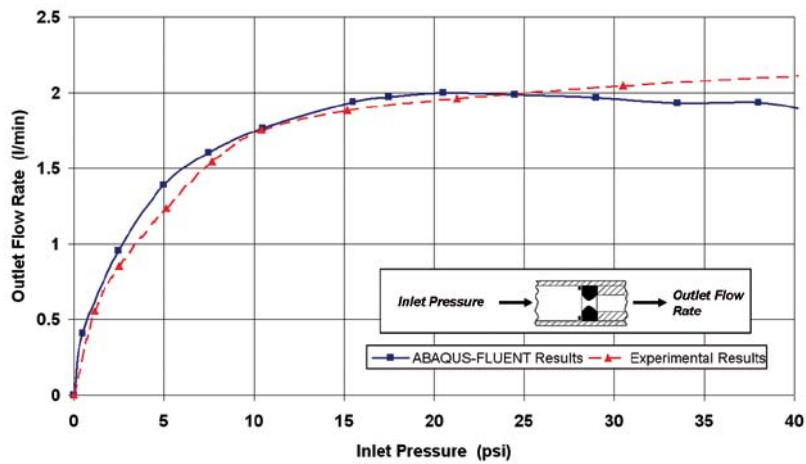
ABAQUS model



ANIMATION OF FLOW LIMITER



OUTLET FLOW RATE VS. INLET PRESSURE



Comparison between numerical and experimental outlet flow rate vs. inlet pressure

Example: Aerodynamic Study of Glider Wing

- DG-1000 glider wing
- Original linear-elastic simulation was performed by
Zentrum für Strukturtechnologien, ETH Zürich and Fraunhofer SCAI
- Example extends the simulation by including large-displacement effects
- Simulation objective
Determine aerodynamic performance for different wing designs



ETH
Eidgenössische Technische Hochschule Zürich
Swiss Federal Institute of Technology Zurich

DG-1000 Glider

Large wing span and body length:

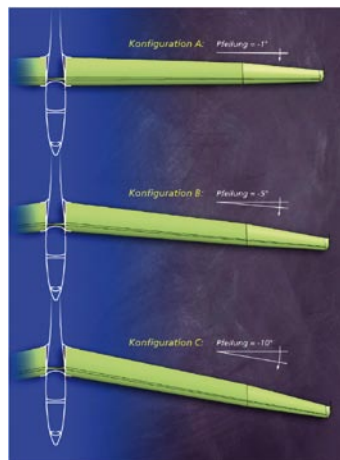
- Two-seater glider, 20m wing span
- Flexible, low-damped structure

Three configurations are analyzed:

- Configuration A, Rake angle = -1°
- Configuration B, Rake angle = -5°
- Configuration C, Rake angle = -10°

The torsion response of the wing changes with the forward rake angle:

This alters the fluid flow around the wing and consequently the aerodynamic behavior



C. Dehning, P. Post, C. Rümppler, K. Wolf, C. Ledermann, F. Hurlimann, P. Ermanni, »Fluid-Strukturkopplungen mit MpCCI,« 2004

Model Specifications

ABAQUS model

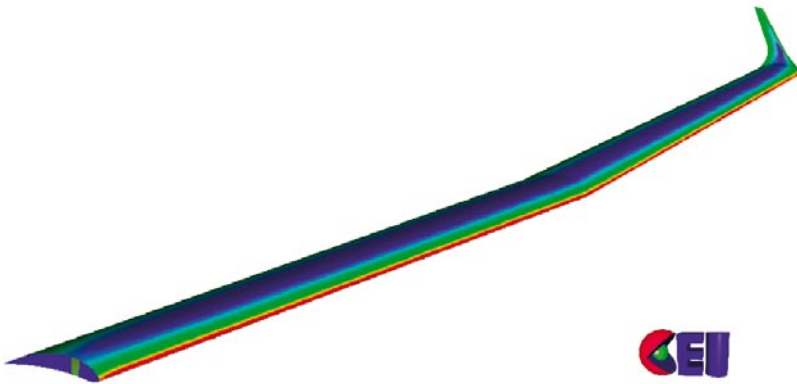
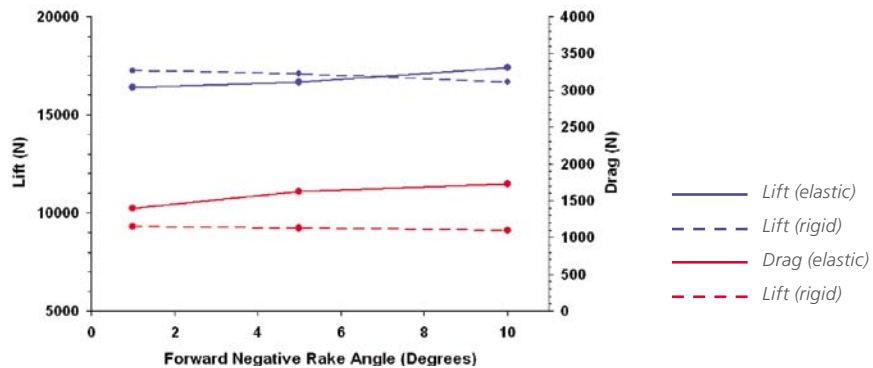
- ~37,000 S4/S3 elements
- Large geometric effects
- Linear-elastic composite properties

FLUENT model

- ~723,000 tetrahedral cells
- Incompressible laminar flow

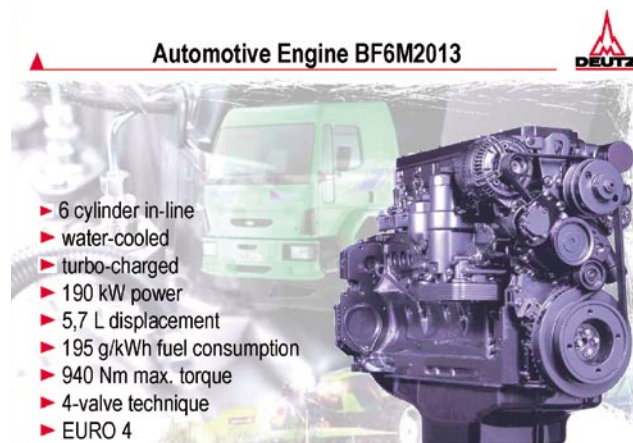


Aerodynamic forces at 140 km/h



Example: Analysis of an Engine Head with Coolant Flow

- ABAQUS-FLUENT conjugate heat transfer analysis, followed by an ABAQUS-only thermal-stress analysis
- Structural and CFD models were provided courtesy of Deutz, AG
- Simulation objectives
 - Obtain steady-state temperature distributions
 - Obtain higher fidelity thermal-stress solutions

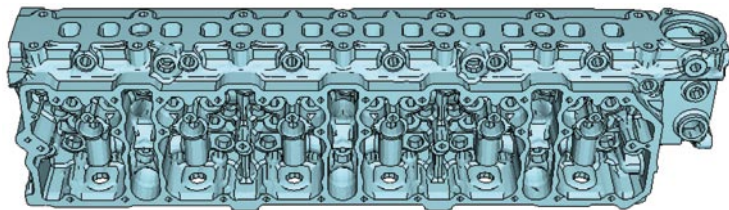


Model of Cylinder Head

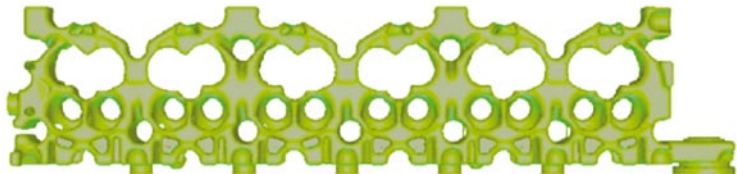
Complex geometry

530,000 tetrahedral cells and 290,000 heat transfer elements

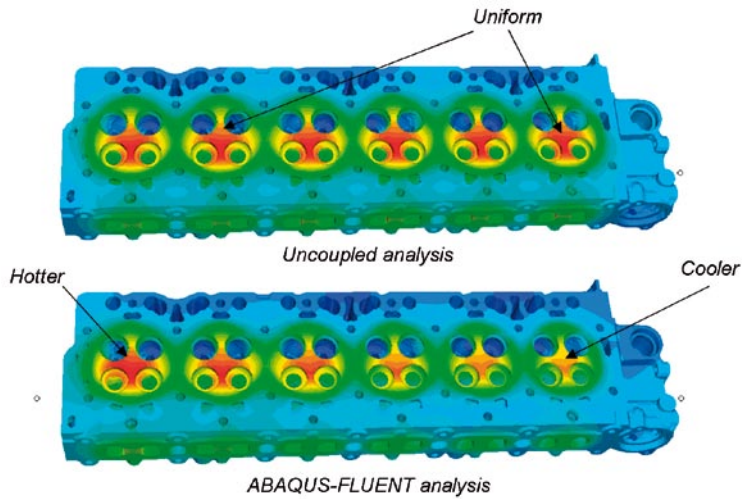
ABAQUS



FLUENT

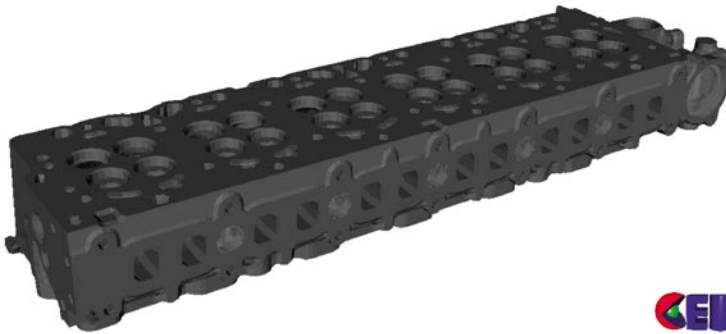


Temperature Distribution



Temperature distribution of ABAQUS-only (top) vs. ABAQUS-FLUENT (bottom)

Animation of Engine Head with Coolant Flow



Example: Ball Valve of Antilock Brake System

- Transient simulation of the a ball valve of an Antilock Brake System (ABS)
- Depending on the brake fluid pressure, the ball valve will open and stay open until the excess fluid pressure is released
- Simulation Objectives:
 - Characterize flow characteristics of the brake fluid
 - Characterize the ball movement



- The ABAQUS-Fraunhofer SCAI collaboration is a success and has delivered a leading FSI capability to the market in under two years
- The ABAQUS FSI strategy using MpCCI provides clear advantages over proprietary closed code coupling methods
 - MpCCI provides time-tested best-in-class code coupling functionality
 - MpCCI provides an open-systems link to more than one CFD product
- Both ABAQUS/Standard and ABAQUS/Explicit can be linked with CFD
- MpCCI avoids the need to obtain additional niche FEA or CFD products to solve FSI problems
- ABAQUS will continue to expand its MpCCI-based FSI functionality to provide additional value to our customers

COUPLED SOLUTIONS WITH STAR-CD

Katsushi Moriyama, CD-adapco JAPAN Co.,LTD.

In the engineering and scientific field, the numerical simulation is an important tool which is helpful to understand a complicated phenomenon. We can obtain the detailed data which are not provided by experiment, and reduce the time and cost to develop the product.

A field of numerical simulation is divided to each specialized area such as the fluid analysis software (ex. STAR-CD) and structure analysis software (ex. ABAQUS, ANSYS). In each area, the most suitable numerical method has been developed. However, many of actual phenomena are multi-physics that the physical fields such as a fluid, structure, electromagnetic field and sound are connected with each other complicatedly. Therefore, in order to simulate such multi-physics, a tool for coupling these software are necessary. MpCCI is interface for coupling different software. For example, the technique of two-way coupling is selected to solve the system that includes the interaction between some physical phenomena such as the fluid and structure, ex. »the structure deformed by a fluid flow« and »the fluid flow controlled by an electromagnetic field«. By using MpCCI, we enable two-way coupling doing data transfer between different software.

CD-adapco JAPAN Co., LTD (CDAJ) carries out sale of MpCCI and technical support in an Asian area including Japan and China since 2004. CDAJ is a member of CD-adapco group and do distribute of STAR-CD. CDAJ uses MpCCI for coupling between STAR-CD and other CAE software such as structure analysis software and electromagnetic field analysis code.

Development of engineering industry is remarkable in an Asian area such as Japan and China. Recently, it rises up the request of high accuracy and complicated physical models for analysis. In such a problem, the coupling analysis play important role and expectation to MpCCI are very high. In this paper, some examples of coupled solution with MpCCI and STAR-CD are shown.

FLOATING BODY PROBLEM

This is an example analyzed the floating body problem with a rectangular block. The floating body problem is very important in marine engineering such as vibration of a marine construction or a ship by a wave. Influence to a ship by a wave in particular is closely related to our safety of a voyage. The investigation of floating body is very important, so that the behavior of rectangular block on the water surface was solved by using MpCCI coupling simulation.

In the floating body problem, fluid is treated as two phase model of liquid (water) and gas (air). The fluid was analyzed by a free surface function of STAR-CD. On the other hand, ABAQUS was used for analysis of a rectangular block moving. A rectangular block floats on the surface of water at first and moves by a wave induced forcibly (see Figure 1). A block made by wood is influenced by gravity force and fluid force. Under this condition, it almost is moving as a rigid body.

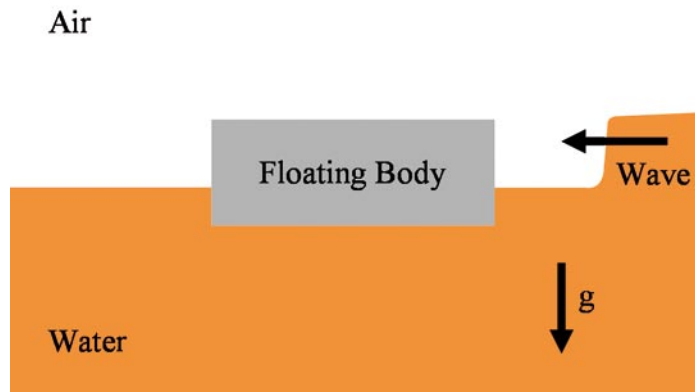


Figure 1: Simulation Model of Floating Body

The fluid force acting on a floating body is calculated by STAR-CD, and is transported to ABAQUS through MpCCI. Then ABAQUS calculates the moving of block and the displacement is transported to STAR-CD through MpCCI again. STAR-CD receives displacement data, and the mesh is reconstructed by a grid morphing function of MpCCI and then the next flow field is calculated. This coupling procedure is executed by each time step. This scheme is shown in Figure 2.

CONTACT

Katsushi Moriyama
CD-adapco JAPAN Co.,Ltd.
Kansai Branch,
Nihon Bldg 8F, 79.
Kyomachi, Chuo-ku
Kobe, Hyogo
Japan
Phone: +81 (0) 783 265353
katsushi.moriyama@cdaj.co.jp

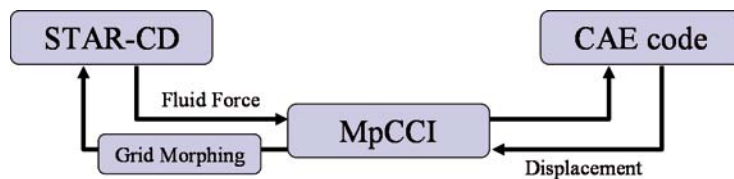


Figure 2: Coupling Scheme between STAR-CD and Other CAE Code via MpCCI

Analysis result is shown in Figure 3. A floating block that rests at first is moved by wave induced forcibly from right side. Then a block moves more complicatedly by a reflected flow.

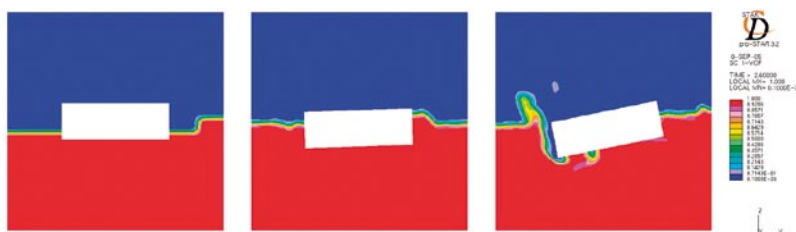


Figure 3: Analysis Result of Floating Body Problem

FLOW-INDUCED VIBRATIONS

It is shown an example of flow-induced vibration of a cylindrical structure. The flow-induced vibration of a structure is important in the engineering field such as atomic energy and chemical plant. In atomic energy plants, there is the case that the destruction of a structure breaks out by such fluid-related vibration and it often causes serious accident. On the other hand, the noise by fluid-induced vibration of a structure is also important problem.

The fluid-structure interaction (FSI) simulation using MpCCI was used in order to analyze a column vibrating by interaction with fluid flow. An elastically-supported column is located in uniform flow as shown in Figure 4. The flow field is analyzed by STAR-CD. The fluid force acting to a column is transported to ANSYS through MpCCI, and the structure displacement is calculated by ANSYS. The displacement of a column is given back from ANSYS to STAR-CD through MpCCI, and the flow field is calculated by STAR-CD again.

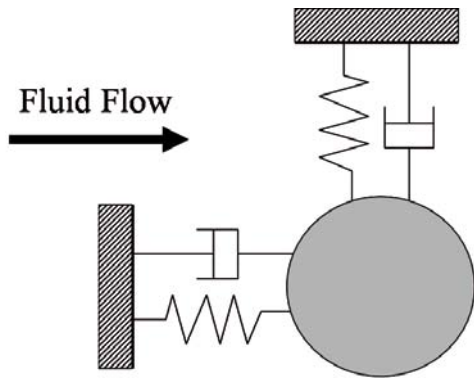


Figure 4: Simulation Model of Flow-Induced Vibration of a Cylindrical Structure

Figure 5 shows the flow field around a cylinder. The fluid flow varies with a difference of flow speed. As flow speed generally increases, the self-induced vibration with symmetric vortex and lock-in vibration by Karman vortex appear. The vibration amplitude of a cylindrical structure with flow speed is represented in Figure 6. By using the coupling simulation with MpCCI, these fluid-induced vibrations can be predicted.

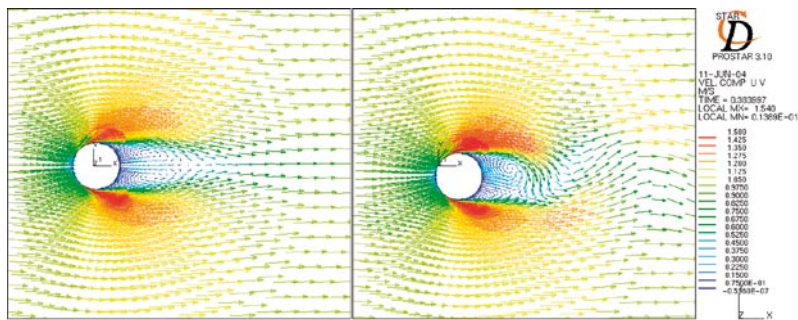


Figure 5: Flow Field around a Cylinder

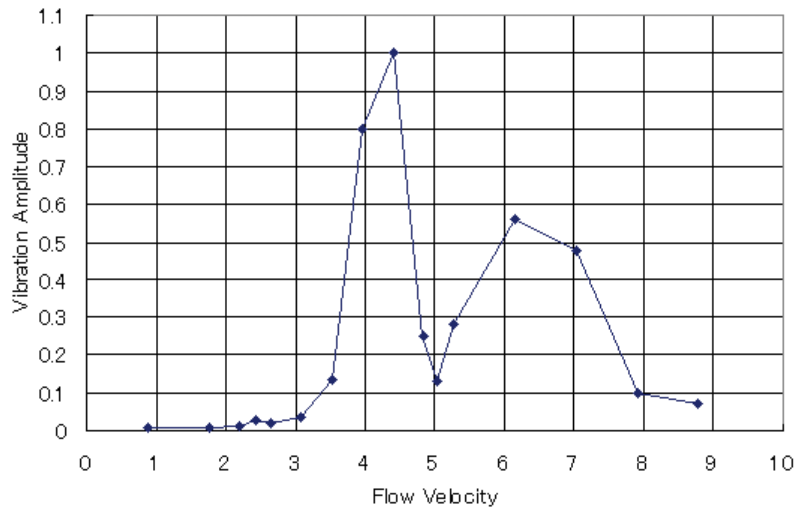


Figure 6: Maximum Vibration Amplitude of a Cylinder

CONCLUSION AND OUTLOOK

As well as above examples, the coupling simulations such as deformation of a thin film by fluid flow and fluttering of a plane wing are also carried out in CDAJ. In various engineering and scientific problem, the coupling simulation with MpCCI will become more important tool. In addition, with version up of MpCCI, the number of CAE software which can be coupled with STAR-CD will increase, so that analysis ability of STAR-CD in the field of multi-physics will be expanded more and more.

MULTIPHYSICS WITH FLUENT AND MPCCI

Mark Pelzer, FLUENT Deutschland

INTRODUCTION

So called »multi-physics« problems have been of high interest for recent years. Fields of combination of multi-physics are structural analysis, fluid dynamics, aeroelastics, heat transfer, radiation, electrodynamics, magnetodynamics, stamping, crash. Simulations have been able to address some of these combination within single tools. For example fluid dynamics, combustion, multiphase, conjugated heat transfer and radiation within FLUENT or structural dynamic, heat transfer and electrodynamics in FE tools are already feasible. For some cases one could also use CFD and FE tools' programmable interfaces to implement additional multi-physics. This is currently very often done in CFD codes since CFD tools often provides an option to account for moving geometry.

If such on-board means are not sufficient the user can couple software tools manually. A prerequisite then is identical computational meshes in both tools.

A one-way coupling can be established by exporting mesh and results from one tool in the appropriate format and import the result into the other tool. In case of a loose physical coupling of the problem even a two-way coupling can be achieved this way.

A closely coupled problem or a problem that requires different computational meshes in both tools requires the use of a coupling software. This software has to handle data exchange, mapping of data from one mesh to the other and the synchronization of physical time in both tools. For some application also the deformation of the geometry is handled by the coupling software. Following we will discuss the various level of complexities by examples between finite element programs and the CFD software FLUENT using the coupling software MPCCI [1].

FLUENT

FLUENT provides comprehensive modeling capabilities for a wide range of incompressible and compressible, laminar and turbulent fluid flow problems. Turbulence models include Spalart-Allmaras, k-e, k- ω , RSM and LES. Steady state and transient analyses can be performed. In FLUENT a broad range of mathematical models for transport phenomena like heat transfer and chemical reactions is combined with the ability to model complex geometries. The following Radiation models are included: P1, Rosseland, surface to surface, DTRM (discrete transfer radiation model), DOM (discrete ordinate model) and

the solar load model. Furthermore the key function for FSI, that is a dynamic moving/deforming mesh capability for arbitrary large boundary deformations is available.

Another very useful group of models is the set of free surface and multi-phase models like ASMM (algebraic slip mixture model), Euler-euler model, Euler-granular model, VOF (volume of fluid model) and the DPM (discrete particle model) [2].

SOLVING MULTI-PHYSICS PROBLEMS WITH A COUPLING SOFTWARE

A closely coupled problem or a problem that requires different computational meshes in both tools requires the use of a coupling software. This software has to handle data exchange, mapping of data from one mesh to the other and the synchronization of physical time in both tools. For some application also the deformation of the geometry is handled by the coupling software.

MpCCI (Mesh-based parallel Code Coupling Interface) has been developed at the Fraunhofer Institute SCAI as a general software platform for coupling different simulation codes.

MpCCI is a software environment which enables the exchange of data between the meshes of two or more simulation codes in their coupling region. Since the meshes belonging to different simulation codes are not compatible in general, MpCCI performs a flux conservation interpolation. In case of parallel codes MpCCI keeps track on the distribution of the domains onto different processes.

MpCCI allows the exchange of nearly any kind of data between the coupled codes; e.g. energy and momentum sources, material properties, mesh definitions or global quantities. The intricate details of the data exchange are hidden behind the concise interface of MpCCI.

Most of the commercial CFD/FEM applications allow users to add additional features, physical models, or boundary conditions via a programming interface. Within these user routines access to internal data structures is possible, either through subroutine parameters and global variables, or via internal modules for reading and storing data. MpCCI uses these capabilities for code adaptation. A user-subroutine called after each iteration or time step works as a hook to MpCCI [3].

CONTACT

Mark Pelzer
Fluent Deutschland GmbH
Birkenweg 14 a
64295 Darmstadt,
Germany
Phone: +49 (0) 6151 3644-0
mp@fluent.com

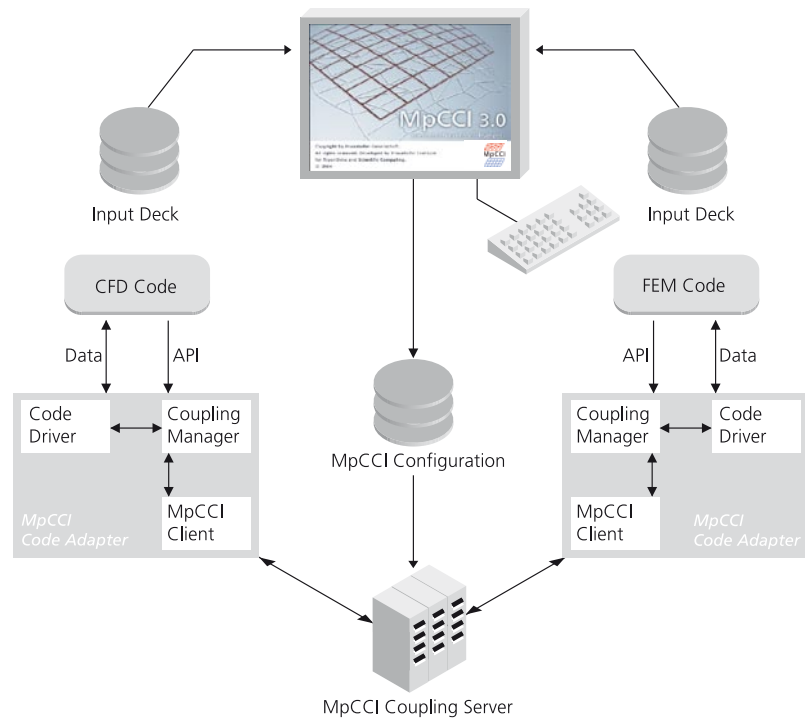


Figure 1: MpCCI uses a client-server architecture. The »MpCCI Code-Adapter« links ABAQUS/Standard and ABAQUS/Explicit to FLUENT through the MpCCI Coupling Server.

COUPLING EXAMPLES ABAQUS-FLUENT (FSI)

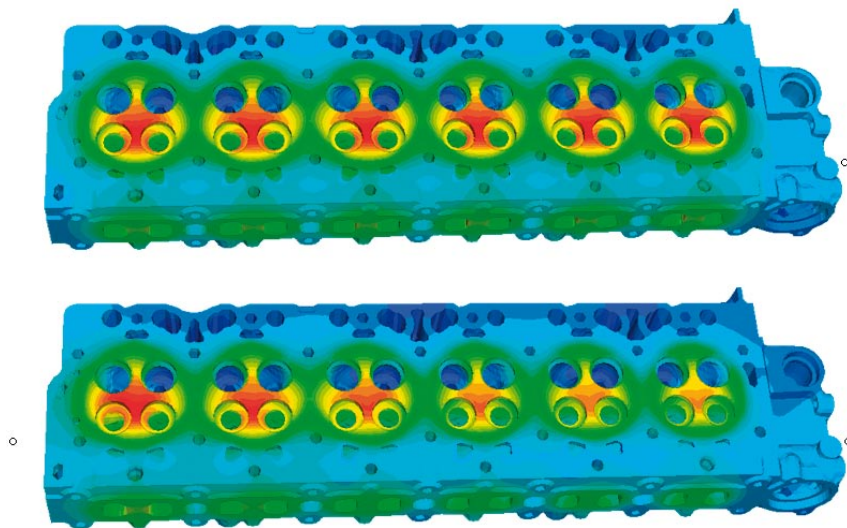
The coupling capabilities between FLUENT and ABAQUS includes both sequential and coupled simulations. The following list of quantities gives an overview about the possible data exchange.

	DESCRIPTION	SENDER	RECEIVER
NPosition	Nodal positions	ABAQUS	FLUENT
OverPressure	Relative pressure	FLUENT	ABAQUS
RealWallForce	Relative wall force	FLUENT	ABAQUS
Temperature	Ambient (fluid) temperature	FLUENT	ABAQUS
WallForce	Absolute wall force	FLUENT	ABAQUS
WallHTCcoeff	Wall heat transfer coefficient (film coefficient)	FLUENT	ABAQUS
WallHeatFlux	Wall normal heat flux density	FLUENT	ABAQUS
WallTemp	Wall temperature (nodal temperature)	ABAQUS	FLUENT

CYLINDER HEAD THERMAL-STRESS PREDICTION

The prediction of thermal stresses in an cylinder head depends strongly on the influence of the fluid. The heated air enters the flow domain and heats up the material. The temperature gradient in the material causes thermal stresses. Via one way code coupling it is possible to send the fluid temperature and heat transfer coefficient from FLUENT to ABAQUS. With these values ABAQUS can calculate the heat flux and so the temperature distribution in the material. Afterwards ABAQUS calculates the thermal stresses. Red shows the hottest regions and blue the coldest regions (Figure 2).

A comparison between an ABAQUS stand alone simulation and an ABAQUS-FLUENT coupled simulation shows a significant difference in the temperature distribution on the surface of the cylinder head.

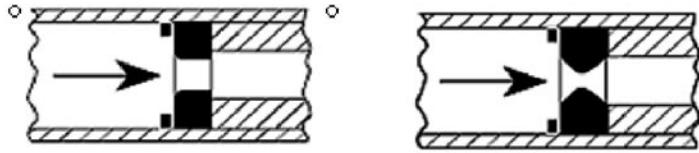


Plotted in EnSight Gold from CEI. Courtesy of Deutz, AG

Figure 2: Prediction of temperature on the surface of a cylinder head. Red shows the hottest regions and blue the coldest regions.

VERNAY-VERNAFLO® FLUID FLOW VALVE

In this application a liquid flow through a valve is examined. The pressure inlet boundary condition changes from 0-40 psi and deforms the valve more and more (Figure 3). A steady state analysis was done in both FLUENT and ABAQUS. FLUENT started with a low pressure inlet boundary condition (Figure 4) and sent the relative forces after getting the converged flow field. ABAQUS calculates the new shape (Figure 4a) of the geometry and send back this information via MpCCI. After this the inlet bc. will be increased and the complete procedure is repeated until it reached the maximum value of 40psi at the inlet (Figure 4b). A comparison between experimental data and simulation results shows a good agreement (Figure 5).



Under low pressure

Under high pressure

Flow control value cross-section

Figure 3: Illustration of the undeformed and deformed shape of the fluid flow valve

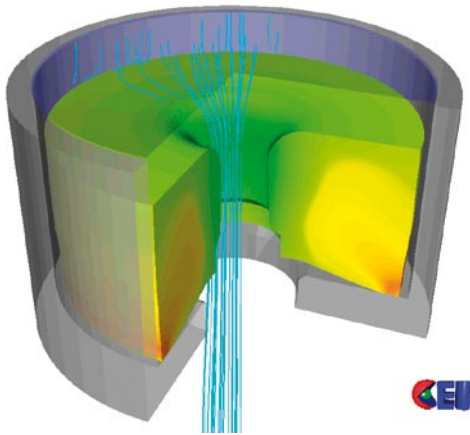


Figure 4a

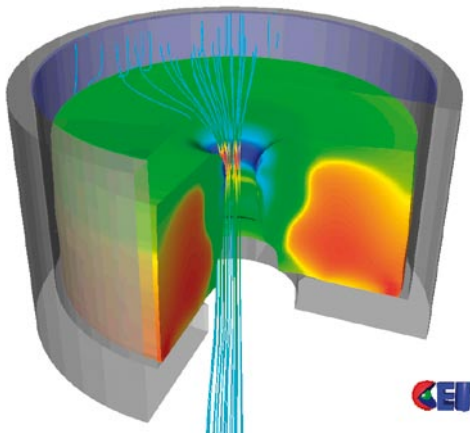


Figure 4b

Plotted in EnSight Gold from CEI

Figure 4: Contours of pathlines of the flow field and von Mises stresses in the valve.

Figure 4a shows the starting point, figure 4b shows the end shape of the valve.

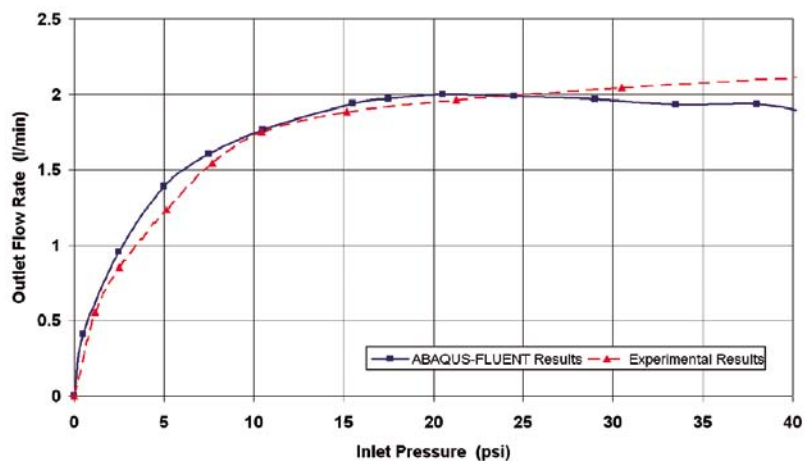


Figure 5: Comparison between experimental- and simulation results. The values are in good agreement.

ELECTRIC ARC SIMULATIONS

For the simulation of electric arcs based on the magneto-hydrodynamic approach volume coupling between ANSYS (electromagnetic fields) and FLUENT (fluid/plasma) is necessary.

ANSYS and FLUENT were used for 3D simulations of an electric arc running on copper busbars. Magneto-hydrodynamic equations are solved in FLUENT and Maxwell's equations are solved in ANSYS.

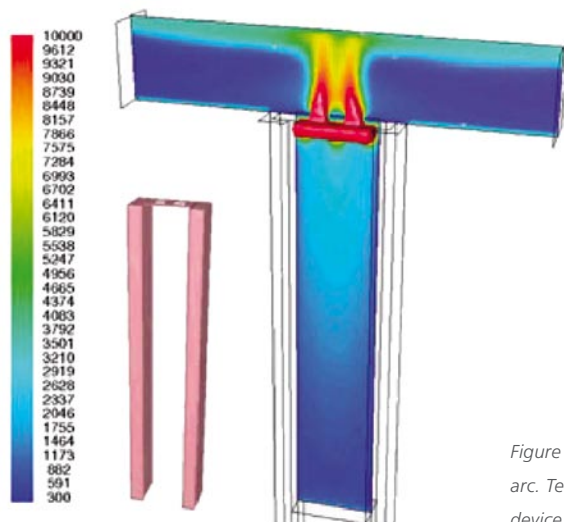


Figure 6: Simulation of an electric arc. Temperature distribution in the device.

CONCLUSION

With the capability of automatic data exchange via MpCCI it is possible to describe different complex multi physics systems. The interpolation method guaranteed a correct data exchange between the CFD- and FEM code. This avoids time consuming file based exchange between the codes and gives the flexibility to use different meshes.

ABAQUS, FLUENT and Fraunhofer SCAI collaborate with their development activities to improve the coupling of the codes for FSI applications.

REFERENCES

- [1] Sitzki L., Kaufmann F.H., Dehning C.: »Fluid-Structure Interaction: Status and Strategy«, 2004 Conference Virtual Product Development (VPD) in Automotive Engineering
- [2] FLUENT.Inc: »FLUENT 6.2 User Guide Vol 2A«, 2005, 9-2
- [3] Fraunhofer SCAI: »MpCCI 3.0 Overview and Release Notes«, 2004, 4

FLUID-STRUCTURE INTERACTION SIMULATIONS WITH MSC.MARC AND STAR-CD OR FLUENT

Pieter Vosbeek, MSC.Software Benelux B.V.

INTRODUCTION

MSC.Marc is a general-purpose nonlinear finite element solver. It offers automated nonlinear analysis of 2-D and 3-D contact problems, automated remeshing in 2-D and 3-D and has strong multi-physics capabilities. MSC.Marc is in use at many sites around the world to analyze and optimize designs in the aerospace, automotive, biomedical, chemical, consumer, construction, electronics, energy, and manufacturing industries.

MSC.Marc has a long history with MpCCI. The choice for MpCCI is based on the desire for a general-purpose coupling interface to other commercial solvers. Emphasis has been on computational fluid dynamics (CFD) codes, to solve fluid-structure interaction problems. The first coupling interface in MSC.Marc dates back to MpCCI's predecessor COCOLIB. Later on, a prototype interface to MpCCI versions 1.3 and 2.0 was developed. Examples of the latter can be found in Refs. [1] and [2].

Recently, in a joint effort by Fraunhofer SCAI and MSC.Software, MSC.Marc has been fully integrated into the MpCCI 3.0 environment. The MSC.Marc code adapter is available with the new MpCCI 3.0.5 and MSC.Marc 2005r3 releases and has been implemented through a new set of user subroutines specially developed for MpCCI. It allows MSC.Marc customers with access to commercial CFD solvers such as STAR-CD and FLUENT to analyze fluid-structure interaction problems involving large deformations of the structure and heat transfer. In the present paper, the main features of the MSC.Marc-MpCCI coupling will be discussed. On-going interface development will be illustrated using the local mesh refinement capabilities of MSC.Marc.

FEATURES

The MpCCI code adapter for MSC.Marc, available with the new MSC.Marc 2005r3 and MpCCI 3.0.5 releases, has been designed primarily to solve fluid-structure interaction problems with commercial CFD solvers such as STAR-CD and FLUENT. The main features of the code adapter are:

- The adapter is available in thermal, structural and coupled thermal-structural analyses, that can be of steady state, transient, quasi-static or transient dynamic nature;
- The adapter supports surface interaction and volume-based coupling between the fluid and the structure;

- The adapter can be used with a wide range of linear and non-linear material behavior, including elastic, plastic and rate-dependent materials as well as composites;
- The adapter supports geometrically linear and non-linear effects;
- The adapter can be used with MSC.Marc's automated contact algorithm.

All the usual thermal and structural quantities, such as displacement, temperature, fluid pressure, heat flux, film coefficient and -temperature can be exchanged with CFD solvers via the code adapter on predefined parts of the surface or volume of the structural model. In addition, in a transient analysis in which adaptive time stepping is used, the CFD solver can prescribe the coupling time steps after which MSC.Marc must exchange data with the solver.

The MSC.Marc code adapter adheres to the MpCCI 3.0 convention to identify the parts of the surface or volume of the structural model where it interacts with the fluid by user defined sets. The MpCCI graphical user interface (GUI) allows users to couple these sets with corresponding surfaces or volumes of the CFD solver and to specify the physical quantities that are to be transferred between these regions. Depending on the model dimension and the type of coupling, the following set types are supported:

- sets of finite element edges or geometric curves, for 2-D surface coupling;
- sets of finite element faces or geometric surfaces, for 3-D surface coupling;
- sets of finite elements or contact bodies, for volume-based coupling in any dimension.

These sets can be defined in the MSC.Marc Mentat pre- and post-processor (see Figure 1).

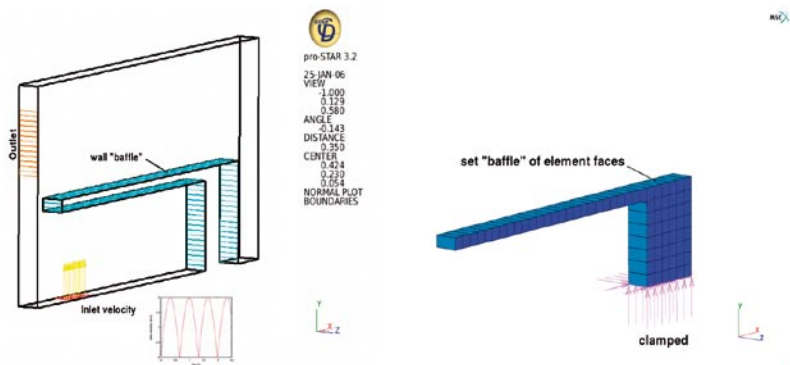


Figure 1: The STAR-CD and MSC.Marc models of the transient analysis on an elastic flap in a laminar flow. The coupling surfaces are the wall »baffle« defined in Pro-STAR and the element face set »baffle« defined MSC.Marc Mentat.

CONTACT

Pieter Vosbeek
 MSC.Software Benelux B.V.
 Groningenweg 6H
 2803 PV Gouda,
 The Netherlands
 Phone: +31 (0) 182 536444
 pieter.vosbeek@
 mscsoftware.com

IMPLEMENTATION

The MSC.Marc 2005r3 release includes a number of new features specially designed for MpCCI. These new features allow the MpCCI code adapter for MSC.Marc to access connectivity, coordinates and current values of solution quantities such as displacement, reaction force, temperature and heat flux, on predefined parts of the surface or volume of the structural model. In addition, quantities that are typically computed by a CFD solver, like fluid pressure and temperature, heat flux and film coefficient and environment temperature, can be prescribed on these parts of the model.

The basic new notion in MSC.Marc 2005r3 is that of a coupling region, which is the part of the surface or volume of the structural model where it interacts with the fluid. A new input option, called COUPLING REGION, is available to define such regions and to specify the physical quantities that are to be prescribed on them. Three types of coupling regions are supported. These types depend on the model dimension and the type of coupling and correspond to the set types listed at the end of the preceding section. Any number of regions can be defined in a model.

An extensive and public API that consists of three new user subroutines and a number of utility routines accompanies the new option. MSC.Marc calls the user subroutines during the analysis if coupling regions have been defined. Utility routines can be used in the user routines to obtain the connectivity, the coordinates and the current values of solution quantities on these regions as well as to set the new values of prescribed quantities on the regions.

All the usual thermal and structural quantities, such as displacement, temperature, heat flux, film coefficient and environment temperature and pressure can be accessed via the API. In addition, the coupling time step (the time between two data exchanges) can be prescribed by the CFD solver in transient analyses, if the AUTO STEP automatic time stepping algorithm is employed. In that case, MSC.Marc may divide the coupling time step into a number of smaller time steps and call the user subroutines only after the coupling time step has elapsed.

The MpCCI 3.0.5 code adapter for MSC.Marc is implemented through the new user subroutine API. The MpCCI GUI scans the MSC.Marc input file for user defined sets of the above mentioned types and allows users to couple any of these sets with corresponding surfaces or volumes defined in the CFD grid. At startup of the coupled analysis, the MpCCI GUI creates a copy of the selected MSC.Marc input file and adds the new COUPLING REGION option in order to define a coupling region for each set that is coupled with a CFD surface or volume and to specify the prescribed physical quantities on the set.

EXAMPLES

Elastic Flap in a Laminar Flow (STAR-CD)

Figure 1 shows the STAR-CD and MSC.Marc models of an elastic flap in a laminar flow. The periodic inflow velocity is depicted in the graph. The models are coupled via the wall »baffle« and the finite element faces in the set of the same name. The coupling is purely mechanical. The fluid pressure on the wall computed by STAR-CD is applied to the element faces of the MSC.Marc model and the displacements of the nodes of these faces are used to move the fluid grid points of the wall. The MpCCI grid morpher is employed to adjust the interior vertices of the CFD grid, to avoid cells with zero or negative volumes. The final fluid velocity and structural deformations are shown in Figure 2, as well as the normal stress distribution in the x-direction. In the graph, the vertical displacement of the left-most node of the flap is plotted versus time. The frequency of the vertical displacement matches that of the inlet velocity.

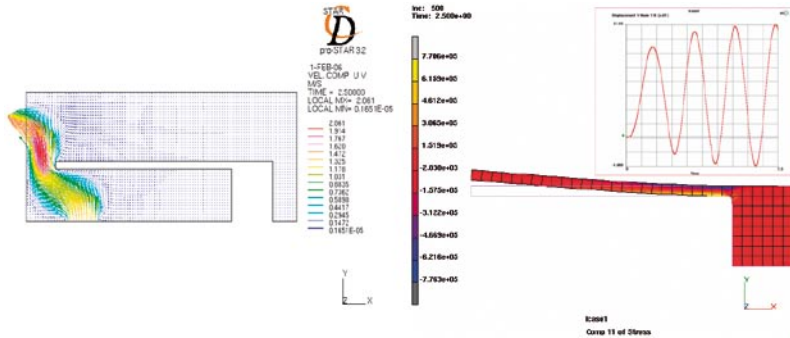


Figure 2: The final velocity field of the fluid and deformations of the elastic flap. The graph shows the vertical displacement of the left-most node of the structure versus time.

Steady State Heat Transfer of an Exhaust Manifold (FLUENT)

Figure 3 shows the FLUENT and MSC.Marc models of a steady state heat transfer analysis of an exhaust manifold. At the four inlets, a constant temperature of both fluid and structure is prescribed, as well as a constant inlet fluid velocity. The outer surface of the structure is subject to a convective (film) boundary condition with a constant environment temperature. At the coupling surfaces, heat flux and temperature are exchanged. The heat flux is computed by FLUENT and applied to the interior surface of the manifold by MSC.Marc. The temperature at this surface is computed by MSC.Marc and applied as the wall temperature of the fluid in FLUENT. In Figure 4, the final temperature distribution in the fluid, at the wall with the structure and in the structure is depicted.

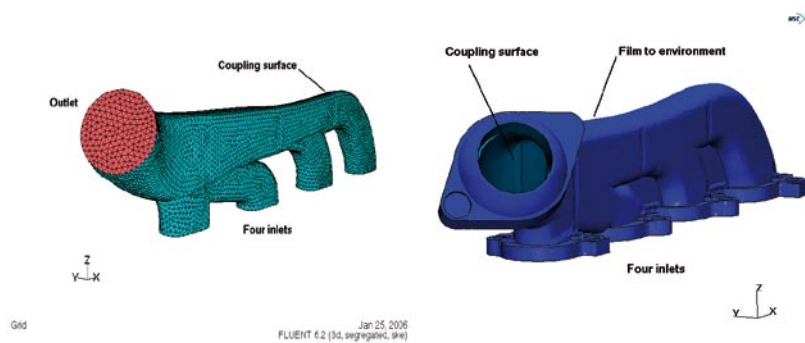


Figure 3: The FLUENT and MSC.Marc models of the steady state heat transfer analysis of an exhaust manifold.

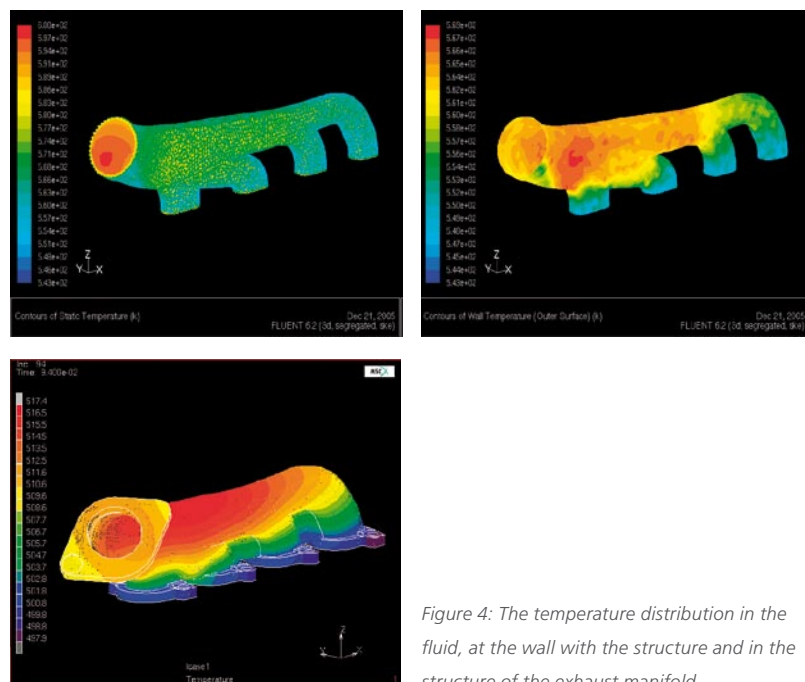


Figure 4: The temperature distribution in the fluid, at the wall with the structure and in the structure of the exhaust manifold.

Four-Cylinder Twin Catalyst Exhaust System (STAR-CD)

In the presentation, the results of an industry-strength example will be discussed. The analysis was performed with STAR-CD and the geometry, depicted in Figure 5, comes from pre-production analysis on a four-cylinder twin catalyst exhaust system.

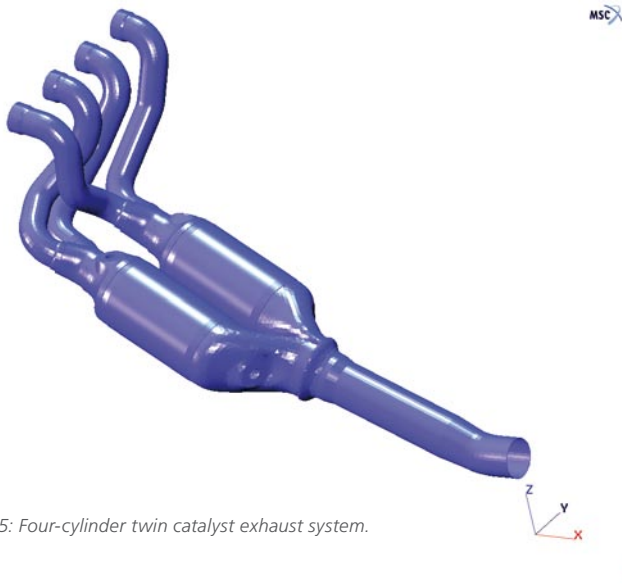


Figure 5: Four-cylinder twin catalyst exhaust system.

DEVELOPMENT

A next development item of the MSC.Marc code adapter is the support for the automatic remeshing capabilities of MSC.Marc (see Ref. [3]). Two types of adaptive meshing are available in MSC.Marc: local and global. The local adaptive meshing feature locally refines finite elements of the structural model during the analysis if a certain criterion has been satisfied. The criterion is usually defined in terms of the stress and/or strain components in the element. This feature is normally used to automatically refine the mesh at high stress or strain gradients, so that they can be described more accurately. The global remeshing feature involves automatic creation of an entirely new mesh for one or more parts of the structural model during the analysis. This is particularly useful in analyses involving large deformations, for example, with rubber-like materials or in forging processes. If, due to the large deformations, finite elements become severely distorted, an entirely new mesh can be created fully automatically. The solution variables are mapped to the new mesh and the analysis continues with the new mesh.

In both cases, the finite element mesh of the coupling region changes. This implies that MpCCI will have to re-compute the geometrical relationship between the CFD grid and the structural mesh. It also means that the utility routines in MSC.Marc that give access to the connectivity and coordinates of the coupling regions will have to return the new mesh after remeshing. The basic idea is illustrated in Figure 6. This is a variant of the elastic flap problem discussed in the preceding section. The local adaptive meshing feature is used to automatically refine the finite elements at the sharp corner. The newly created nodes at the surface are automatically positioned on a geometric surface that represents the true curvature of the corner. It can be seen from the graph, in which the blue curve represents the new solution and the red curve the old solution, that the global deformation of the flap, and consequently the fluid flow, is hardly affected by the local mesh refinement. However, the normal stress in x-direction is 30% higher in the refined mesh. This is because the high stress gradient caused by the bending of the flap cannot be described accurately with only one element through the thickness. The original solution therefore underestimates the stress. The advantage of the local adaptive meshing feature is apparent. The finite element mesh can be refined only in critical areas and accurate results can be obtained with a limited number of degrees of freedom.

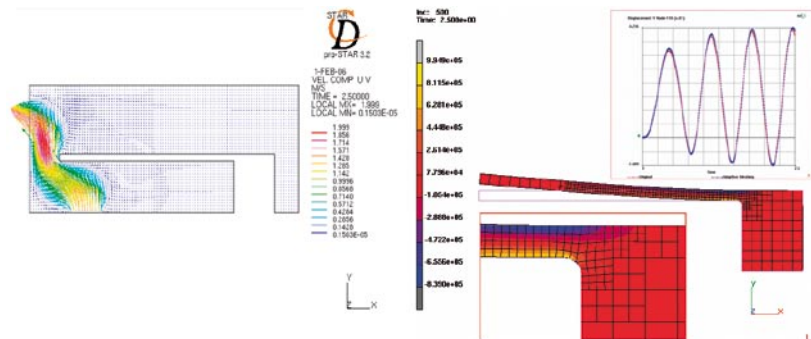


Figure 6: The final velocity field of the fluid and deformations of the elastic flap using local adaptive remeshing. The graph shows the slight increase of the vertical displacement of the left-most

TRADEMARKS

All products mentioned are the trademarks, service marks, or registered trademarks of their respective holders.

REFERENCES

- [1] Nafems, »A Software Collaboration to Predict Aquaplaning«, Benchmark, pp. 24-25, January 2006.
- [2] Dinescu, C., Hirsch, Ch., Leonard, B., Baran, O. U., Platschorre, A.-W., Alessio, R., Beluzzo, D., »Fluid-Structure Interaction Model for Hydroplaning Simulations«, Technical Paper 2006-01-1190, SAE World Congress, 2006.
- [3] MSC.Software Corporation, »MSC.Marc 2005, Volume A: Theory and User Information«, 2004.

1D AND 3D CO-SIMULATION BETWEEN FLOWMASTER AND CFD PACKAGES

Abdul Ludhi, Flowmaster Ltd.

SYNOPSIS

Flowmaster® is a 1D fluid system modelling tool. It enables engineers to simulate various fluid systems such as fuel systems for aircrafts, Vehicle Thermal Management Systems with Air-conditioning and Air-side for automotive industry, piping systems for ship building organisations, cooling systems for satellites etc. Flowmaster is equipped with libraries of components populated with loss data, allowing users to build and analyse a model of complete systems with compressible or incompressible fluid flows.

CFDLink is a 1D\3D boundary coupling software developed by Flowmaster Ltd. It enables engineers to perform co-simulation between a Flowmaster 1D network and 3D CFD models, such as FLUENT™ or STAR-CD.

Recently Flowmaster and MpCCI have started working together developing the next generation of the coupling capabilities between Flowmaster and 3D packages. This partnership between Flowmaster and MpCCI will enable Flowmaster users to couple with CFD, FEA, Radiation and various other packages giving our users a greater choice in integration modelling to meet their design objectives.

INTRODUCTION

In today's competitive engineering world, reducing overall design time and costs have become key factors to the future success and growth in many parts of the industries. 1D and 3D tools are leading the way to meet such engineering and business challenges. This process can be further strengthened or enhanced with utilising coupling methods between 1D and 3D tools, which can provide strengths from both approaches.

Interaction between CFD (such as FLUENT and STAR-CD) software and Flowmaster can enable design or system engineers to build virtual prototype test bed or models for small or large systems thereby reducing significant prototyping costs and design time. For example, in the automotive industry various parts of the Underwood vehicle thermal management system are simulated using CFD packages. Such models with complex geometry consist of many hundreds of thousands of cells and take considerable time to construct and validate. Modelling in isolation can compromise the accuracy of

the overall system performance. At the same time, at the earlier design stage it is impractical to represent a complete system in CFD that consists of water jacket, pump, expansion tank, valves, heat exchangers, grills, thermostat etc with individual physical characteristics. In such scenarios, 1D modelling can provide a significant advantage by both reducing model complexity and computational design time. This can allow the engineers to design and analyse system performance more rapidly.

By coupling 1D and 3D models together it can provide a more flexible and robust approach in fluid system design that can be utilised throughout the design cycle in numerous applications.

BACKGROUND

What is Co-simulation?

Co-simulation is a process that enables to share boundary data such as pressure, flow and temperature between one dimensional and three dimensional models in single or multi-domain systems. This means that engineers can simulate the interaction of fluid system with 3D effects on CFD.

CFDLink Setup:

There are two parts to the CFDlink installation.

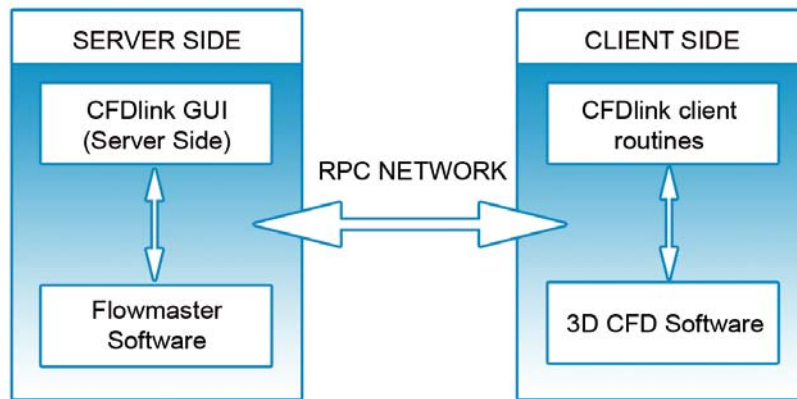


Figure 1: Data transfer & communication processes during a CFDlink co-simulation

CONTACT

Abdul Ludhi
Flowmaster Ltd
The Maltings, Pury Hill
Alderton Road, nr Alderton
Towcester,
England
NN12 7TB
Phone: +44 (0) 1327 306000
abdul.ludhi@com

1D/3D Co-simulation:

Advantages can be gained by using 1D and 3D co-simulation:

- Reduces the error in assumptions made
- Better simulation accuracy
- Accurately model flows in complex geometries, taking account of transient boundary conditions
- Reduced boundary condition set up times
- Allow component interactions to be taken into account
- Increased product knowledge and quality

FLOWMASTER AND FLUENT MODELS IN STANDALONE FORM

Flowmaster Marine Cooling System:

The model shown below in Figure 2 is a Marine cooling system network that consists of various Flowmaster standard components. Designing such models in Flowmaster enables engineers to analyse system performance at various scenarios. This includes pipe, pump and heat exchangers that can be sized and optimized by the engineers through simulation.

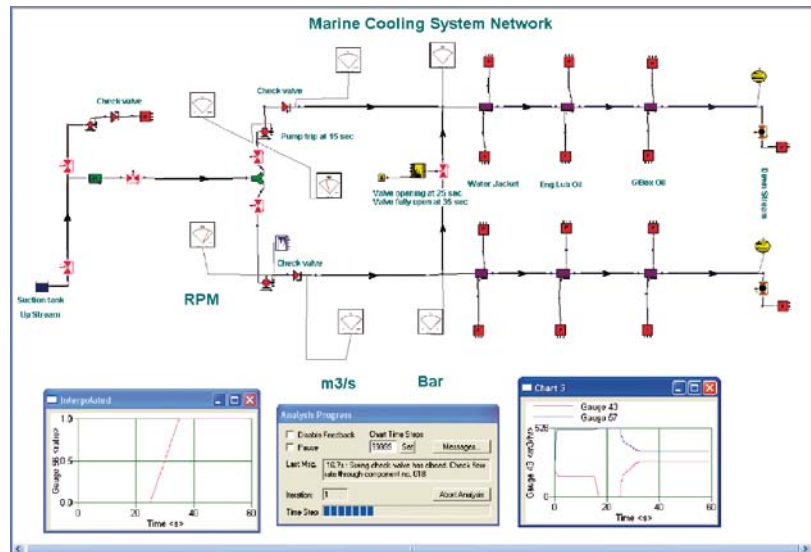


Figure 2: 1D Flowmaster model representation of a Marine cooling system

FLUENT Y-Junction Model:

The model below in Figure 3 is a 3D Y-junction modelled in FLUENT that can be used to perform detail flow behaviour.

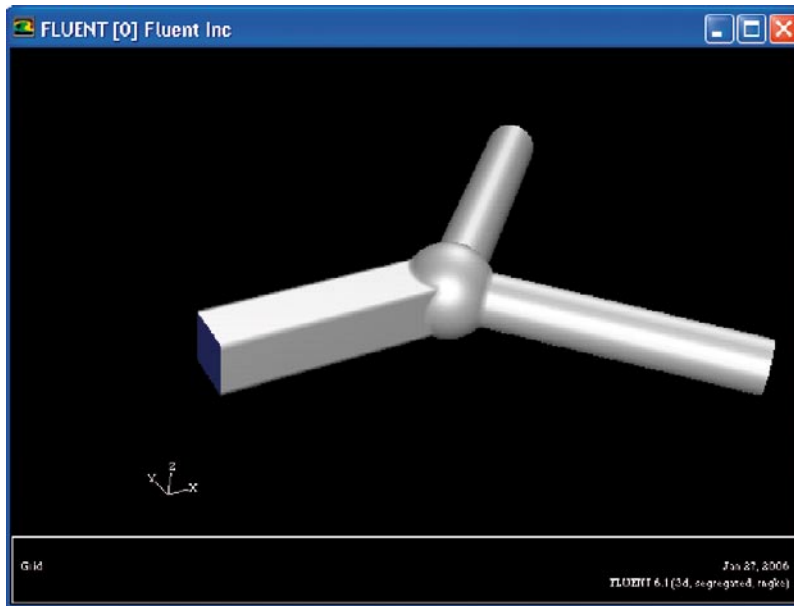


Figure 3: FLUENT Model

Co-Simulation Configuration Procedure

The steps below shows the setting up procedure for co-simulation between Flowmaster and FLUENT.

Step 1: Configuring the Flowmaster boundary connections with COM Controller and Gauge components (as shown in Figure 4, highlighted with blue boxes).

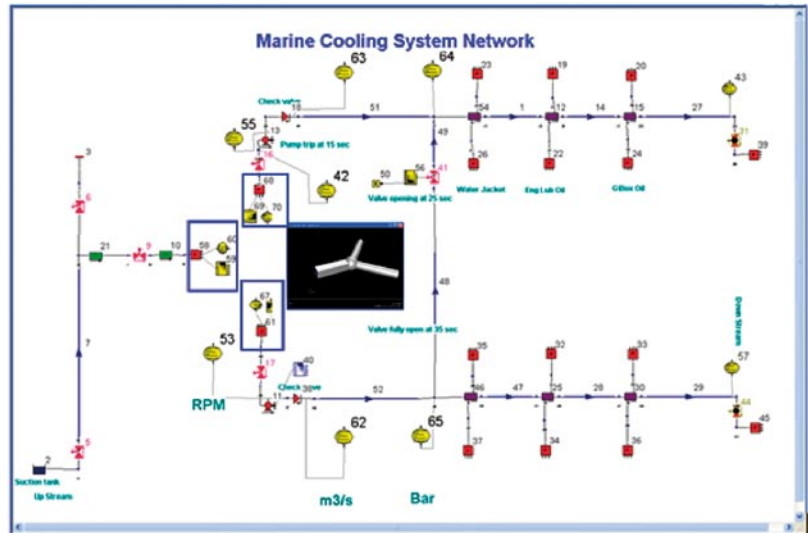


Figure 4: Marine Cooling system Network schematic

Step 2: Configuring in CFDLink GUI

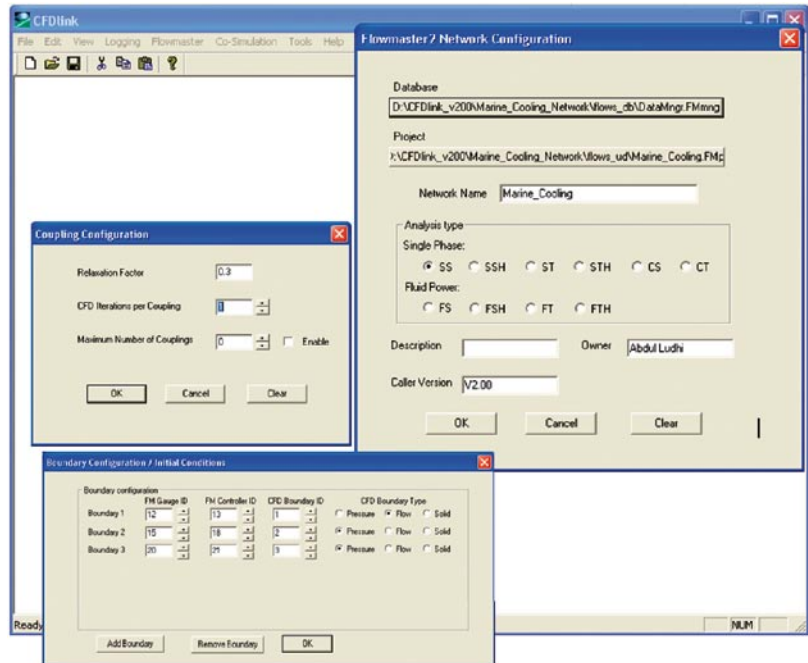


Figure 5: CFDLink Configuration

Step 3: Configuring FLUENT Model and co-simulation execution

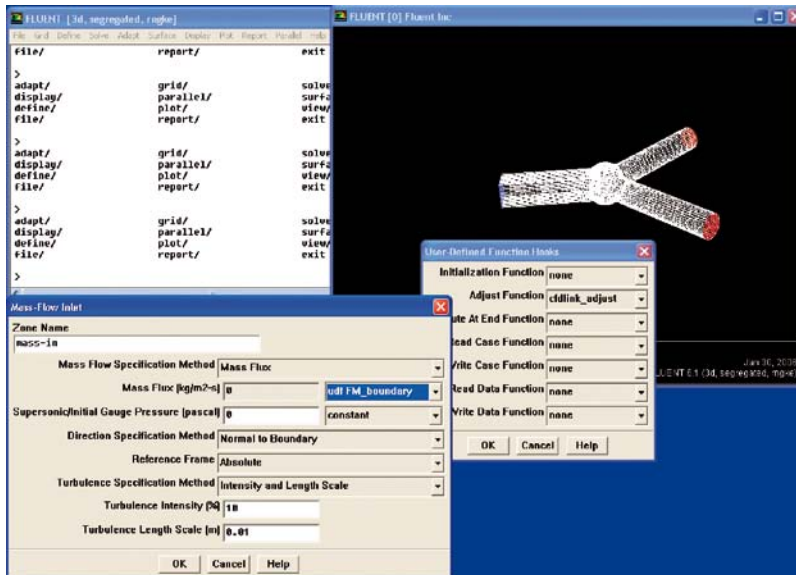


Figure 6: FLUENT model Configuration

The total process of co-simulation is summarised below:

1. Create and validate the CFD model
2. Create and validate 1D model
3. Start and configure the server with 1D and CFD model information
4. Include FLUENT client side routines in the CFD model
5. Run CFD model

FLUENT Co-Simulated Results:

Figure 7 and 8 shows pressure contour and velocity flow pattern plots of the Y-Junction.

Total Pressure Results:

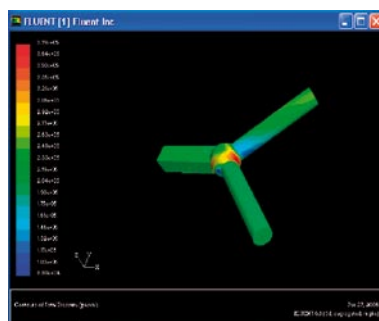


Figure 7: FLUENT Total Pressure results (Pa)

Velocity Magnitude Results:

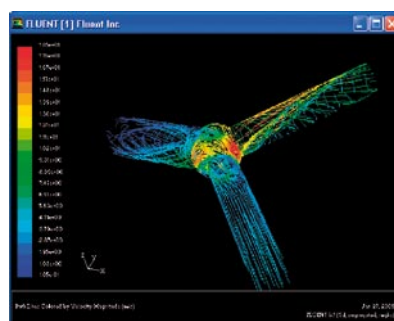


Figure 8: FLUENT velocity magnitude (m/s)

FLUENT Residual Plots:

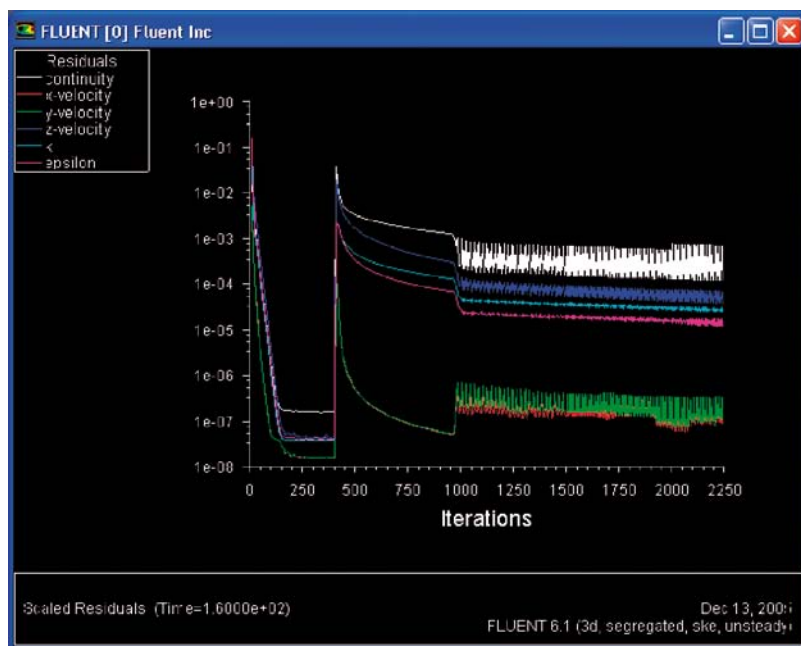


Figure 9: FLUENT residuals

CFDLink Co-Simulated Results:

The diagram below shows the CFDLink displayed boundary shared data between Flowmaster and FLUENT.

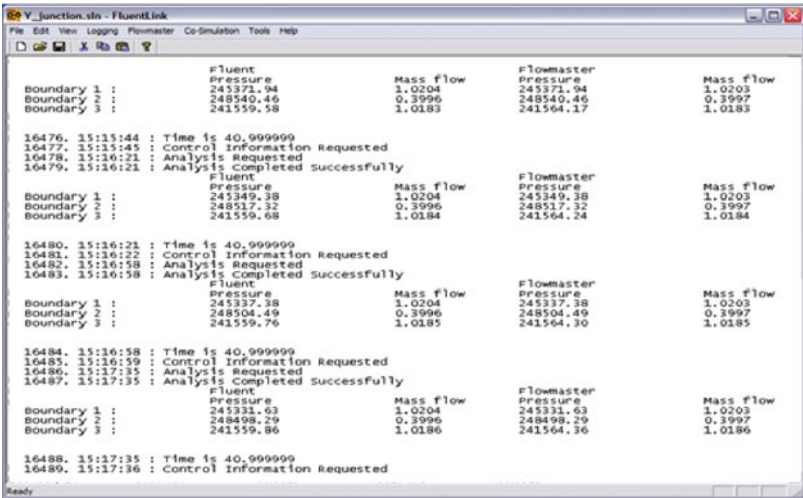


Figure 10: Co-simulated boundary results in the CFDLink GUI

FLOWMASTER RESULTS

The graph below shows transient result of the various Flowmaster components.

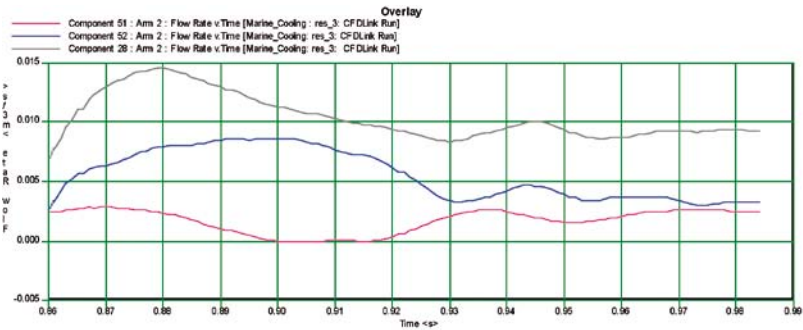


Figure 11: Incompressible transient results in Flowmaster

CONCLUSION

Using the CFDLink, co-simulation between 1D and 3D software can maintain the internal fluid flow details within a complicated 3D geometry whilst allowing the component to interact with 1D fluid network. The convergence of the co-simulation has been tested with various models including turbo-machinery. The ability to model heat transfer in a transient co-simulation offers the potential to model many phenomena relevant in various industries.

The future versions of the CFD or FEA Link will be carried out in partnership between Flowmaster and MpCCI. The diagram below shows how the interaction will be performed between Flowmaster – MpCCI – CFD/FEA/Rad-Therm etc.

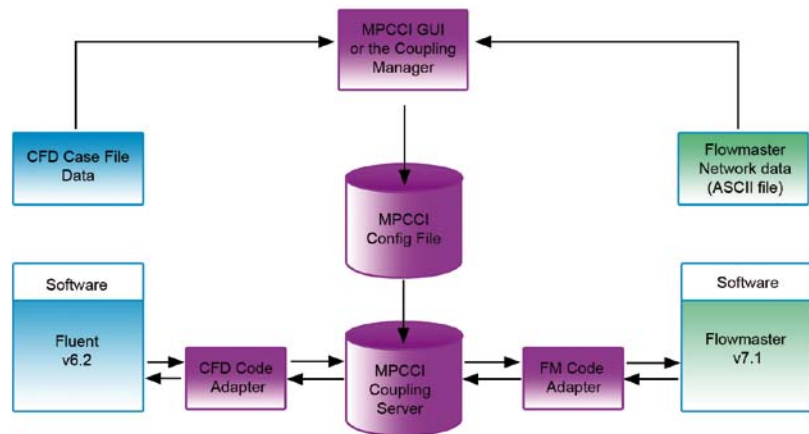


Figure 12: Schematic of CFD/FEA-MPCCI-Flowmaster Interaction

REFERENCES

- [1] Daniel J. Groce, Keith Austin, Flowmaster Ltd. 01VTMS-18 Coupling of one dimensional and three dimensional simulation models.
- [2] CFDLink User Guide – v2.0.0, Flowmaster Ltd.

MULTIDISCIPLINARY SIMULATION AND VISUALISATION WITH MPCCI AND ENSIGHT

Johannes Grawe, Graphics; Klaus Wolf, Fraunhofer Institute SCAI

Visualizing and interacting with engineering analysis results can provide valuable insights into a system's performance and aid in engineering decision-making. Currently, the majority of analysis codes are developed as isolated solutions focusing only on the most prominent physical influence to a system, such as thermal, structural, fluid, etc. Frequently, more than one of these physical influences combines forcing engineers to evaluate complex, coupled systems. The Mesh-based Parallel Code Coupling Interface (MpCCI) developed at Fraunhofer Institute for Algorithms and Scientific Computing SCAI allows for separate world class solvers to be externally coupled solving multi-physics problems.

The object of this publication is to demonstrate new methods for visualizing and interacting with these externally coupled results allowing a greater level of interpretation to support engineering decision-making. Commercial application cases will show the use of these new visualization and interaction techniques.

This new solution – MpCCI based simulation coupling and advanced visualisation by EnSight – allows the engineer to significantly interact with and visualize more complex problems, solved in preferred world class tools, in a timely and streamlined manner.

CODE COUPLING AND FSI VISUALISATION

MpCCI – The Standard for Simulation Code Coupling

MpCCI (Mesh-based parallel Code Coupling Interface) has been developed at the Fraunhofer Institute SCAI in order to provide an application independent interface for the coupling of different simulation codes. MpCCI is a software environment which enables the exchange of data between the meshes of two or more simulation codes in the coupling region.

MpCCI allows the exchange of nearly any kind of data between the coupled codes; e.g. energy and momentum sources, material properties, mesh definitions, or global quantities.

For debugging and basic visualisation purposes MpCCI provides its own visualisation tool. The main intention of this module is to allow the user to have a quick view on those data which are relevant for MpCCI itself: e.g. the definition of coupling surfaces and source and sink of quantity transfers. Acting as a coupling interface between fluid and structure implies that MpCCI does not have information about (all) the volume data of the codes themselves.

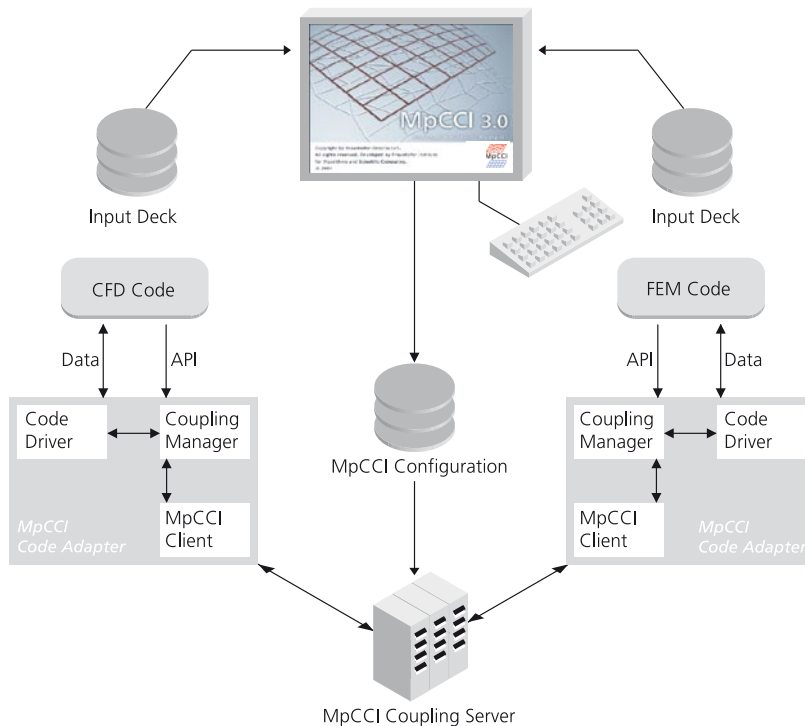


Figure 1: Module Architecture of MpCCI

Due to that limitation the input file for the MpCCI visualiser does not contain enough information for a combined CFD and FEM animation. The current way of tracing data for a FSI visualisation thus is to use the codes' own export routines to generate data sets which can be read in by a high-end tool like EnSight.

Advanced Visualisation with EnSight

EnSight has been developed by Computational Engineering International of Apex, North Carolina to provide advanced general purpose post-processing and visualization of results from different simulation codes. And since EnSight was designed as general purpose there is functionality already for FEA post-processing such as failed elements, displacements, mode shape animation and frequency response calculations as well as CFD post-processing features such as particle traces, isosurfaces, and boundary layer feature extraction. Interestingly both FEA and CFD codes have a growing need for particle-based simulations such as SPH for FEA simulating massive failures of structures and DEM for CFD simulating fluidized beds such as cereals, grains, and catalysts. EnSight also supports these particle-based results.

CONTACT

Johannes Grawe
 Genias Graphics Software GmbH,
 Regensburgerstr. 31
 93128 Regenstauf,
 Germany
 Phone: +49 (0) 9402/9480-0
johannes.grawe@genias-graphics.de

EnSight uses a client-server architecture in which the data is read from files by the `ensight.server` application. The server sends extracted visualization constructs like isosurfaces, streamlines, part boundary faces to the `ensight.client` application which is responsible for displaying the data and providing the user interface. Because the architecture allows up to 16 datasets (a current limit which could be extended) to be read simultaneously by 16 different `ensight.server` applications sending geometry to a single `ensight.client`, it is of no difficulty to display simultaneously 2 different datasets, even from different commercial solvers.

There is a file interface to every simulation code currently supported by the current version of MpCCI 3.0.5:

- ABAQUS 6.5 – .fil or .odb direct readers
- Ansys 7.1 to 9.0 – direct reader
- FLUENT 6.1.22 to 6.2.16 – export to EnSight Case Gold format or direct reader
- MSC.Marc 2005R3 – t 16 or t 19 files
- Permas 10 – direct reader
- StarCD 3.1.50 to 3.2.4 – export to EnSight Case Gold format
- RadTherm 7.1.1 – export to EnSight Case Gold format

Principles of coupled Simulation and Visualisation

In order to accomplish the goals of a user-friendly simulation and visualisation environment, a process has been developed to automate the transfer of MpCCI coupled results to EnSight and allow for 3D visualization of and interaction with the data.

Before visualization and interaction with externally coupled analysis data can take place, the coupled data must first be generated. MpCCI manages the communication between the coupled solvers, but the result consists of two independent files separate from one another and in their original file formats. For the shown here, FLUENT and ABAQUS will each be writing out separate result files, though the meshes and time domain between them will be synced through the MpCCI coupling engine.

The focus of this new approach is a new automated input file method or data structure for transferring two separate, though coupled, result files into EnSight. EnSight has a wide variety of analysis data readers available and can currently load up to 16 cases at a time.

ENSIGHT VISUALISATION SYSTEM

Easy Data Visualization and Post-processing

EnSight provides an easy CAD-like user interface for data visualization and post-processing. EnSight uses OpenGL graphics when run interactively and Mesa software rendering when run as a batch process. Modifying the visualization scene and requires no programming or even pseudo-programming skills to operate and produce images, animations, plots, or explorations of the data. Everything done in EnSight interactively is recorded in a journal file, called a »command file« for easy replay, modification, or building of macros. EnSight can export to standard image and animation or movie formats such as TIFF, JPG, AVI, MPEG, MPEG2. In addition CEI provides some unique formats to support additional features and cross platform compatibility. CEI EnVideo movie format (file extension .evo) is cross platform and provides high quality graphics using less memory than uncompressed AVI and supports stereo playback. EnVideo is also useful for displaying a movie on multi-tile displays such as a PowerWall or CAVE Virtual Reality display. CEI's EnLiten »scenario« geometry format (file extension .els) allows the saving of the EnSight 3D scene including all types of animation for playback and presentation. Both EnLiten and EnVideo are free to download and are used to share visualization work among colleagues, suppliers and customers, and with management.

File Format Support

EnSight supports a number of common data formats as well as interfaces to various simulation packages. There are three different methods to get your data into EnSight: a direct reader to the native format of the solver code, a standalone translator which converts the data to a format EnSight can read, and an exporter built into a solver or solver post-processor which exports the data into an EnSight-readable format. The most authoritative list of supported file formats is found on the CEI website at: <http://www.ensight.com/products/solvers.html> However, it is recommended to contact CEI if a format is not listed on the web page as interfaces are added more frequently than the web page can be updated. CEI can be contracted to develop or will contract others to develop additional interfaces for EnSight.

In many cases EnSight reads the native format of the solver code (FLUENT, ABAQUS, ANSYS, for example). This is known as a »direct reader«. For example CEI has developed a Direct FLUENT Reader that allows FLUENT data to be read into EnSight. And CEI has developed a Direct ABAQUS Reader that allows .fil or .odb datasets to be read into EnSight. In general reading the data in the EnSight native formats, which are public and well documented, is faster than reading the native file formats of the codes, but this is also

generally less convenient to the user. User-defined readers can be written by the solver code developers, CEI, EnSight users, or other 3rd parties. Some solver code companies write their own direct reader and provide this to CEI to bundle with EnSight. CEI supports and encourages this as the most direct and efficient way to help the customer visualize their data. A user-defined reader can be written in a day or two by anyone familiar with the format which is being read, so it is best developed and maintained by a member of the solver code development team or by someone who regularly uses the solver code and EnSight.

Loading Multiple Simulation Cases to Combine CFD and FEA

Once the data is in a format that EnSight can read then EnSight can be started using several different methods. EnSight 8 can be launched either by double-clicking on a result file from either solver, or by using File -> Open from the EnSight user interface, or by using File -> Data Reader from the EnSight user interface. This will load either the CFD data or the FEA data first into EnSight, whichever was chosen and this first dataset is known as case1. To load the other dataset in EnSight 8 simply choose File -> Open and select the 2nd dataset, EnSight will ask whether to keep the data from case1 or replace it with the new dataset. Select to keep the data, and a new case will be created, case2 and the 2nd dataset will be loaded into case2. EnSight provides a »Case« menu for managing which cases are visible and being manipulated.

Up to 16 cases are permitted. Thus, if one wanted to compare 8 different MpCCI-coupled solutions of a CFD solver and FEA solver it would be possible using a continuation of this process. However it is not necessary to load the cases in any particular order, so all 8 CFD datasets could be loaded first if desired and then the 8 corresponding FEA datasets. However it is reasonable to ask if this can be automated, and can additional cases be formatted in a consistent way as they are read in. Yes, everything in EnSight can be scripted and reused, and even run in batch rather than interactive if desired. To apply the same format to the 2nd and 3rd CFD dataset as used by the 1st the user should select the »apply context« toggle provided in during the data loading process. EnSight refers to its templating capability as »context« files, »saving context«, »applying context« and »restoring context«.

If loading more than one pair of coupled simulations it is recommended to consider using the EnSight »casemap« variable function in order to map the values from one run onto another coupled run to enable differencing which can dramatically display the effect of changes to the input file of the runs, much more effective then trying to view two models side by side.

»Context Files« Templates for Automatic Post-processing

Saving and restoring context files is designed to allow the automation of loading data, applying EnSight visualization techniques, and producing output images, movies, etc. for multiple runs of a simulation. Some customers run hundreds of simulations in batch and apply a standard context to these runs to post-process them in EnSight automatically in batch. And EnSight is compatible with Grid computing methods as it will attempt to obtain a license from the license server repeatedly in order to run a batch post-processing session until user-defined stopping points such as time of day, or number of attempts, or duration of attempts.

3D Model Control for Interactive Post-processing

With the data loaded it will be visible on the screen and can be manipulated in 3D space by the mouse and the display properties changed through various menus, typed commands, recorded macros, and other program controls. Some customers have added even voice, Palmpilot, body tracking devices or gesture control to manipulate and visualize their data in EnSight. But the most common way is through a 3 button mouse and menu selections. See the EnSight Getting Started Manual and the How-To Manual for an introduction into EnSight model manipulation.

Working with CFD and FEM Data in one FSI-View

EnSight provides flexible control over the page layout of the scene of displayed data including multiple resizeable and overlapping viewports, 3D and 2D viewports, with or without perspective, and with a variety of backgrounds, rendering styles, transparency and coloring available for each independent viewport. This permits the user to include CFD and FEM in a single viewport in the EnSight window as well as have other viewports in the window which show only the CFD model or only the FEA model or a mixture of parts of each. Viewports can have independent or linked 3D transformations allowing to view the model from multiple points of view simultaneously or look at multiple copies of the model interactively with the same 3D view. For advanced work users can animate transparency using EnSight's keyframe animator to fade the structural housing of a model to reveal beneath the flow path of the CFD model, for example. In addition to 3D data, EnSight can also query the dataset for transient plot data or query the dataset in 3D space along a line or path for spatial data and provide this information in another viewport of the window, or in EnSight version 8 in a detached plot window. The plot will animate over time or through space depending on the type of data query being performed.

Displaying Test Data as a Bitmap Background

In EnSight 8 it was also added that the user can attach a bitmap background to the EnSight window providing either context to the model such as terrain or scene, or to display test data against which the model will be compared, for example a crash simulation or the photographed footprint of a hydroplaning tire during a hydroplaning test.

EXAMPLE – THERMAL COUPLING IN A MANIFOLD

Application Setup

An important issue for numerical analysis in automotive industry is the provide solutions for the thermal management of cars. A fully coupled (two-way) temperature-stress analysis is used to simultaneously solve for both displacement and temperature fields for problems in which both the stress and temperature are dependent upon each other. The transfer of temperature fields and heat transfer coefficients in an engine exhaust manifold may illustrate the importance of thermal coupling in the transient heating due to the flow of the internal hot exhaust gas stream. The internal flow was modelled in FLUENT while the structural heating and extraction are calculated by ABAQUS. MpCCI provides the transfer of the wall heat flux from FLUENT to ABAQUS and passes back the resulting surface temperature from ABAQUS to FLUENT. ABAQUS further computes the thermal stress and deformation of the exhaust manifold due to heating.

Generating Multidisciplinary Visualisation

In this example we load the FLUENT results in case1 and then the ABAQUS results in case2. If these two cases were not prepared in a consistent position and orientation we would select one of the cases and switch to Frame Mode in order to reorient or position the models so they are in a consistent position.

The two models will be colored by default by part colors. The ABAQUS case2 results can then be colored by »temperature« variable, and the FLUENT case1 results can be colored by »temperature« variable as stored by FLUENT. The result will look like shown in the image below. The ranges of »temperature« and »temperature« variables will have to be adjusted in EnSight for consistency if the user desires. EnSight provides very flexible control over the color palette and each variable has its own customizable color palette.

It is easy to explore the model now. Changing the timestep is done through the time solution dialog and animating over time is easy through the flip-book animation dialog. The ABAQUS results can be displaced by using the

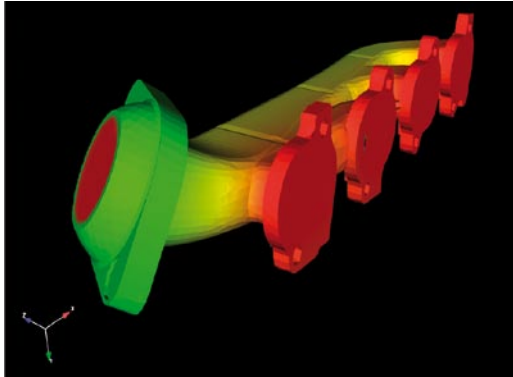


Figure 2: Visualisation of FEM results

Displacement dialog. Exaggerated displacements will probably be necessary in order to see them.

EnSight provides an Annotation Mode in order to add text and labels to the scene as show to the right. Annotations can be static text or based on data extracted from the dataset or from system commands such as the max value of a variable, the date of post-processing, or the file name and path to the data. Logos or images from other applications such as test data can also be inserted in Annotation mode to provide additional information. Items added in Annotation Mode will sit on top of the scene like a overlay.

Further changes to the scene can display internal flow. First we made the ABAQUS parts semi-transparent and gave them a thick feature angle border line to show its outline. Then we have created a clip plane through the FLUENT flow field and colored by a variable. Then we have colored the background by a gradient of beige for a more pleasing neutral background image.

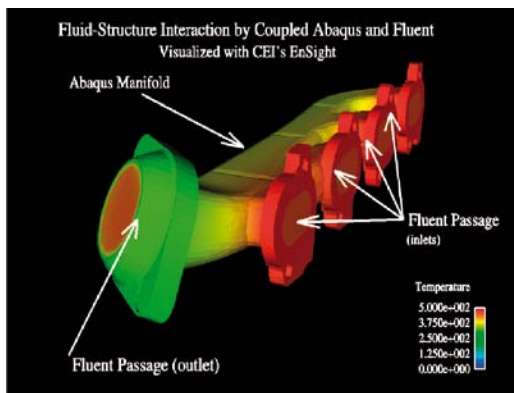


Figure 3: Annotation of result model

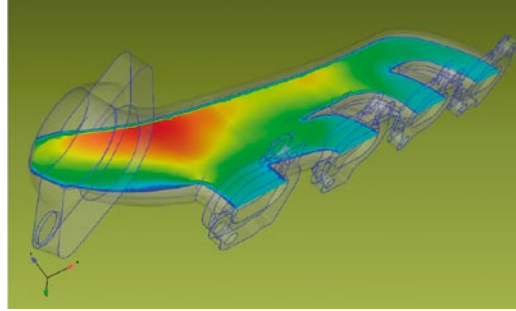


Figure 4: Visualisation of CFD results

CONCLUSION

Currently MpCCI has a powerful coupling engine but lacks a method for visualizing and interacting with the externally coupled analysis results in 3D. This new joint approach from CEI and Fraunhofer SCAI proposes to integrate MpCCI with EnSight and add needed functionality, allowing for the visualization of and interaction with the coupled data in 3D.

Yes, there remain additional requirements as users of MpCCI and EnSight are just in 2004 and 2005 beginning to explore these new programs and find limitations to the currently provided capabilities. For example, today results from different cases are displayed together but cannot easily exchange data during post-processing. And if the two programs use different names for the same variable there is not an easy way to map them together. Another development to consider is the reading of the MpCCI data into EnSight to combine with the case for CFD data and the case for the FEA data. So then 3 cases would be loaded and visualized in EnSight. Fraunhofer SCAI and CEI look forward to tackling these emerging requirements. It is certain that new levels of product performance, safety, and reliability will be reached by employing coupled simulations using best-of-breed simulation codes coupled by MpCCI and visualized with EnSight.

APPROACHES TO INDUSTRIAL FSI – AN OVERVIEW WITH CASE STUDIES

Fred Mendonça, CD-adapco

ABSTRACT

The purpose of this paper is to summarise the promising approaches to fluid-structures coupled interaction (FSI) that have evolved over now many years of practice. Several examples are shown, covering different sectors of industry including automotive, power generation, nuclear engineering, marine engineering and with applications ranging from tube-bundle vortex induced vibration (VIV), automotive exhaust system thermal stressing and tyre aqua/hydro-planing, to floating bodies. The most promising and most general of these is that offered by MpCCI; yet it is worth considering efficient alternatives towards which MpCCI may evolve later.

INTRODUCTION

Virtual Product Development (VPD) continues to place demands on CAE software and an ever-increasing emphasis on multi-disciplinary analysis such as fluid-structure interaction. FSI covers a wide range of applications. Simulation methodologies in FSI are similarly broad. We summarise some of the more promising ones as follows;

- Parallel execution of single-discipline software, such as CFD and FEA, communicating relevant information during execution (MpCCI). Capable of dealing with the full non-linearities in both fluid and structure systems, the coupling tends to be done explicitly, that is the structural response to the fluid and vice versa, is delayed by one time-step.
- Single execution of multi-discipline software, in which the finite-volume or finite-element methodology solves simultaneously both the fluid dynamics and solid mechanics [1,2]. Again, the full non-linearities in both fluid and structure systems are accounted for, and additionally caters for truly interacting systems including casting, melting and solidification, is fully implicitly coupled, but currently is limited to certain classes of problems which do not involve shell- or plate-like structures.
- Substructure matrix approach in which the mass, stiffness and damping matrices for the structure are exported to the fluids code and inverted through an API on the basis of the fluid loading. This methodology is limited to linear deformations.

- 6-DOF (six degrees of freedom) systems in which the deformations may or may not be rigid, whilst the structure is allowed to rotate and translate, e.g. floating bodies and store release. Such systems may be regarded as a subset of the first two listed above, but is here listed separately because of the uniqueness of applications.

Examples of each of the above are given in the following sections.

APPLICATIONS

MpCCI approach

This is clearly the most general FSI simulation methodology currently available. It permits established, consequently well-validated, single-discipline codes to be coupled together in multi-physics applications. Supporting routines for non-conformal mesh interpolation between fluid and structures meshes, and mesh morphing makes MpCCI open to very wide applicability.

In the next sub-sections, two examples are expounded. First, we add further details of the fluid and thermal coupling between STAR-CD and MSC.Marc through MpCCI for the pre-production automotive exhaust system presented elsewhere in this compendium [2]. Secondly, we illustrate the coupling of complex physics in a hydro-planing example for a treaded tyre using the two-phase volume-of-fluid (VOF) method including rubber deformation and tyre-road contact reduction due to the hydrodynamic forces. STAR-CD presently interfaces to all structures codes via MpCCI, including ABAQUS, ANSYS and PERMAS.

CONTACT

Fred Mendonça
CD-adapco, UK
200 Shepherds Bush Road,
Hammersmith
London, W6 7NL
United Kingdom
Phone: +44 (0)20 7471 6250
fred@uk.cd-adapco.com

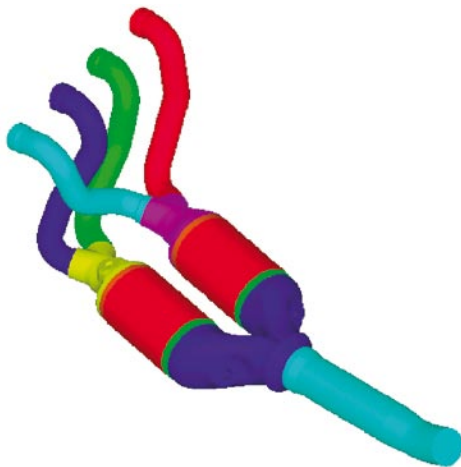


Figure 1: 4-runner, twin catalyst geometry

Thermal analysis in a 4-cylinder twin-catalyst exhaust system

Of primary concern here is that the metal is exposed to temperatures which are beyond linear elastic limits, therefore are susceptible to plastic deformation over many heat-up/cool-down cycles.

Four runners admit periodic flow at close to 1200K from the engine. We presume that the solid thermal response is too slow to see the dynamic variation of the flow and temperatures during the engine cycle, therefore the solid thermal response arises from »mean« flow and thermal field, which determines the fluid to solid heat transfer. Also presumed is that the structural deformation is too small to affect the flow field, in which case the fluid model is not deformed (though this is within the capabilities of the MpCCI-coupled system, as illustrated in [3]).

Therefore, the STAR-CD fluid flow model comprises a steady, mean-representative flow field, coupled to respond to the exhaust system metal skin and catalyst mat-insulation surface temperatures during warm-up.

The structural model comprises a 6mm insulating mat around the monolith and a 1.5 mm metal skin. The metal skin is modelled using linear triangular shell elements with 5 layers through the thickness; the insulating mat using linear hexahedral solid elements. Linear thermal and temperature dependent structural properties (Young's modulus, yield stress and thermal expansion) are assumed. MSC.Marc's automated contact algorithm is used to describe the contact between the insulating mat and the skin, with a constant heat transfer coefficient and mechanical glue conditions (permanent sticking) at the contact interface.



Figure 2: Arrows indicate fixed mounts. (Inset) exhaust metal skin and catalyst insulating mat

In the coupled transient heat transfer analysis with STAR-CD, the structure interacts with the CFD model at the interior surfaces of the insulating mat and the metal skin. The surface temperature is the wall temperature in the CFD analysis and the reaction heat flux (density) is applied at the interior surfaces of the structural model. The convection to the environment is taken into account by a film boundary condition at the exterior surfaces of the metal skin. Fixed time stepping is used in both solvers with 450 time steps of 2 seconds each.

The temperature histories calculated in the transient heat transfer analysis are prescribed at all nodes of the structure in a subsequent thermal stress analysis to determine the thermal expansion of the structure. In this quasi-static stress analysis, the displacements of all nodes at the inlets and at four locations on both sides of the catalysts are suppressed in all three directions (see Figure 2). In addition, gravity loading is applied to all elements.

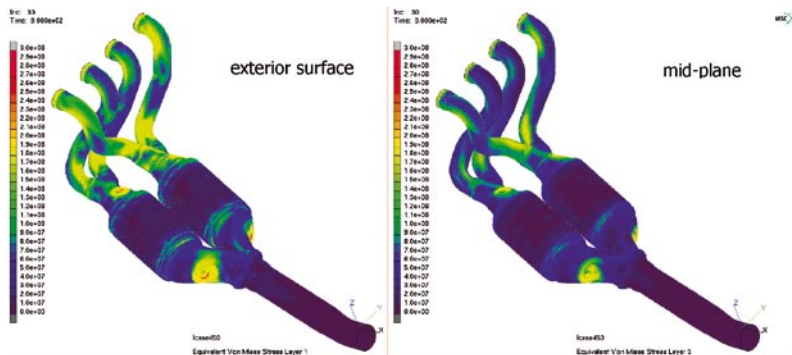


Figure 3: von Mises Stresses, exterior surface (left) and mid-plane (right)

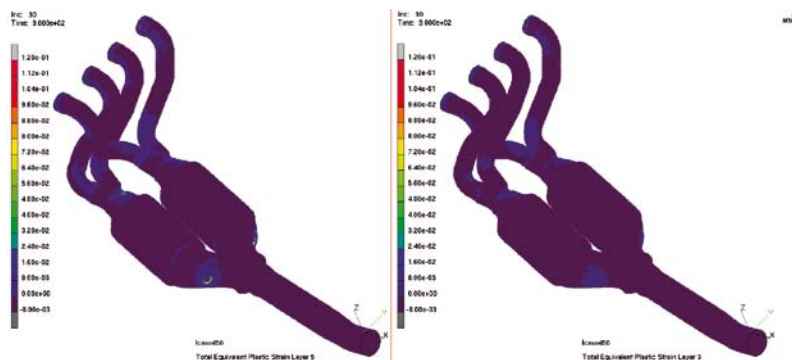


Figure 4: Plastic strain, exterior surface (left) and mid-plane (right)

The temperature histories are applied in 30 increments, each covering 30 s of the transient analysis. The final Von Mises stress distribution in the metal skin is depicted in Figure 3. Note that particularly in the runners, the stresses at the exterior surface are larger than at the mid-plane (i.e., at the centre layer of the shell elements), which points to bending of the runners. Figure 4 shows the final equivalent plastic strain distribution in the metal skin. The largest plastic deformations are found at the exterior surface near the four support points on both sides of the catalysts. The amount of plastic deformation at these locations is probably overestimated due to too rigid support conditions.



Figure 5: Instantaneous VOF shortly after striking the surface water sheet (left) and after the flow conditions become pseudo-steady (right) – the wheel is travelling left to right, rotating clockwise.

Hydro-planing and tyre deformation using the volume-of-fluid (VOF) method

Tyre contact with the road in the presence of surface water affects the traction and therefore dynamic stability of the vehicle. The major challenge to the modelling of hydro- or aqua-planing is to combine the non-trivial handling of the complicated treaded tyre geometry (simple longitudinal as well as complex grooves) with deformation caused by the forces induced in a two-phase water/air system whilst the tyre is rolling. This is achieved by STAR-CD's dynamic mesh motion and sliding capability together with an efficient transient solution methodology, in which the net fluid dynamic forces are calculated, then communicated to the purpose-built rubber deformation code of the tyre manufacturer, which in turn returns the information necessary to deform the fluid mesh.

Figure 5 shows a grooved tyre in instantaneous snap-shots against the liquid free-surface sheet disturbed by the rolling motion of the tyre. The front face

creates a pressurisation against the cusped contact between the rubber and road surfaces, and the build up of water there forces a deformation of the tyre which leads to a reduction in the area of the road-rubber contact patch. The reduction in contact patch area is shown in Figure 6 together with a characterisation of the final deformation of the tyre based on a vehicle speed of 55 mph and a water sheet 0.6 inches, indicating a 40% reduction of the contact surface area due to the water sheet.

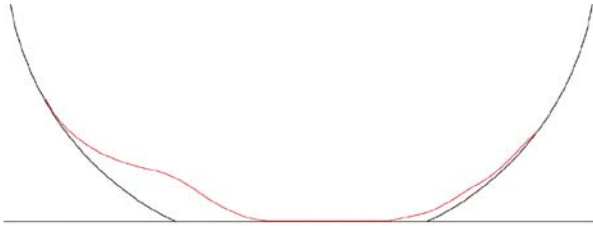


Figure 6: Final deformation ($\times 10$) relative to circular profile. The wheel is rotating counter-clockwise.

Finite Volume combined fluid and structural approach

Computational Continuum Mechanics (CCM) is the term coined for a combined approach to multi-physics such as fluid and structural mechanics. As described in [2] the conservation equations apply to both and may be solved using a finite volume methodology whereas the constitutive relations and material properties differ between the two systems. CCM for FSI, enabled in STAR-CD version 4, offers some advantages compared to traditional FE methodologies, and is applicable to a wider range of applications including casting, solidification, melting and floating bodies, but becomes potentially unstable for structural analysis of thin structures (plates/shells).

In the next sub-sections, we briefly describe two types of examples; a ship rudder inclined to the flow; and secondly, floating body motion in a liquid/air free-surface multi-fluid 6DOF system.

Rudder in cross flow

This is a common application in marine engineering, in which the manoeuvring effectiveness of the rudder in the wake of the ship's hull and vicinity of the propeller(s) is simulated. In this example, a rudder comprising a symmetrical NACA cross-section is inclined at 20° to the flow and rigidly fixed at the top via a shaft. Figure 7 illustrates fluid velocities and pressures exerted on the rudder, showing the pressurisation on the inclined face and suction on the opposing face which result in a tip vortex which trails the rudder due to induced flow from the pressure to the suction surfaces.

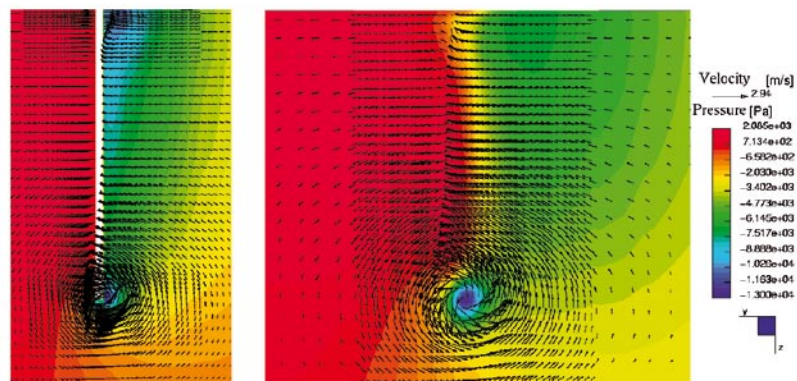


Figure 7: Fluid pressure contours and flow cross-sections through (left) and behind (right) the rudder

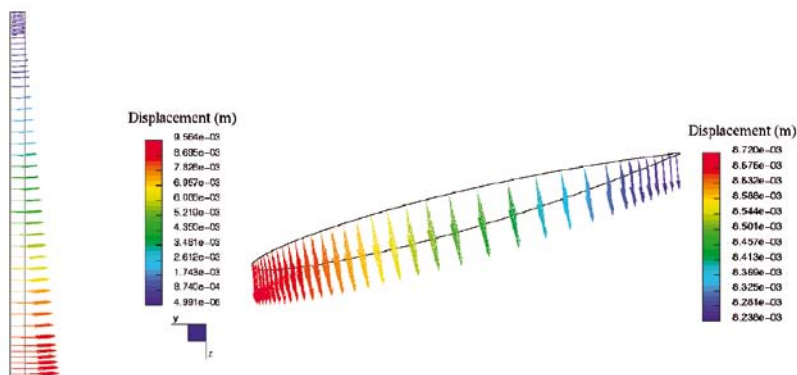


Figure 8: Displacement in the longitudinal (left) and lateral (right) directions through the rudder

Figure 8 depicts the fluid-induced displacements, whilst figure 9 illustrates the stresses in the rudder.

Cylinders falling into water

Slamming of ship structures in rough sea-weather conditions imposes severe structural loading on the hull. Two representative simulations are described here, in which a hollow cylinder and a solid inclined wedge are dropped from a height onto a water free surface. Motion due to gravity together with the flow, associated wall deformations and/or 6DOF motion due to the fluid forces are computed.

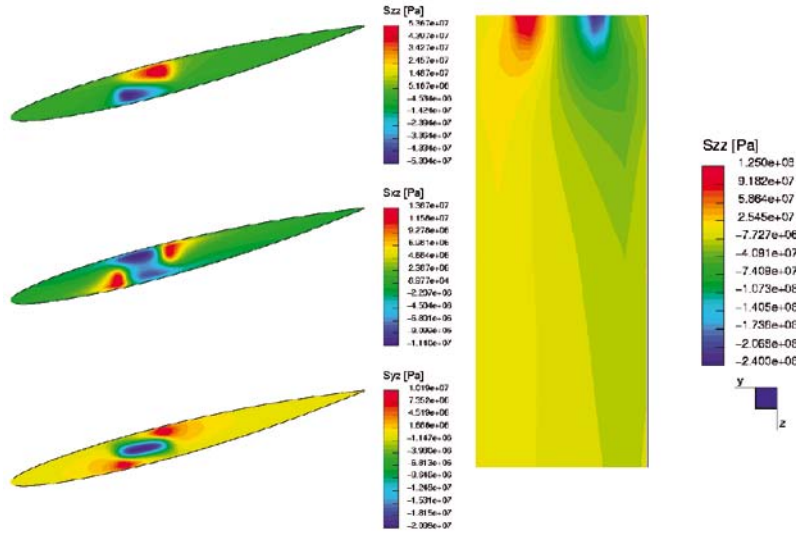


Figure 9: Stresses in lateral (left) and longitudinal (right) rudder cross-sections

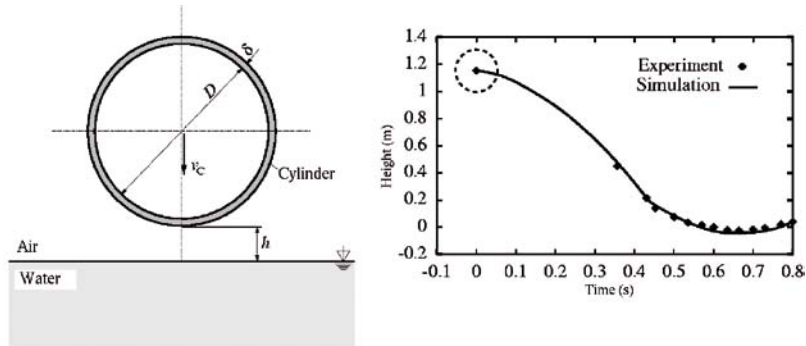


Figure 10: Schematic (left) and vertical free-body motion compared with measurement (right)

Figure 10 (right) shows for the hollow cylinder drop test the free-body simulated vertical motion compared with a drop test. Figure 11 shows that the cylinder wall displacement increases even though the peak impact pressure decreases.

Next, full 6DOF motion is illustrated in the form of a wedge drop-test – here the linear and angular acceleration, together with the heel angle and impact velocity, are compared with experiment [4].

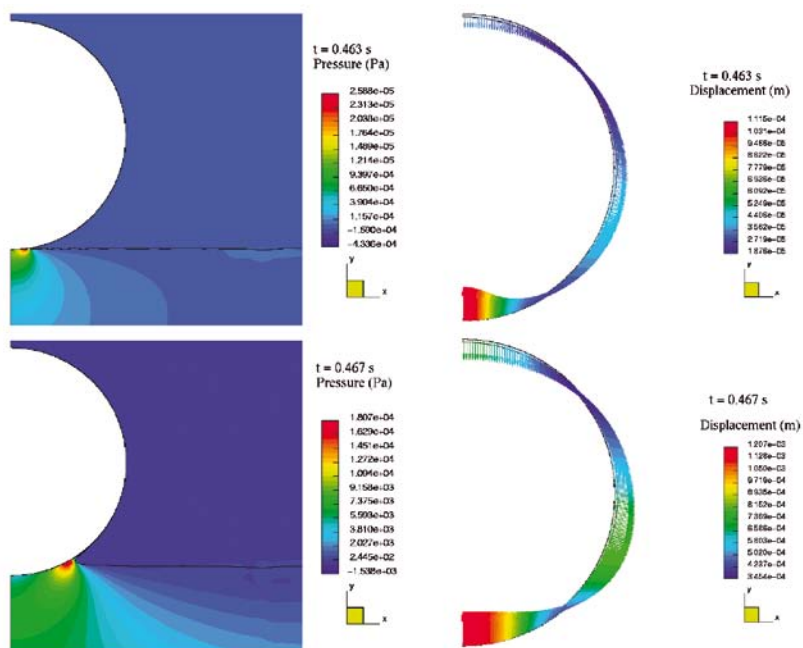


Figure 11: Fluid pressurisation and cylinder hollow-wall displacement prediction at and shortly after free-surface impact.

Figure 12 shows the water free-surface disturbance shortly after the wedge impacts the water. In Figure 13, the simulated linear and angular acceleration are compared with measurements.

Substructure matrix approach



Figure 12: 140o wedge free-fall test – 5o inclination (from Azcueta [4])

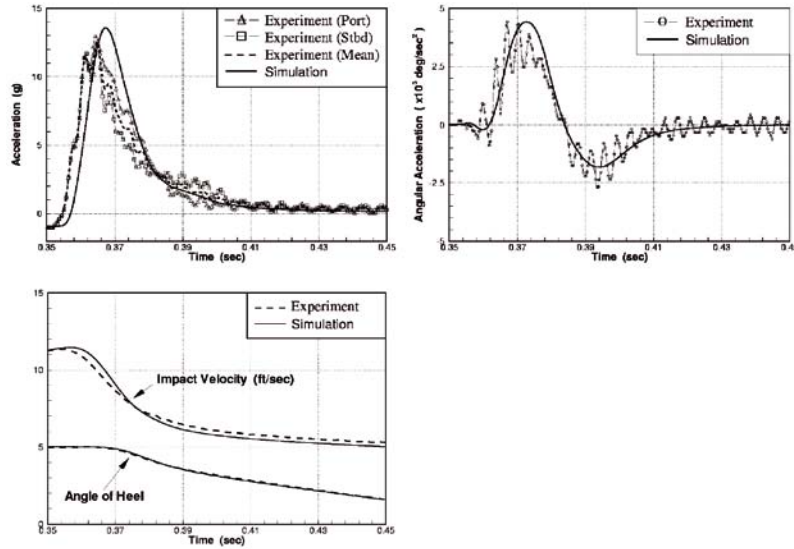


Figure 13: 140o wedge free-fall 5o inclination test – linear (top, left) and angular (right) acceleration; heel angle and impact velocity (bottom) (from Azcueta [4])

This is a unique approach in which any well-established structures code may be used to generate the mass, stiffness and damping matrices, then exported to files. CD-adapco offers an expert system, es-fsi, which reads in the matrix file and solves the dynamics equations for the structural displacements within the CFD solutions system. Substructuring is used to condense out many degrees of freedom with respect to the fluid mesh. The fluid forces computed by STAR-CD are interpolated onto the substructure nodes and the matrix inverted in a special-purpose API to compute the displacements using the Newmark method at each time-step. Though the coupling method is explicit, it benefits by eliminating all communication overheads.

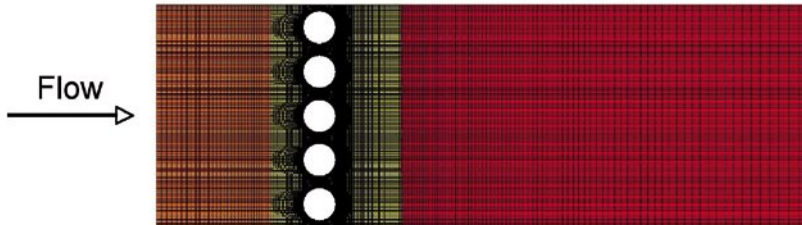


Figure 14: Linear tube array in cross-flow

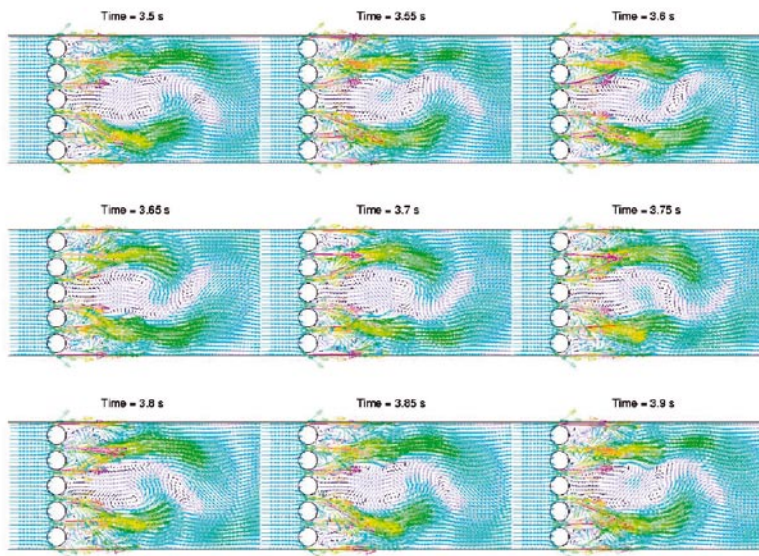


Figure 15: Flow patterns showing wake flow through one complete oscillation cycle

The method is exemplified here by analysing the vortex-induced vibration (VIV) in a tube array in cross-flow such as experienced in heat-exchanger applications in the power generation, process and nuclear industries. In this particular case illustrated in Figure 14, the flow past each tube in the array creates a vortex shedding pattern, which induces a perturbation on it and

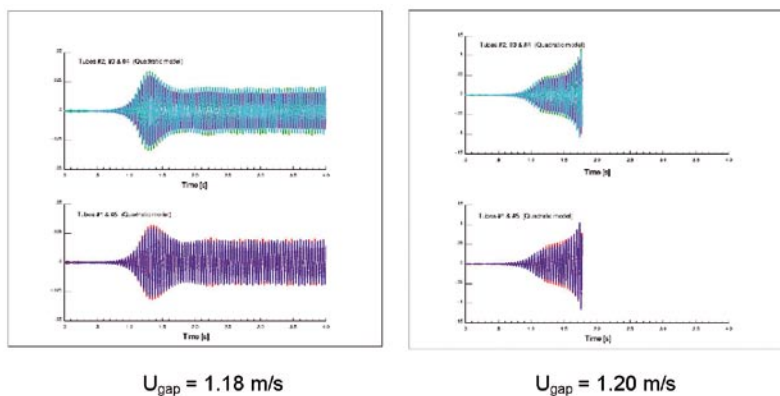


Figure 16: Stable oscillations (left) and unstable (right) oscillations beyond critical velocity.

the neighbouring tube, as shown in Figure 15.

The perturbations result in oscillations, growing to a limiting and self-sustaining amplitude. The limiting amplitude of oscillation increases with the oncoming flow velocity. At some critical flow velocity, in this case 1.2 m/s, the amplitude exceeds the separation between tubes, causing them to collide, Figure 16.

SUMMARY

Several years of serious FSI applications have led to a number of complimentary approaches for simulation of the coupled fluid and structures systems. We have summarised four methodologies in this paper. The most generally applicable is that offered through MpCCI, whilst efficiencies may be achievable through complimentary simulation strategies or future developments in MpCCI.

ACKNOWLEDGEMENTS

Thanks go to the following for contributing the material presented; Dr. Pieter Vosbeek, MSC, Netherlands; Prof. Ismet. Demerdzic, Dr. Samir Muzaferija, Prof. Milovan Peric, Dr Alan Mueller, and several others in the CD-adapco team.

REFERENCES

- [1] Demerdzic I., Muzaferija S. and Peric M., »Benchmark solutions of some structural analysis problems using finite-volume method and multgrid acceleration«, Int. J. Num. Meth. Eng. 40, p.1893-1908, 1997
- [2] Demerdzic I., Muzaferija S., »Numerical method for coupled fluid flow, heat transfer and stress analysis using unstructured moving meshes with cells of arbitrary topology«, Comp. Meth. Appl. Mech Engrg., Vol 125, pp. 235-255, 1995
- [3] Vosbeek P., »Fluid-Structure Interaction Simulations with MSC.Marc and STAR-CD«, 7th MpCCI User Forum, Feb 2006

SIMULATION OF BLAST-STRUCTURE-INTERACTION WITH COUPLED EXPLICIT HYDRO-CODES

Arno Klomfass, Fraunhofer Ernst-Mach-Institut, Freiburg, Germany

ABSTRACT

The paper addresses conceptual and numerical aspects regarding the coupled simulation of blast-structure interaction. As examples of coupled explicit codes we discuss our inhouse developed codes APOLLO (CFD) and SOPHIA (CSD), which are equipped with MpCCI software interfaces. A number of selected studies will be presented, where the coupled codes have been applied and validated against test data. These studies include a basic shock tube experiment, tests conducted with a container-like structure in the Large Blast Simulator LBS 501, and model scale experiments of underwater shock propagation in ducts.

INTRODUCTION

The interaction of a blast wave with an object consists of the initial refraction of the wave front and the subsequent transient flow about the object. The stresses exerted on the object during these phases lead to a structural response, which in general consists of

- induced stress waves and vibrations,
- structural deformation and potentially failure (elastic-plastic response),
- transferred momentum and displacement (rigid body motion).

The terminology interaction refers to an inter-dependency of loading and response. Such can exist in both phases of the process: the refraction and transmission of the incident wave front is affected by the impedance ratio between ambient medium and loaded object, the transient flow phase can be affected by changes in shape or displacement of the object. Estimates concerning the significance of the interaction can thus be based upon impedance ratios of the involved materials and ratios of time scales (duration of the blast wave vs. characteristic time of structural deformation). The relevance of the different modes of response clearly depend on the type of object, the ambient medium and the strength and duration of the incident wave: glass windows might scatter due to blast loads from bomb explosions, a heavy military vehicle might topple over in a nuclear blast wave, equipment within a hardened shelter might be damaged due to severe vibration. The numerical methods used for the analysis of blast-structure interaction should therefore be capable of the prediction of any such response modes and damaging mechanisms.

Traditionally, the numerical analysis of blast loaded structures has been performed in a sequential approach, where first the blast loads on the idealized rigid structure was calculated as a pure fluid dynamic problem. The response of the real structure to the idealized loads was then calculated as a pure structural dynamics problem in a second step. The application of coupled numerical methods, as those addressed here offers two advantages over the traditional approach. First, the inter-dependency of loading and response is accounted for. Second, a precise application of the blast load to the structure even for load distributions which are strongly non-uniform in space and time is ensured. Coupled methods are thus useful also for cases without significant interaction. An adequate strategy to enable a coupled simulation is the usage of readily available CFD (fluid dynamics) and CSD (structural dynamics) codes. Equipped with suitable communication interfaces, the codes can be run in parallel to obtain coupled solutions of the fluid-dynamic and the structural dynamic equations.

PHYSICAL MODELS AND SIMULATION CODES

CFD Code APOLLO

The fluid dynamic aspects of blast-structure interaction are adequately described by the conservation equations for the time dependent flow of a compressible fluid in three space dimensions. For typical scenarios the effects of viscosity and heat conduction can be neglected. The favourable numerical solution is thus an explicit time integration of the equations. In order to adapt the computational grid to moving and deforming objects the equations are formulated for arbitrarily moving and deforming control volumes. This so-called ALE-formulation (Arbitrary Lagrangian Eulerian) in integral form is the basis of our APOLLO flow solver. These equations are closed by an equation of state $p=p(\rho, e)$. The numerical method implemented in APOLLO is a spatially three dimensional finite-volume scheme with explicit time integration, which works with cell-centered conservative variables on block structured, body-fitted hexaeder grids. In order to treat strongly non-linear equations of state (e.g. 2-phase water) in an accurate and robust manner APOLLO uses a two-step scheme, which consists of a Lagrangian update and a subsequent remap step. An acoustic HLL-type Riemann solver is applied in the first step for the calculation of the conditions at the material interface. The subsequent remapping from the Lagrangian updated cells onto the actual grid cells is achieved with a donor cell method. Both steps are performed with a higher order of accuracy by employing a MUSCL-type extrapolation of the conservative cell-averaged quantities. For the treatment of multiple fluids within one computational domain APOLLO uses a VoF-Method (Volume of Fluid) in a conservative formulation.

CONTACT

Arno Klomfass
 Fraunhofer-Institut für Kurzzeiddynamik,
 Ernst-Mach-Institut EMI
 Eckerstr. 4
 79104 Freiburg
 Phone: +49 (0) 7 61/27 14-313
arno.klomfass@emi.fraunhofer.de

CSD Code SOPHIA

The continuum mechanical conservation equations are also used for the simulation of highly transient solid dynamics and structural dynamics processes. For numerical solution the equations are in this case formulated in Lagrangian description with primitive variables. These equations are closed with material models in the form where σ and ϵ are the stress and the strain tensor, $\dot{\epsilon}$ is the strain rate tensor and the temperature T is in general a function of both, ϵ and $\dot{\epsilon}$. A variety of formulations can be derived from the conservation equations, as e.g. simplifications for thin structures, which form the basis of FE-shell elements. As in the fluid dynamic equations, heat conduction is neglected, as it is typically of minor importance in highly transient processes.

The multi purpose CSD solver SOPHIA solves these equations by means of a finite element method with lumped mass matrix and explicit time integration. The code uses standard underintegrated 8-node solid elements with viscous hourglass stabilization and 4-node underintegrated shell elements. Artificial viscosity terms are included for the treatment of strong shock waves. A penalty-type contact-algorithm is implemented for the treatment of contact interaction problems.

Coupling Conditions

That part of the structural surface, which is in contact with the ambient fluid forms an internal boundary of the coupled systems of equations. The conditions that apply on this contact surface demand the continuity of the material velocity v , the surface stress (traction) $t = \sigma n$, the temperature T and heat flux q_n across the surface. For a non heat-conducting fluid the latter two conditions are dropped. Furthermore, for an inviscid fluid the conditions imposed on the traction and the velocity apply for the normal components only.

COUPLED SIMULATION

Concepts

There are three prominent concepts for fluid-structure coupled simulations. These are frequently called the ALE-, Chimera- and GLE-coupling method. The first uses CFD grids that are fitted and attached to the structure and adapt to the structural motion by suitable deformation. The coupling surfaces coincide in this case always with boundaries of the CFD grid. This approach provides both high accuracy and efficiency. However, it is obviously limited to moderate structural deformations and small displacements. There are two subclasses: the CFD grid might either stick to the structure's surface or slide along it.

The Chimera-coupling makes use of overset CFD grids. Here we typically use stationary (Eulerian-) background grids together with overset grids, which form a narrow band around the object. The overset grids are treated according to the ALE-coupling method, i.e. they deform and follow the motion of the object's surface. This approach allows for large displacements and offers additional flexibility with respect to grid generation. However, the required interpolation processes between background and overset grids slightly degrade the accuracy and demand additional computational effort.

Neither the ALE- nor the Chimera-coupling are applicable in cases which exhibit topological changes. Two initially separate bodies that come into contact can serve as an example: the CFD grid originally filling the space between the bodies must recede completely at the point of contact. For such cases the GLE-coupling (General Lagrangian-Eulerian) offers a suitable method. Here, the CFD-grid is not a body fitted but typically a stationary cartesian grid, into which the structure is embedded through blanked-out and cut grid cells. The GLE method offers the widest capability with respect to structural motions and also the least effort with respect to grid generation. However, a numerical treatment of cut cells with higher than first order accuracy is in general hardly possible. Also, the location of a moving structural surface within the CFD-grid must be re-identified frequently, which demands extra computations.

In order to enable efficient computations, the overset grid method in APOLLO is restricted on cartesian background grids only. Also will the GLE coupling, which is presently under development, be restricted to cartesian CFD grids.

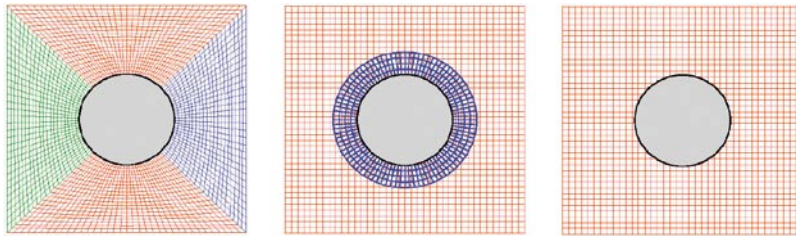


Figure 1: Schematics illustrating ALE-, Chimera- and GLE-coupling between a CFD grid and a cylindrical structure.

CFD-Grid Motion

A major task for the CFD solver in ALE- or Chimera-coupled simulations is the calculation of the grid motion. Given the grid velocity at the coupling surfaces, the node velocities in the interior of the grid must be determined such, that the grid maintains proper cell shapes and size distributions. This can be achieved by the solution of three additional boundary value (diffusion-) problems for the components of a velocity field, which govern the node velocities. Different types of boundary conditions can be used, which enable the simulation of either fully prescribed boundary motion, sliding boundary motion or rigid body motion.

The sliding motion is typically used on non-coupled walls, where the nodes have to move along the wall in order to allow a grid stretching imposed on a coupled moving boundary. The rigid body type is mostly used at free surfaces of overset grids, if large displacements must be handled. The diffusion equations are numerically solved in APOLLO with a standard central differences and explicit time stepping scheme, which works with a time stepping independent of the fluid flow.

Time Integration Scheme

Both codes, CFD and CSD, are in general integrated with identical time steps. Within each step, the fluid pressure on the coupling surfaces is once supplied to the CSD code and the structural velocity is once supplied to the CFD code. The CFD code then applies a velocity boundary condition on its coupling surfaces, while the CSD code enforces a stress boundary condition to its side.

In cases, where the time steps in both codes differ significantly, the code with the smaller time step can be operated in a subcycling mode, i.e. it carries out a number of successive time steps which are tailored to an equal sized, single time step of the other code. During the subcycles no communications between the codes take place. The quantity imported by the subcycling code at the beginning of the subcycling is kept constant during the subcycles, while the quantity exported at the end of the subcycles is averaged over the subcycles. In typical simulations the CSD code carries out 5-10 time steps during one CFD time step. The velocity of the coupling surface is time-averaged over these time steps and supplied to the CFD code after each sequence of subcycling. The high frequency part of the structural motion is thus not seen in CFD solution in this case. Neither can the presence of the fluid affect the high frequency motion of the structure in this case.

Software Implementation

Technically, the code coupling requires two capabilities: i) the exchange of data between the two codes, and ii) the interpolation of grid based discrete fields (pressure, velocities) between the CSD- and the CFD-grids on the common coupling surfaces. Those aspects are in our applications handled with the MpCCI software (Meshbased parallel Code Coupling Interface) which enables the inter-process communication and data exchange between simultaneous multi-processor applications. It also provides the required data interpolation between the CSD and the CFD grids for a variety of grid types. MpCCI is based on the MPI standard and is thus well compatible with codes that are parallelized with MPI. In order to control the correctness of the coupling, especially on significantly mismatching grids, the global quantities total area, total force, and total power on both sides of the coupling surfaces are calculated, controlled and corrected if necessary.

EXAMPLE APPLICATIONS

Interaction of a Shock Wave with a thin Aluminium Sheet

In 2001 a series of shock tube experiments was performed with the aim to provide high quality test data for the validation of fluid-structure coupled simulation methods. The following pictures were obtained with a 24 spark camera and show the deformation of a 1mm thin aluminium sheet of height 4.75 cm and width 3.9 cm, which was fixed in the 20 cm x 9.4 cm large test section of the shock tube. The sheet was loaded with a shock wave of shock Mach number $M_0 = 1.48$ (overpressure = 1.37 bar) in air. The pseudo Schlieren pictures below the experimental results were obtained from quasi 2D simulations (one grid cell over the width of the shock tube) with ALE-coupled codes APOLLO and SOPHIA.

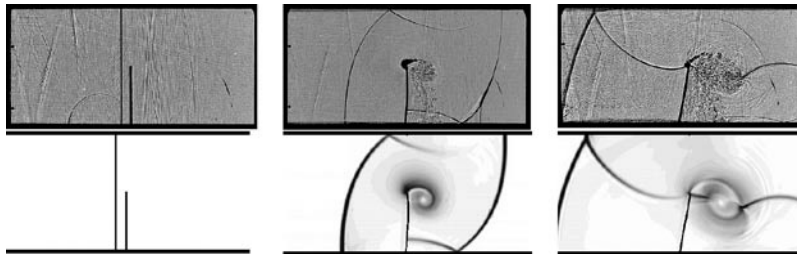


Figure 2: Interaction of a shock wave with an aluminium sheet. Above: Shadowgraphs from experiments (EMI 1999), below: results from coupled APOLLO/SOPHIA simulation. From left to right: $t = 0$, $t = 0.17\text{ms}$, $t = 0.35\text{ms}$

Blast loading of a closed Container

The Large Blast Simulator LBS 501 is operated by the German Armed Forces Technical Center WTD52, Oberjettenberg. The main purpose of the facility is testing of military vehicles and equipment for blast resistance. The LBS 501 is a 100 m long tunnel with an about semi-circular cross section of 75 m² area. The tunnel is equipped with an array of 4 baffles near its open end, which serves as blast wave shaper and silencer. The other, closed end holds the blast wave generator system, an array of 100 pressure reservoirs. Each of about 6 m long steel bottles has 385 l volume and a short nozzle of about 10 cm throat diameter, which is initially closed by a membrane. These reservoirs can be filled with dried air up to 200 bar; they are opened simultaneously with small amounts of explosive. Test objects are typically placed 50 m away from the nozzle exits. Peak overpressure and duration of the pressure wave are adjusted through the number of used bottles and their initial pressures.

Figure 3 displays the numerical model of the tunnel which consists of about 1.5 Mio cells with average resolution of 20cm in 352 grid blocks. The pressure reservoirs are not modelled directly but incorporated as customized boundary conditions: the time dependent free stream at each nozzle exist is obtained from a 1D flow model and is fed into the 3D-flow field at the respective position on the model end wall.

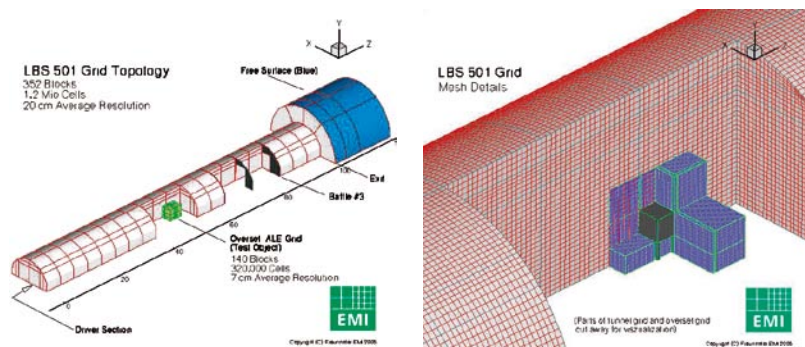


Figure 3: CFD model of the LBS 501. Left: Wire-Frame view. Right: Enlargement showing back-ground grid (red), overset grid (blue) and surface of the container (grey). Parts are cut away for visualization of details.

The results presented here are taken from a 2004 test campaign conducted by WTD 52 which was devoted to validate the coupled simulation. The object tested was a closed container with dimensions 2 m x 1 m x 1 m, built as a steel frame with aluminium walls and mounted on four stands (rigid steel tubes) 0.8 m above the floor. The container was equipped with pres-

sure transducers, optical displacement sensors and accelerometers. The CSD model of the container (figure 4) consisted entirely of shell elements with elasto-plastic material models. An overset grid was fitted to the container and placed into the tunnel model. Some representative results with respect to the loading and the response are shown in the figures below.

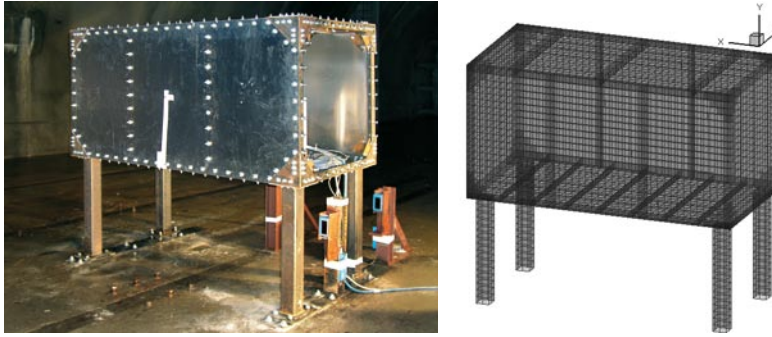


Figure 4: Instrumented container before test and its numerical model (CSD-part)

The comparisons with the test data indicated that the methods and models are suitable for this type of application. It should be noted however, that the deformations were small and a decoupled simulation would provide similar results.

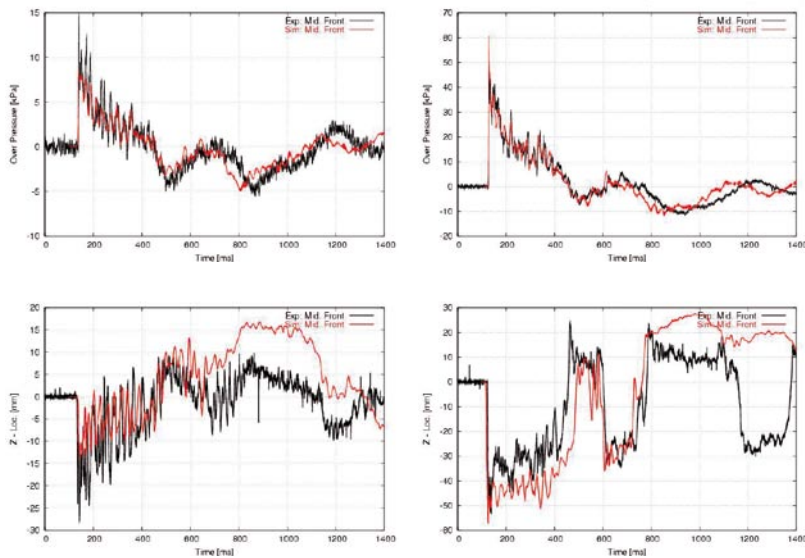


Figure 5: Measured (black) and computed (red) pressures (above) and displacements (below) in the middle of the front plate for two different loading conditions (blast waves of different strength).

Underwater Explosion in an open Duct

This example exhibits a significant interaction between loading and response. The set-up shown in Figure 6 was designed for validation purposes, as the simulation tools were to be used in the safety analysis for nuclear power plant's water supply buildings. The shown model consisted of a square basin and a slender duct with cross section of 12cm x 30cm and length 120cm. The model was built from 1cm thick, welded steel plates with a concrete backing of about 20cm thickness. A few steel struts were mounted onto the plates to improve the connection with the concrete backing. The explosion was generated in the duct through detonation of a spherical charge of 1g PETN near to the connection to the basin. Shown below are the pressures obtained by measurements, from an ALE-coupled calculation and from a fluid dynamic calculation under the simplification of rigid walls. Due to the very small displacements, an adaption of the CFD grid was not required in this coupled simulation; it was sufficient to take into account the surface velocities imposed by the CSD solver. As can be seen, the uncoupled results (legend »APOLLO« in the diagram) are far off the measured pressures. The remaining deviation of the coupled simulation has its origin in the insufficient modelling of the complex dynamic behaviour of the binding between steel and concrete.

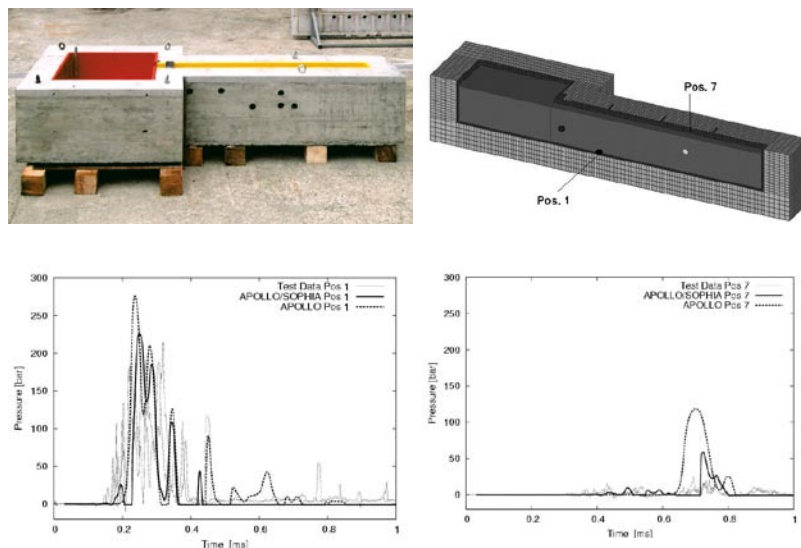


Figure 6: Picture of the steel/concrete duct and the numerical model (CFD/CSD); measured and computed wall-pressure (side-on pressure) records.

REFERENCES

- [1] Smith, P.D.; Hetherington, J.G.: Blast and Ballistic Loading of Structures
Butterworth-Heinemann Ltd, 1994
- [2] Toro, E.: Riemann Solvers and Numerical Methods for Fluid Dynamics,
Springer Verlag, 1997.
- [3] Benson, D.J.: Computational methods in Lagrangian and Eulerian Hydro-
codes, Computer Methods in Applied Mechanics and Engineering, vol. 99
(1992), pp. 235-394
- [4] Belytschko, T.; Liu, W.K. and Moran, B.: Nonlinear Finite Elements for
Continua and Structures, John Wiley & sons, Chichester, England, 2000
- [5] Klomfass, A., Heilig, G. Thoma, K.: Analysis of Blast Loaded Structures by
Numerical Simulation, Fluid-Structure-Interaction 2005, WIT Press

COMPUTATIONAL AEROACOUSTICS USING MPCCI AS COUPLING INTERFACE BETWEEN FLUID MECHANICS, STRUCTURAL MECHANICS AND ACOUSTICS

F. Schäfer, I. Ali, S. Becker, Institute of Fluid Mechanics, University of Erlangen; M. Kaltenbacher, M. Escobar, G. Link, Department of Sensor Technology, University of Erlangen

ABSTRACT

This paper describes a coupling scheme for the simulation of flow induced sound based on fluid-acoustic and fluid-structure-acoustic interactions. A direct coupling between the flow field and the acoustic field is performed in the time domain by applying Lighthill's acoustic analogy. For the simulation of fluid-structure interactions, an implicit coupling between the flow field and the mechanical structure is applied. The exchange of physical quantities between the structured mesh of the flow computation and the unstructured meshes of the acoustic computation and of the structural computation is performed by MpCCI.

INTRODUCTION

Computational aeroacoustics is a multiphysics discipline dealing with the numerical simulation of flow induced sound. In a very general situation, it involves the complex interaction between fluid mechanics, structural mechanics and acoustics. The main difficulty with the coupled simulation of this multiphysics problem is, that usually different spatial discretizations are used for the prediction of the three physical subproblems. This is also a consequence of length scale disparities between the involved fields. Therefore, in order to simulate the sound generation due to fluid-acoustic and fluid-structure-acoustic interactions, we propose a coupling scheme which applies the Mesh-based parallel Code Coupling Interface (MpCCI) [1] for the exchange of data between the different discretizations.

In the present work, a partitioned approach is applied which employs two different simulation codes for the prediction of flow induced sound. The numerical flow computation based on the large eddy simulation method (LES) is carried out with FASTEST-3D [4], a CFD tool developed at the Institute of Fluid Mechanics. In the underlying numerical scheme, a fully conservative second-order finite volume space discretization together with a pressure correction method of the SIMPLE type for the iterative coupling of velocity and pressure is applied. For time discretization, an implicit second-order scheme

is employed, while a non-linear multigrid scheme, in which the pressure correction method acts as a smoother on the different grid levels, is used for convergence acceleration. For the LES method a Smagorinsky-Model is used. Block structured, boundary fitted grids are applied for the spatial discretization of complex flow domains. The code is optimized for the application on parallel and vector computers. The parallelization is based on a grid partitioning approach and implemented using MPI.

For the computation of the generated sound field, the finite element implementation of the inhomogeneous wave equation obtained by Lighthill's acoustic analogy is employed. This formulation has been implemented in CFS++ (Coupled Field Simulation) [11], developed at the Department of Sensor Technology. The time discretization is performed by a predictor-corrector method of the Newmark family. CFS++ is also used for the computation of structural deformations due to pressure and shear stress forces, which are exerted on the structure by the fluid flow. These deformations give rise to changes of the fluid flow, thereby also influencing the flow induced sound field. Moreover, it is possible to take mechanical vibrations as acoustic sources into account.

NUMERICAL SCHEMES

Fluid-Acoustic Computation Scheme

Our approach for the computation of flow induced sound is motivated by the acoustic analogy of Lighthill [12], which is based on the assumption, that one can perform the fluid flow simulation and acoustic field computation separately. This assumption means that the noise induced by the flow does not affect the flow characteristics of the fluid itself.

Starting point of the numerical scheme is the inhomogeneous wave equation, which results from Lighthill's analogy:

$$\frac{\partial^2 \rho_a}{\partial t^2} - c^2 \frac{\partial^2 \rho_a}{\partial x_i^2} = \frac{\partial^2 L_{ij}}{\partial x_i \partial x_j} \quad (1)$$

In (1) ρ_a denotes the acoustic density (density fluctuation), c the speed of sound and L_{ij} the components of Lighthill's stress tensor $[L]$. The right hand side of (1) represents the flow induced acoustic sources, which are computed by using

$$L_{ij} \approx \rho v_i v_j \quad (2)$$

CONTACT

Frank Schäfer
 Technical faculty University
 Erlangen
 Institute of Fluid Mechanics
 Cauerstraße 4
 91058 Erlangen,
 Germany
 Phone: +49 (0) 9131 85-29572
 frank.schaefer@
 lstm.uni-erlangen.de

with v_i the velocity components obtained from the flow simulation. Multiplying (1) by an arbitrary test function $\omega \in H_o^1$, we arrive at the weak form given by

$$\int_{\Omega} \omega \frac{\partial^2 p_a}{\partial t^2} d\Omega + c^2 \int_{\Omega} \nabla \omega \cdot \nabla q_a d\Omega = - \int_{\Omega} (\nabla \omega) \cdot (\nabla \cdot [L]) d\Omega + \int_{\Gamma} \hat{c} \omega \frac{\partial p_a}{\partial n} d\Gamma. \quad (3)$$

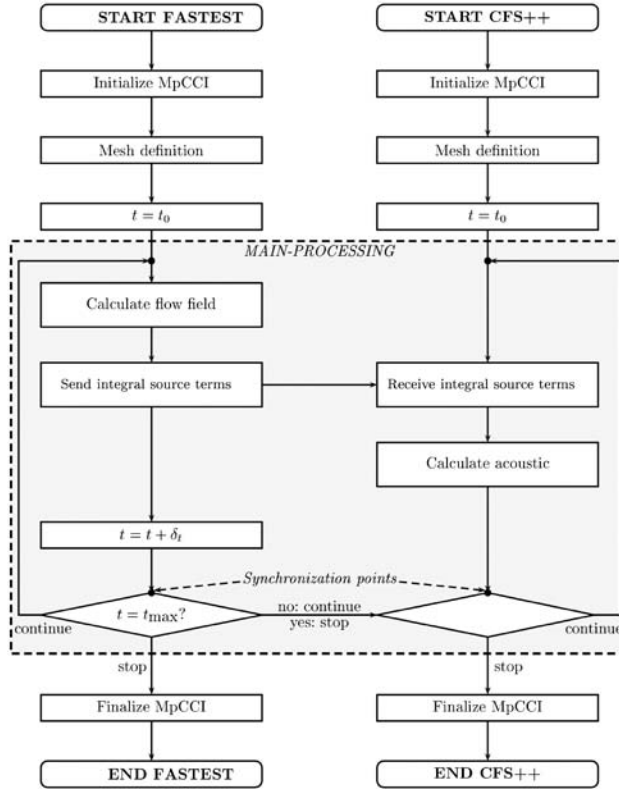


Figure 1: Coupled fluid-acoustic simulation scheme using MpCCI.

By solving (3), we obtain the fluctuation of the density, which for linear acoustics has the following relationship to the acoustic pressure p_a :

$$p_a = p - p_0 = c^2 (\rho - \rho_0) = c^2 \rho_a . \quad (4)$$

By applying the finite element method to (3), we solve for the acoustic field directly in the time domain. Time discretization is performed by a predictor-corrector method of the Newmark family [8]. At the boundary of our acoustic domain, we apply a set of first order absorbing boundary conditions derived from Padé approximations to account for free field radiation [5]. For a detailed discussion on this formulation we refer to [9].

The coupled fluid-acoustic simulation scheme is depicted in Figure 1. During the actual simulation (shaded in gray) the acoustic sources are transferred from FASTEST-3D to CFS++ at the nodal positions of the grids by means of interpolation algorithms provided by MpCCI. The straightforward approach would be to transfer the fluid velocity components and compute Lighthill's tensor (see (2)) within CFS++. In order to minimize the amount of the data transfer, we compute the right hand side of (3) from the velocity vector on the flow grid and obtain so called acoustic nodal loads (scalar quantity). These nodal loads have then to be interpolated by a conservative technique, since they are integral quantities. Subsequently, with the nodal loads it is possible to carry out the computation of the acoustic propagation.

Fluid-Structure Interaction

When a fluid is flowing around a flexible or moving structure, the structure is deformed or displaced due to pressure and shear stress forces exerted on it by the fluid. Since this changes the boundary of the flow domain, the fluid flow changes as well. In order to simulate this complex interaction, we use an implicit coupling between fluid mechanics and structural mechanics. The basic scheme is depicted in Figure 2. At the heart of the algorithm, there is a fluid-structure iteration loop within each time step to assure a strong coupling between the two physical fields. The calculation of fluid loads, resulting structural deformations and resulting change of fluid flow is iterated until a dynamical equilibrium is reached within the time step. The convergence criteria is based on the change of the mechanical displacement u between two subsequent iterations:

$$\frac{\|u_{t+1} - u_t\|_2}{\|u_{t+1}\|_2} \leq \varepsilon . \quad (5)$$

In (5) l denotes the iteration counter, $\| \cdot \|_2$ the L^2 -norm and ε a selectable accuracy, which we set for most cases to 10^{-3} . For a detailed discussion on this topic we refer to [7].

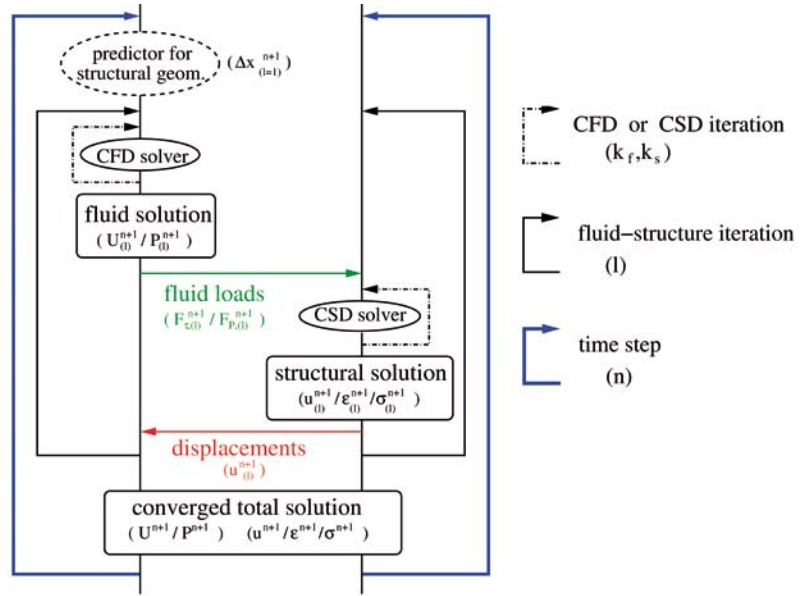


Figure 2: Implicit coupling scheme for fluid-structure interactions using FASTEST-3D (left branch), CFS++ (right branch) and MpCCI

At the beginning of each time step, optionally a prediction of the new structural deformation is performed based on an extrapolation of the deformations at previous time steps. This can reduce the cumulated number of CFD iterations k_f needed throughout the simulation by 25% to 45%, depending on the order of the extrapolation [7].

The exchange of data via MpCCI is performed at the surface patches of the structure. For the transfer of fluid loads from FASTEST-3D to CFS++ a conservative interpolation scheme is employed. This guarantees that the sums of all forces are the same on both grids. The transfer of mechanical displacements from CFS++ to FASTEST-3D is accomplished by means of a bilinear interpolation. The data exchange is fully parallelized in FASTEST-3D, so that all processors can take part in the communication with CFS++. This is important for the simulation of fluid-structure interactions in large and complex domains.

Since the boundary of the flow domain changes within each fluid-structure iteration, the computational grid of the flow simulation has to be adapted accordingly. For this purpose, we use fast and robust algebraic methods such as linear and transfinite interpolation. In a simple case, where the deformation of two opposing faces of a grid block is known (compare Figure 3), linear interpolation is applied as follows:

$$\Delta x(\xi) = \xi \Delta x(0) + (1 - \xi) \Delta x(1) \quad (6)$$

Here ξ denotes the local coordinate along a grid line and $\Delta x(\xi)$ the grid displacement at the position ξ . In a more complex situation involving the deformation of adjoined faces, transfinite interpolation is employed [7]. Depending on the state (deformed or not deformed) of each face of a given block, also a mixture of different linear and transfinite transformations can be necessary to adapt the grid within the block.

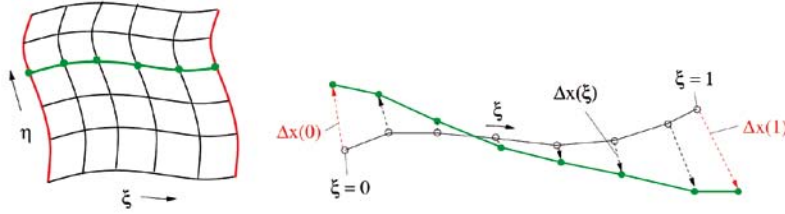


Figure 3: Grid adaptation by linear interpolation along grid lines.

Since the whole grid consists of several blocks, the order in which the transformations are applied to the blocks is crucial. In the case of moderately complex multiblock configurations, we use an automatic grid adaptation scheme which determines automatically the order of the necessary transformations. For arbitrary complex situations, which cannot be handled by the automatic scheme, the order of transformations is defined manually.

As a consequence of the grid adaptation algorithm, the grid cells are changing with time. The movement of the control volume faces introduces additional fluxes which have to be taken into account in the finite volume scheme. This is done by using the Arbitrary-Lagrangian-Eulerian formulation (ALE) of the generic transport equation of some quantity ϕ (see [10] for details):

$$\frac{d}{dt} \int_{\Omega} q_f \phi \, d\Omega + \int_{\Gamma} \rho_f \phi (v_i - v_i^g) n_i \, d\Gamma = \int_{\Gamma} \Lambda_{\phi} \frac{\partial \phi}{\partial x_i} n_i \, d\Gamma + \int_{\Omega} q_{\phi} \, d\Omega. \quad (7)$$

In (7) ρ_f denotes the density of the fluid, v_i the i -th component of the velocity vector, Λ_ϕ the diffusive constant and q_ϕ the source term. Additional grid fluxes are caused by the grid velocity v_i^g . As shown in [6], this scheme can introduce artificial mass sources. Therefore, in order to obtain mass conservation, we have also to enforce the so-called space conservation law (SCL):

$$\frac{d}{dt} \int_{\Omega} d\Omega = \int_{\Gamma} v_i^g n_i d\Gamma. \quad (8)$$

NUMERICAL CASE STUDIES

Flow around an Oscillating Square Cylinder

Our first numerical case study concentrates on a square cylinder immersed in a turbulent flow at a Reynolds number of about 13,000. The computational domain of the flow simulation is depicted in Figure 4. In a previous investigation [3], we computed the flow induced sound field for the case of a rigid square cylinder located at a fixed position in space. In the present investigation, we take fluid-structure interactions into account by treating the square cylinder as a rigid body which is allowed to oscillate in two space directions. The oscillation is governed by a 2D spring equation with spring constant Λ and damping constant b . With F_β being the overall force which is exerted on the square cylinder by the fluid flow, the equation of motion of the cylinder reads as follows:

$$m \ddot{x}_c = F_\beta - \Lambda x_c - b \dot{x}_c. \quad (9)$$

Here $x_c = (x_c, y_c)$ denotes the position of the square cylinder's center line relative to the cylinder position in the fixed case. The mass m of the cylinder and the spring parameters Λ and b are chosen in such a way that the maximum cylinder elongation in the main flow direction is of the order of magnitude of the cylinder size D . The exact values are $D = 0.02\text{m}$, $m = 0.005\text{ kg}$, $\Lambda = 10\text{N/m}$ and $b = 0.1\text{Ns/m}$. This implies that the resonance frequency of the spring oscillation is about 7.12 Hz.

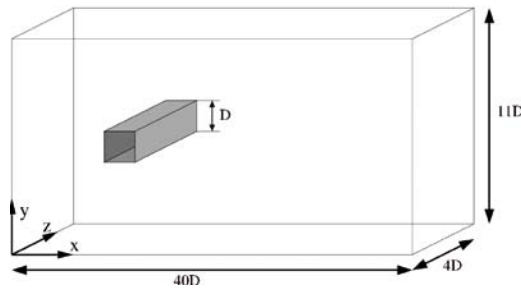


Figure 4: Computational domain of the flow simulation.

For temporal integration of (9), the initial conditions are set to $x = 0$, $\dot{x}_c = 0$. The boundary conditions for the flow simulation are chosen as follows:

POSITION	BOUNDARY CONDITION
$x = 0$	block flow profile of 10 m/s
$x = 40D$	convective outflow boundary condition
$y = 0$	symmetry boundary condition
$y = 11D$	symmetry boundary condition
$z = 0$	periodic boundary condition
$z = 4D$	periodic boundary condition
Surface of cylinder	no-slip boundary condition

The computed instantaneous pressure field in the vicinity of the square cylinder is depicted in Figure 5. Two consecutive instances of time are shown, where the temporal difference roughly corresponds to the time between two von-Karman vortices emerging downstream of the cylinder. As can be seen, the influence of the pressure force on the cylinder motion is twofold: on the one hand, there is a pressure force pushing the cylinder into the main flow direction x ; on the other hand, there is an alternating force in the transverse direction y which is due to the alternation of the von-Karman vortices.

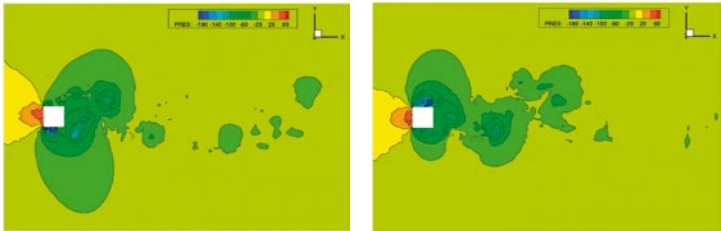


Figure 5: Instantaneous pressure field at time t (left) and $t + 0.01s$ (right) in a cutting plane at $z = 2D$.

Resulting time series and frequency spectra of the cylinder motion in the main flow direction and the transverse direction are shown in Figure 6. The frequency spectra show strong peaks at about 7 Hz corresponding to the resonance frequency of the cylinder oscillation. Additionally, there are also some higher frequency components which are partly induced by the periodic structures in the flow: in the transverse direction, there is a strong peak at about 58 Hz corresponding to the frequency at which two alternating von-Karman vortices are created; at the double frequency (117 Hz) there is a weakly pronounced peak in the main flow direction which is due to the creation of single von-Karman vortices.

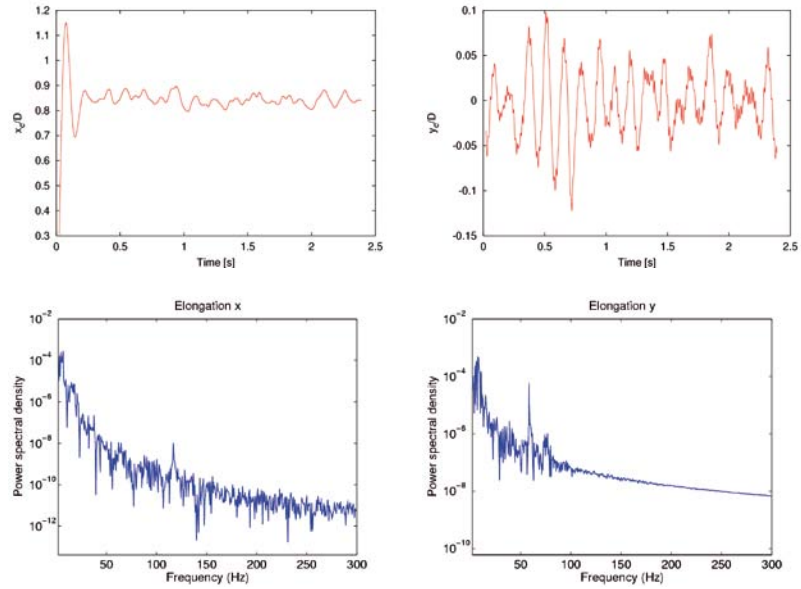


Figure 6: Normalized square cylinder elongation (top) and corresponding frequency spectra (bottom) in main flow direction (left) and the transverse direction (right). The spectra were obtained by considering only the time $t > 0.8$ s

A comparison between the oscillating and the fixed square cylinder is shown in Figure 7. Time series of the fluid pressure were recorded at two positions at a distance $5D$ behind the cylinder (in case of the oscillating cylinder the distance was $5D$ behind the average cylinder position). The two positions are aligned with the center or with the upper corner of the square cylinder, respectively. For the fixed cylinder, there are pronounced peaks at 67 Hz and 132 Hz, corresponding to the single and double frequency of the von-Karman flow structures. In the oscillating cylinder case, the same dominant peaks can be identified, but the frequencies are shifted towards lower values. We assume that the square cylinder's elastic response to the fluid flow leads to a delay in the creation of von-Karman vortices and thereby reduces the frequency.

We expect that the shift to lower frequencies is also present in the acoustic field emanating from the flow around the cylinder and its structural oscillation. Acoustic computations of the oscillating square cylinder case are currently in preparation.

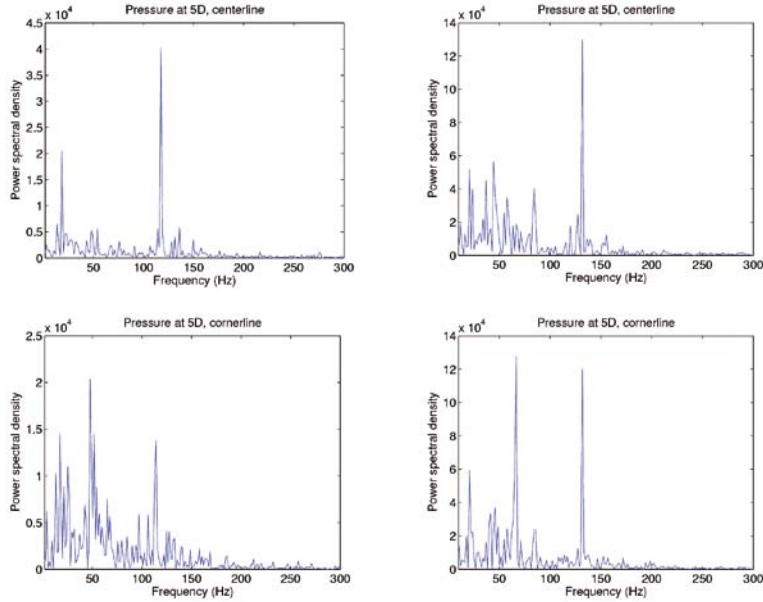


Figure 7: Comparison of fluid pressure frequency spectra for the oscillating cylinder (left) and the fixed cylinder (right).

POSITION	BOUNDARY CONDITION
$x = 0$	block flow profile of 10 m/s
$x = 40D$	convective outflow boundary condition
$y = 0$	symmetry boundary condition
$y = 11D$	symmetry boundary condition
$z = 0$	no-slip boundary condition
$z = 11D$	symmetry boundary condition
Surface of cylinder	no-slip boundary condition

Flow around a Square Cylinder Obstacle

The second numerical case study presented here is the turbulent flow around a square cylinder obstacle at a Reynolds number of about 13,000. Figure 8 represents the configuration chosen for the simulations, where Ω_F denotes the domain for the flow computation and $\Omega_F \cup \Omega_A$ defines the computational domain for acoustics. The square cylinder has a length D of 0.02m and a height of $H = 6D$. The dimensions of the flow domain are also shown in Figure 8. The boundary conditions for the flow computation are defined as follows:

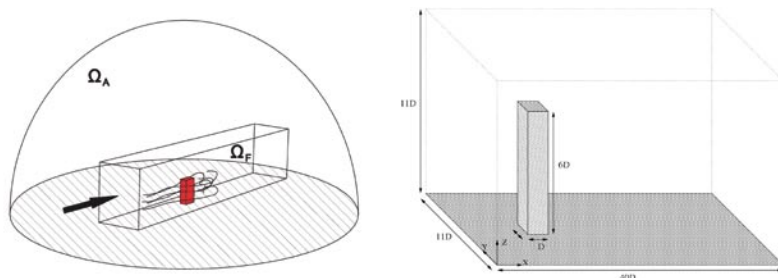


Figure 8: Principle setup for the aeroacoustic computation (left) and dimensions of the flow domain (right).

For the acoustic field computation, we have extended the domain Ω_F to a semi-sphere with a radius of about 10m (see Figure 8). On the surface of the semi-sphere, we apply absorbing boundary conditions to omit reflections of outgoing waves.

The generation and propagation of flow induced sound was computed for a rigid, fixed cylinder without considering fluid-structure interactions. The coupling between FASTEST-3D and CFS++ was performed in the complete 3D intersection of the flow domain and the acoustic domain by using hexahedral elements in MpCCI.

A timeline visualization of the instantaneous velocity field next to the square cylinder is depicted in Figure 9. After the fluid has passed the cylinder at the sides and at the top, a complex flow field is evolving behind the obstacle.

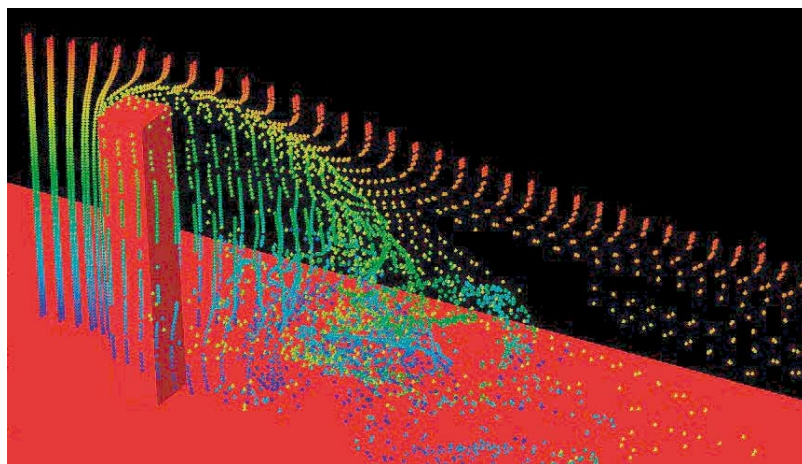


Figure 9: Timeline visualization of the flow field next to the square cylinder.

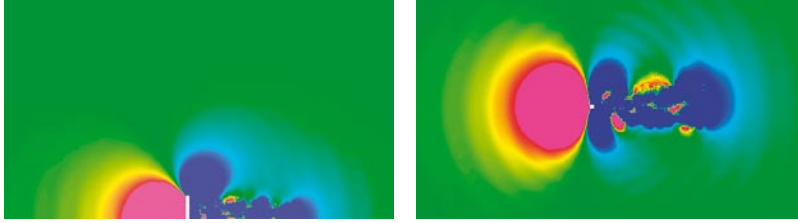


Figure 10: Instantaneous acoustic pressure field in a cutting plane at $y = 5.5D$ (left) and $z = 0$ (right)

The resulting acoustic pressure field in the vicinity of the square cylinder is shown in Figure 10. In these images, a white rectangle or square is indicating the location of the cylinder. Our results show that the acoustic field is mainly dominated by a dipole which is located next to the cylinder. There are also some acoustic sources in the wake of the obstacle, but they are much weaker and their contribution to the acoustic far field is less important.

The flow simulation with FASTEST-3D was carried out using an LES model and a grid consisting of 3.1 million control volumes. Since the computational cost for LES is very high, it is attractive to consider also other turbulence models which require less resources. Therefore, we have compared our

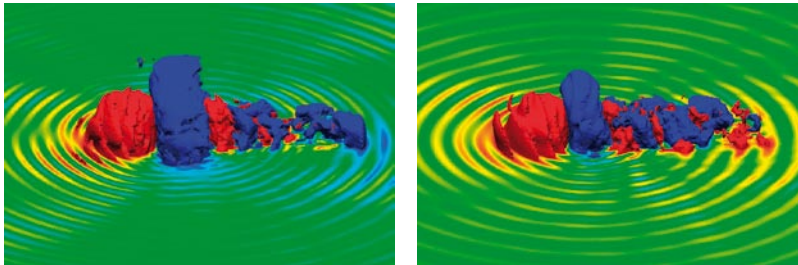


Figure 11: Instantaneous acoustic pressure field for a flow computation using FASTEST-3D (LES, left) and ANSYS CFX (SAS, right).

LES-results with computational data obtained with the CFD package ANSYS CFX. In the latter case, the flow data and the acoustic nodal sources were provided by ANSYS based on a scale adaptive simulation (SAS) with a grid consisting of 1.1 million grid cells. A comparison of the resulting acoustic fields for the LES case and the SAS case is shown in Figure 11. As can be seen, the main features are very similar. However, further investigations are necessary to compare the LES and the SAS approach in more detail.

CONCLUSION AND OUTLOOK

We have presented our computational aeroacoustics environment using MpCCI as a coupling interface between fluid mechanics, structural mechanics and acoustics. In the case of fluid-structure interaction MpCCI provides the data exchange between surfaces, whereas in the case of fluid-acoustic coupling the data exchange is performed within the volume.

Currently we are preparing a coupled fluid-structure-acoustic simulation of the oscillating square cylinder case. In this simulation, also the noise generated by the structural oscillation will be taken into account.

ACKNOWLEDGEMENTS

The computational results of the simulations using ANSYS CFX have been kindly provided by M. Kuntz, ANSYS Germany GmbH.

REFERENCES

- [1] <http://www.mpcci.org/>
- [2] I. Ali, M. Escobar, C. Hahn, M. Kaltenbacher, and S. Becker, Numerical and Experimental Investigation on Flow Induced Noise from a Square Cylinder, 10th Aeroacoustic Conference, Manchester, 2004.
- [3] I. Ali, M. Kaltenbacher, M. Escobar, and S. Becker, Time Domain Computation of Flow Induced Sound, Euromesh Colloquium 467, Turbulent Flow and Noise Generation, Marseille, July 18th – 20th, 2005, submitted.
- [4] F. Durst and M. Schäfer, A Parallel Block-Structured Multigrid Method for the Prediction of Incompressible Flows, Int. J. Num. Methods Fluids 22 (1996), 549-565.
- [5] B. Engquist and A. Majda, Absorbing Boundary Conditions for the Numerical Simulation of Waves, Mathematics of Computation 31 (1977), 629-651.
- [6] J.H. Ferziger and M. Peric, Computational Methods for Fluid Dynamics, Springer, 2002.
- [7] M. Glück, Ein Beitrag zur numerischen Simulation von Fluid-Struktur-Interaktionen-Grundlagenuntersuchungen und Anwendung auf Membrantragwerke, Ph.D. thesis, University of Erlangen, Institute of Fluid Mechanics, Erlangen, 2002.
- [8] T.J.R. Hughes, The Finite Elemente Method, Prentice-Hall, New Jersey, 1987.
- [9] M. Kaltenbacher, M. Escobar, A. Irfan, and S. Becker, Finite Element Formulation of Lighthill's Analogy for Computational Aeroacoustics, (2005), (in preparation).
- [10] M. Kaltenbacher, M. Escobar, G. Link, I. Ali, S. Becker, and F. Schäfer,

Computational Aeroacoustics using MpCCI as Coupling Interface between Fluid Mechanics and Acoustics, 6th MpCCI User Forum, February 22nd-23rd 2005, 52-63.

[11] M. Kaltenbacher, A. Hauck, M. Escobar, and G. Link, Coupled Field Simulation, LSE, University of Erlangen, 2004.

[12] M.J. Lighthill, On Sound Generated Aerodynamically i. General Theory, Proc. Roy. Soc. Lond. (1952), no. A 211, 564-587.

SIMULATION OF FLUID DAMPED STRUCTURAL VIBRATIONS

Sven Schrape, Arnold Kühhorn, Mark Golze, University of Cottbus

ABSTRACT

Aiming at a fully coupled simulation of the fluid-structure interaction two specific examples are presented. At first, in terms of a validation of the recently commissioned coupling-tool MpCCI, a plate set exposed to a transverse flow is considered. In this case the structure responds in a decaying vibration induced by the flow. Furthermore, a computation of the fully coupled blade vibrations considering a two dimensional model of a compressor cascade configuration will be presented. Starting from an inviscid, subsonic flow the discussion is focussed on effects on the vibration behaviour resulting from aerodynamic damping and the vibration frequency shift.

MOTIVATION

In order to achieve an effective reduction of fuel consumption and lower manufacturing costs in aviation, integrated lightweight design solutions have been developed for high-pressure compressors during the last years. These constructions, known as »BLISK« (**blade integrated disk**), are characterised by lower damping values of the blades compared to conventional constructions in which the blades and the disk are separated. While the manifold mechanisms of aerodynamic excitation remain, the lower damping of the integrated type negatively affects the fatigue strength. Influences resulting from geometrical and material imperfections (mistuning [4], [5]) could even worsen the problem. In order to guarantee a save and predictable operation, an estimation of aerodynamically induced stresses close to reality requires an accurate knowledge of the complex and unsteady interaction between fluid and structure. Finally, it is planned to compute the forced vibration response within an engineering approach regarding a simplified structural model which considers aerodynamic damping, oscillating air masses as well as reinforcing effects due to compressible air flow.

COUPLING CONCEPT

For all simulations presented subsequently a partitioned explicit (staggered) coupling approach is applied, which is realised connecting the finite-volume code FLUENT 6.2.16 for the fluid part and the finite-element code ABAQUS 6.5.1 for the structural part via MpCCI 3.04. In this case the transfer as well as the interpolation of mesh based quantities is provided by MpCCI.

In case of explicit methods quantities of flow and structure are computed once in each time step and exchanged via the contact surface in the following. Within the simulations presented here the time steps are sequentially processed. Due to the time delay of the explicit coupling algorithms the coupling conditions (geometric compatibility of fluid and structure as well as of boundary conditions at the interface) are not fulfilled in case of weak coupling. Hence, relatively small time steps have to be chosen for reasons of stability and equilibrium.

Due to different spatial discretisations the interface has to be found applying geometric algorithms, if non-matching grids are used. Thereby the interacting boundary surfaces of both sub-problems are defined by the user. In this way, a so-called Point-Element search algorithm (PE) connected with a standard interpolation based on it has been used for all coupled computations. In doing so, fluid loads are conservatively coupled whereas structural displacements are coupled in a non-conservative way [1].

TRANSVERSAL FLOW AGAINST A FLEXIBLE PLATE

Configuration

Aiming at a basic validation of the coupling approach an example from literature dealing with a flexible plate exposed to transversal flow loading is regarded [2]. In this context a geometrically simple configuration of a cantilever plate is considered, which is flowed by an artificial fluid. The configuration and boundary conditions of the flow area are shown in Figure 1.

The rectangular plate is asymmetrically located inside the flow area at a distance of 10m away from the left boundary. In the publication [2] a 3-dimensional computation has been carried out. Because of the symmetric bound-

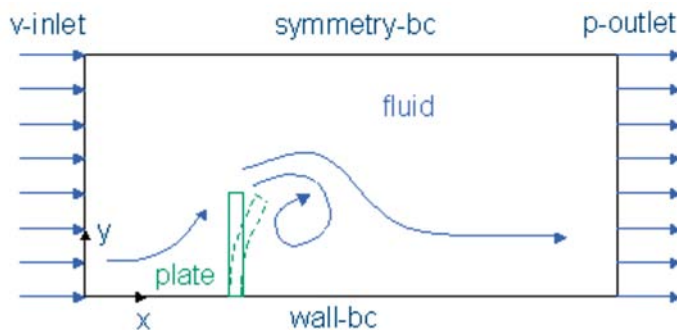


Figure 1: Plate configuration

CONTACT

Sven Schrape
Technical University of Cottbus
Chair of Structural Mechanics
Siemens-Halske-Ring 14
03046 Cottbus,
Germany
Phone: + 49 (0) 355 69-5138
sven.schrape@tu-cottbus.de

any conditions of the lateral surfaces the plate's vibration is characterised by bending around the z-axis without any torsional parts. Thus, with regard to a reduced computation time a 2-dimensional approach is considered in contrast to [2]. A listing of the plate's geometric and material data as well as geometric and fluid data of the flow can be taken from Table 1.

GEOMETRY FLOW AREA	GEOMETRY STRUCTURAL MODEL
$L_x = 50 \text{ m}$	$L_x = 0,01 \text{ m}$
$L_y = 6 \text{ m}$	$L_y = 1 \text{ m}$
$L_z = 0,4 \text{ m}$	$L_z = 0,4 \text{ m}$
FLUID DATA	MATERIAL DATA
$p_f = 1\text{kg/m}^3$	$E = 3500 \text{ N/mm}^2$
$\mu_f = 0,2 \text{ Pa s}$	$\nu = 0,32$
$v = 10 \text{ m/s}$ blockprofile	$p_s = 1200 \text{ kg/m}^3$

Table 1: Structural and fluid data

At the left intake a block shaped velocity profile of $u = 10\text{m/s}$ is applied. Connected with a characteristic plate length of $L_y = 1\text{m}$ the Reynolds number becomes $Re = 50$, from which results a laminar flow (involving friction). At the time $t = 0\text{s}$ a stationary flow field (used as initial solution) is developed around the initially stiff plate. For $t > 0\text{s}$ the now elastic plate is loaded by compressive and frictional forces. Resulting from interacting flow forces and structural displacements a stationary displacement of the plate can be expected after the transient oscillation is decayed.

Numerical model

Because of its laminar, isothermal and incompressible character the configuration considered here corresponds to a flow of a Newton Fluid, which simplifies the solution of the Navier-Stokes Equations consisting of the continuity equation (1) and 3 equations of conservation of momentum (2). Due to the incompressible character of the flow the continuity equation is reduced to the zero divergence of the flow field u_i .

$$\frac{\partial u}{\partial x} + \frac{\partial v}{\partial y} + \frac{\partial w}{\partial z} = \nabla \cdot \mathbf{u} = 0 \quad (1)$$

$$\rho \left(\frac{\partial \mathbf{u}}{\partial t} + \mathbf{u} \cdot (\nabla \cdot \mathbf{u}) \right) = \mathbf{f} - \nabla \cdot \mathbf{p} + \mu \Delta \mathbf{u} \quad (2)$$

with $\Delta \mathbf{u}$ according to the Laplacian operator applied to the velocity vector \mathbf{u} , $\nabla \cdot \mathbf{p}$ for the gradient of the pressure p as well as ∇ for the Nabla operator. The body forces \mathbf{f} also disappears for the configuration considered here.

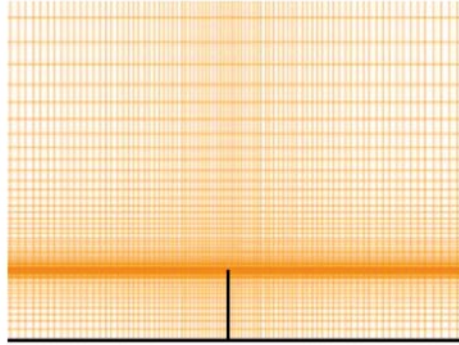


Figure 2: Cutout fluid-grid

Based on a stationary flow analysis of an undeformed rigid plate, in which the grid width of each mesh is halved step by step, the computation mesh could be validated. Figure 2 shows a refined mesh around the plate's tip with 220×60 control volumes. With reference to this spatial discretisation very satisfying results could be achieved applying the second order upwind discretisation method. The time discretisation is realised applying a first order implicit method. A sequential method, applying Patanker's SIMPLE – Algorithm for the pressure-velocity coupling, is used for the solution of the conservative equations. With regard to grid motions in case of coupled simulations, additional terms have to be included to the conservation equation concerning the so called ALE (Arbitrary-Lagrange-Euler) formulation.

On the part of structural evaluations the finite element method (FEM) is used. FEM is based on the principle of virtual displacement which is consistent with the Weak Form of Equilibrium (3).

$$\int_{V_0} {}^{\parallel} \mathbf{P} \cdot \delta \mathbf{G} dV_0 = \int_{V_0} \rho_0 (\mathbf{k}_0 - \ddot{\mathbf{u}}) \cdot \delta \mathbf{u} dV_0 + \int_{A_0} {}^{\perp} \mathbf{t} \cdot \delta \mathbf{u} dA_0 \quad (3)$$

${}^{\parallel} \mathbf{P}$ denotes the second Piola-Kirchhoff stress tensor and ${}^{\perp} \mathbf{t}$ the nominal stress vector. Body forces are neglected for the considered problem. Furthermore a hyperelastic, isotropic material law according to St. Venant (4) is assumed.

$${}^{\parallel} \mathbf{P} = 2G \left[\mathbf{G} + \frac{1}{1-2\nu} (\mathbf{G} \cdot \mathbf{I}) \mathbf{I} \right] \quad (4)$$

G denotes the shear modulus, ν the Poisson's ratio and \mathbf{I} the unit tensor. Corresponding to the problem large deformations and small strains can be expected, so that the Green-Lagrange strain tensor \mathbf{G} (5) is applied, which describes the non-linear relation between displacements and strains. \mathbf{F}_D signifies the deformation gradient tensor.

$$\mathbf{G} = \frac{1}{2} (\mathbf{F}_D^T \mathbf{F}_D - \mathbf{I}) \quad (5)$$

After the spatial discretisation and neglecting the structural damping matrix \mathbf{D} , the coupled system of conventional differential equations results to:

$$\mathbf{M}\ddot{\mathbf{x}} + \mathbf{K}\mathbf{x} = \mathbf{f}(t) \quad (6)$$

\mathbf{M} describes the mass matrix and \mathbf{K} the displacement-dependent stiffness matrix of the structure. It has to be noticed, that during the coupled computation the flow-induced damping is considered as damping force within the vector of external forces $\mathbf{f}(t)$.

Due to the two dimensional approach 2D-continuum elements are used. The so-called »in-plane bending« adversely affects the problem, whereas especially »hourglassing« and »locking«-phenomena have to be considered within the selection of elements. Hence, plane stress 2D-continuum elements with additional inner degrees of freedom (incompatible modes) are applied. As long as the distortion of the mesh expressed by the deviation from ideal rectangular elements is limited, this type of element is particular suitable for such problems (plate thickness: 10 mm). Using the relation between a stationary loading and the expected structural response the finite element mesh has been also validated corresponding to the flow mesh analysis. Sufficiently accurate results are calculated for the plate of 10 mm thickness applying a mesh composed of 2 x 6 elements. In case of thin structures the mesh has been refined to 4 x 24 elements.

With respect to the coupling a geometrical non-linear computation applying an implicit time integration (Hilbert-Hughes-Taylor) has been carried out.

Results

The Figures 3 and 4 shows the displacements of transient oscillations of an elastic plate approaching the stationary solution of a sequential, unsteady coupled computation. It can be seen from Figure 3 (plate thickness: 10 mm) that with decreasing time steps the displacements of the plate vibration increase and approximate to the maximum value, which represents the most accurate solution with regard to the algorithm applied. The stationary solution will be reached earlier if larger time steps are used. The value calculated here is time step independent. Furthermore a phase shift appears.

Additionally the plate width (10 mm, 4 mm, 3 mm) has been varied (Figure 4, time step $\Delta t = 0.01s$). Due to decreasing moments of inertia, larger displacements are calculated with decreasing plate width. The results well accord to those published in [2]. Figure 5 shows the time-dependent development of streamlines considering a coupled computation of a very elastic plate (thickness: 4 mm, time step $\Delta t = 0.01s$). The vortex separation and redevelopment becomes clear.

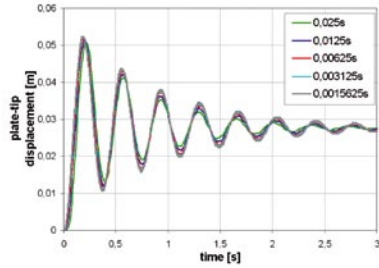


Figure 3: Variation of time step

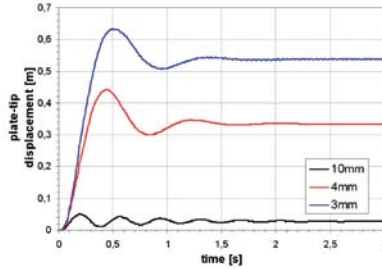


Figure 4: Variation of plate width

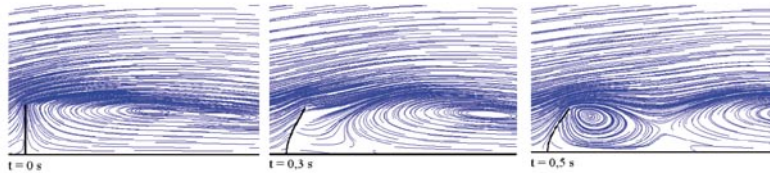


Figure 5: Development of streamlines

SIMPLIFIED AERO ENGINE COMPRESSOR BLADE

Configuration

Applying simplified flow and structural conditions, a first approach of a fully coupled computation of a modified compressor cascade configuration is presented. In this regard a plane compressor cascade corresponding to a NACA3506 profile has been chosen. The used configuration data can be taken from Table 2.

profile	NACA3506
chord length l	0,023 m
blade depth t	0,028 m
blade mass	2,344e-03kg
stagger angle β	40°
inlet mach number Ma_i	0,6
inlet flow angle α	48,3°
pitch to chord ratio τ / l	0,71

Table 2: Configuration data

Subsequently, results of blade bending vibrations are presented considering aerodynamic damping obtained from coupled calculations. Therefore the structure is excited using a linear sine sweep (Figure 6). From the mechanical point of view the blade is modelled as one degree of freedom oscillator. Adjusting mass and stiffness the eigenfrequency of $f_0 = 2500$ Hz is determined. In order to pass through the blade resonance within a forced response calculation a frequency band for the linear sine sweep excitation of 2400 Hz – 2600 Hz (passing time: $t_{ges} = 0,98304$ s) is chosen. Furthermore, a structural damping ratio of $D = 0,1\%$ is assumed. In this way, a reference solution representing the pure structural response is created as basis of comparison for a fully coupled simulation including the passing flow.

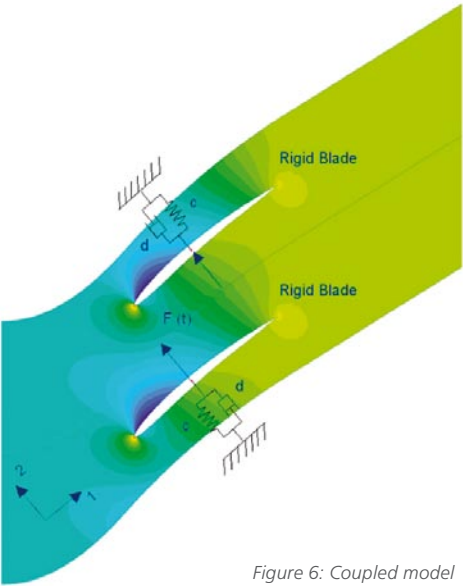


Figure 6: Coupled model

Numerical model and first results

The plane subsonic airflow is computed as compressible flow according to the ideal gas law. Assuming an inviscid flow, the Euler-equations have to be solved by the CFD-code. On the part of FLUENT a coupled, implicit solver is used.

According to Figure 6 a single blade channel has been modelled considering periodic boundaries as well as boundary conditions of in- and outlet and the blade profile. At the inlet boundary the total pressure ($p_0 = 1 \cdot 10^5$ Pa), the total temperature ($T_0 = 300$ K) and the inlet flow angle are defined. The static pressure ($p_2 = 0,865 \cdot 10^5$ Pa) is given by the outlet boundary. This pressure is adjusted using an iterative process to achieve the mach number required at the inlet.

Refining the mesh step by step, a steady flow analysis has been carried out for the purpose of validation. Applying the second order upwind discretisation to a 26×119 control volumes mesh the results awfully match to those published by Grüber [3]. Furthermore effects of numerical dissipation are studied regarding this validated mesh. Numerical dissipation can cause time step dependent oscillation amplitudes within transient coupled simulations.

For the results presented below both, the structural and the fluid time step, has been chosen to $\Delta t = 5 \cdot 10^{-6}$ s, wherewith the computational time remains moderate and numerical dissipation is tolerable. It has to be noted that on part of the structure only the local two degree of freedom is enabled according to Figure 6. As a consequence torsional vibrations of the blade are disabled. Due to the periodic boundary conditions the model describes in-phase bending vibrations of a compressor blade configuration.

Figure 7 shows the time signals and the assigned Fourier spectra of the blade displacement in local 2-direction. The signals results from the coupled computation as well as the structural response without consideration of the passing flow.

As expected the overall damping-ratio of 0.214% clearly increase compared to the pure structural damping. In case of the coupled simulation a decrease of the eigenfrequency can be found, which results from the co-vibrating air mass. Lift arises from the air flow from which results an offset in the time-signal according to the chosen spring stiffness of the 1-DOF-oscillator. Superposed vibrations to be found in the Fourier spectra results from the linear sine sweep excitation of the structure.

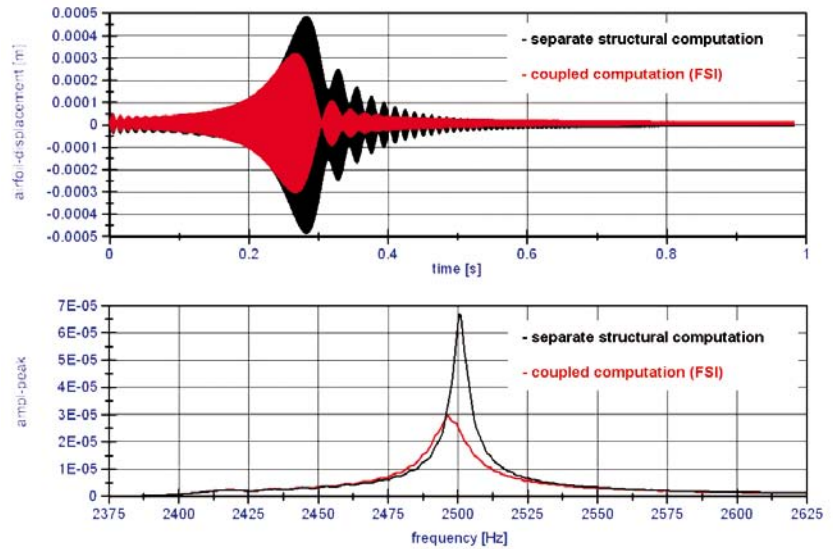


Figure 7: Results blade vibrations

CONCLUSION AND OUTLOOK

Results of a validation problem have been exemplarily presented for a plate exposed to a transverse flow as well as a simplified model for the prediction of the aerodynamically affected over-all damping ratio of compressor blade cascade flow. Within the next steps the plane flow approach will be adapted to real compressor conditions. Aiming at the objectives described in chapter 1, additional parameter studies are planned.

REFERENCES

- [1] Fraunhofer Institute for Algorithms and Scientific Computing SCAI, 2005: MpCCI 3.0.4 Manuals and Tutorials., <http://www.scai.fraunhofer.de/mpcci.html>.
- [2] Glück, M., 2003: Ein Beitrag zur numerischen Simulation von Fluid-Struktur-Interaktionen – Grundlagenuntersuchungen und Anwendungen auf Membrantragwerke. Dissertation, Universität Erlangen-Nürnberg, Shaker – Verlag, Aachen.
- [3] Grüber, B.: Über den Einfluß der Viskosität auf das aerodynamische Dämpfungsverhalten bei schwingenden ebenen Verdichtergittern in transsonischer Strömung, Fortschr.-Ber. VDI Reihe 7 Nr. 437, VDI Verlag, Düsseldorf, 2002.
- [4] Beirow, B., Kühhorn, A., Golze, M., Klauke, Th., Parchem, R.: Experimental and Numerical Investigations of High Pressure Compressor Blades

Vibration Behaviour Considering Mistuning. NAFEMS World Congress 2005, St Julians, Malta.

- [5] Beirow, B., Kühhorn, A., Golze, M., Klauke, Th.: Strukturdynamische Untersuchungen an Hochdruckverdichterschaufelscheiben unter Berücksichtigung von Mistuningeffekten, VDI-Schwingungstagung 2004, Modalanalyse und Identifikation, VDI-Berichte Nr. 1825, 2004.
- [6] ABAQUS, Inc., 2005: ABAQUS Analysis User Manual. ABAQUS, Inc., Providence.
- [7] FLUENT, Inc., 2005: FLUENT 6.2 User Guide. <http://www.fluentusers.com>

AN MPCCI-BASED SOFTWARE INTEGRATION ENVIRONMENT FOR HYPERSONIC FLUID-STRUCTURE PROBLEMS

Reinhold Niesner, M. Haupt, P. Horst, Institute of Aircraft Design and Lightweight Structures, TU Braunschweig; F. Dannemann, A. Schreiber, German Aerospace Center, Simulation and Software Technology

ABSTRACT

The paper describes the techniques used for fluid-structure interaction analyses in the project IMENS+ (DLR, TU Braunschweig), with emphasis on the software concept used. The project's aim is the development of an integrated environment for the multidisciplinary design of hot structures, targeting hypersonic aerospace applications.

INTRODUCTION

Although fluid-structure interaction problems have been the target of research for many years now, there is still a lack of adequate simulation environments for industrial use with regard to user-friendliness and flexibility. The activities in the project IMENS+ aim at developing an integrated environment for coupled simulations, having as main requirements: ability to handle complex physical models, performance, ease of use and flexibility. These requirements led to a modular software concept using existing solvers for the individual disciplines (fluid and structural dynamics). These solvers are optimized for their disciplines (use in general different solution schemes), are very robust and can handle complex physical models.

SOFTWARE CONCEPT

The numerical methods used have an important impact on the design of the software environment. There are three main tasks to consider, from a practical point of view, when dealing with loosely coupled fluid-structure interactions (»loosely« refers here to the different solvers for fluid and structure):

- Time integration;
- Equilibrium iteration;
- Interpolation of data between non-conforming grids.

To facilitate the implementation of a variety of numerical methods for these tasks [1] a centralized architecture with a control instance has been chosen. By introducing a »control code« a flexible simulation steering can be achieved (e.g. starting the fluid or structural solver, checking for convergence

etc.). The different numerical techniques, e.g. iterative or simple-staggered methods for time integration, possibly with adaptive time stepping, Dirichlet-Neumann for equilibrium iteration etc., can be easily implemented.

Figure 1 shows the developed software architecture schematically. It consists of the following components:

- Control code;
- Co-processes (TauCP, AnsysCP);
- Simulation codes (Tau, Ansys, Nastran);
- MpCCI library for interpolation and communication via MPI (the MpCCI version currently used in this environment is MpCCI 3.0 SDK Standard);
- TENT;
- Other (optional) modules for data processing, visualization etc. (e.g. Tecplot).

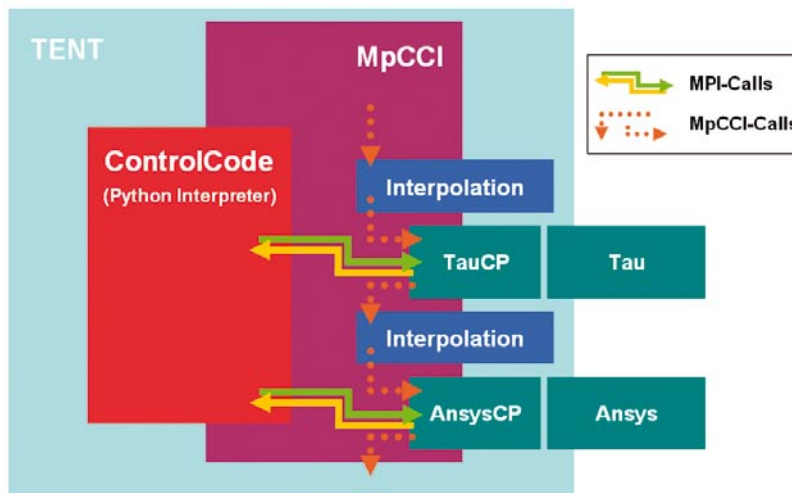


Figure 1: Architecture of the coupling environment

The communication between the individual analysis codes is based on the MpCCI library and the underlying MPI standard. The control code is connected to the analysis codes via MPI. For the communication between the control code and the simulation codes an interface specification has been worked out. This specification defines a set of basic instructions for tasks like:

- send/receive interface state quantities to/from the remote simulation code;
- direct control of the analysis codes (start solver, get/set code parameters, set boundary conditions, get results);

CONTACT

Reinhold Niesner
 Institute of Aircraft Design and
 Lightweight Structures,
 TU Braunschweig
 Hermann-Blenk-Str. 35
 38108 Braunschweig
 Germany
 Phone +49 (0) 531 391-9911
r.niesner@tu-bs.de

- operations on the interface state arrays (such as dot product, multiply, add);
- get/set quantity values directly from the control code (values are transferred via MPI); this makes it possible to perform post-processing tasks or implement specialized interpolation techniques by getting access to the grid data.

These instructions are sent by the control code via the MPI communicators provided by MpCCI to the simulation codes. The simulation codes have to either implement this specification directly or to make use of so-called »co-processes«. These are independent codes that are connected to their respective analysis codes either directly (socket connection or similar) or by file transfer. The configuration presented in Figure 1 uses two such co-processes for the DLR code Tau as flow solver and the commercial FEA package Ansys as structural solver.

CONTROL CODE

The control code is implemented in Python. Python is a powerful, high-level interpreted language. It features a very clear syntax and a vast collection of external modules for a variety of tasks. Most notable modules in the context of this paper are Numerical Python and Scientific Python. Numerical Python and provides very efficient data structures and algorithms. The data structures are fixed-type arrays of any dimensionality. Since the underlying code is well-optimized C, any speed limitations of Python's interpreter usually go away when major operations are performed in Numerical Python calls. Furthermore there are a number of operations on arrays that are much elegant to express in Numerical Python than they are with standard Python data types and syntax. Scientific Python provides, among other things, an MPI and a NetCDF interface.

The Python interpreter was extended with an MpCCI interface, consisting of two Python modules:

- `_cci` – a low-level Python module written in C;
- `cci` – a higher level module written in Python (uses the `_cci` module).

The mapping of data arrays between C in Python is done via Numerical Python arrays. The computing overhead is thus kept minimal.

A major advantage in using an interpreted language is the scripting capability offered. The steering of the simulation is performed via a Python script which is executed at runtime. The script contains the instructions that are

processed during the coupled simulation. Changing the employed time integration scheme or iteration techniques is just a matter of replacing/adapting this script. The code fragment in Figure 2 shows the implementation of the Dirichlet-Neumann iteration for a thermal coupling problem.

```
# ...

# relaxation coefficient and number of iterations
w = 0.8
maxIter = 10

# initialization
TempStruct[:] = 400.

# coupling iteration
for i in range(maxIter):

    # copy array
    TempStructOld = TempStruct.copy()

    # send temperature from StructCode to FluidCode:
    StructCode.SendInterfaceQuantity(TempStruct, FluidCode)
    FluidCode.ReceiveInterfaceQuantity(TempFluid, StructCode)

    # solve fluid:
    FluidCode.SetBCQuantity(TempFluid)
    FluidCode.Solve()
    FluidCode.GetResultQuantity(FluxFluid)

    # send flux from FluidCode to StructCode:
    FluidCode.SendInterfaceQuantity(FluxFluid, StructCode)
    StructCode.ReceiveInterfaceQuantity(FluxStruct, FluidCode)

    # solve structure:
    StructCode.SetBCQuantity(FluxStruct)
    StructCode.Solve()
    StructCode.GetResultQuantity(TempStruct)

    # relaxation:
    TempFluid = (1-w)*TempFluidOld + w*TempFluid
```

Figure 2: Code fragment showing a Dirichlet-Neumann iteration

FluidCode and **StructCode** are the analysis code objects. They are instances of the Python class **iflsSimulationCode**. This class has methods that implement the instructions defined in the interface specification mentioned above, e.g. **SendInterfaceQuantity**, **SetBCQuantity**, **Solve** etc. **TempFluid**, **TempFluidOld**, **FluxFluid**, **TempStruct** and **FluxStruct** represent the grid data on the coupling interface and are instances of the class **iflsCodeArray**. The implementation of this class allows for a simple arithmetical notation using the standard arithmetical operators $\gg + \ll$, $\gg - \ll$, $\gg \cdot \ll$ and \gg / \ll , as it can be in the last line of the code fragment in Figure 2.

In first lines of the code fragment the relaxation parameter and the maximum number of iterations are defined and the structural temperature on the coupling interface is initialized. The for-loop contains the Dirichlet-Neumann iteration: A copy of the temperature array is being made (needed later for relaxation), the temperature array is send from **StructCode** to **Fluid-Code** (via MpCCI, interpolation is performed). The temperature data is set as boundary condition for the fluid solver (**SetBCQuantity**) and a fluid analysis is performed (**FluidCode.Solve()**). The resulting heat flux on the coupling interface is then transferred to the structural code and a structural analysis is performed. The resulting interface temperature array is being relaxed with the given relaxation factor.

The operations conducted on the interface arrays (e.g. the relaxation) are performed in the simulation codes or in their co-processes for efficiency reasons. Thus, there is no need to transmit large amounts of data over MPI. However, direct access to the data can be beneficial in some situations (visualization, changes to transfer algorithm etc). Getting and setting array values from the control code is also possible in a straight-forward manner, using the Python indexing/slicing notation.

CO-PROCESSES

The direct implementation of the instruction set mentioned above in the simulation codes is not possible for commercial solvers (closed code). Furthermore, even for solvers where the source code is available, a separation between the simulation code and the coupling functionality is desirable. For this reason the developed environment makes use of so-called »co-processes«. They can be implemented in C, Fortran or Python and participate directly in the coupling process by implementing the defined instruction set.

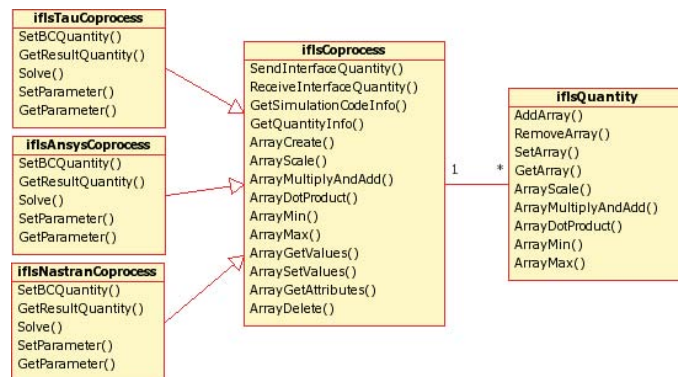


Figure 3: Class diagram for co-processes

The tasks performed by a co-process are:

- communication with the control code via MPI;
- exchange of grid data with remote simulation codes (co-processes) via MpCCI (interpolation);
- quantity operations (dot product, multiply, add etc.);
- steering of the simulation code (setting parameters, setting boundary conditions, starting the simulation, getting the results).

Of these tasks only the last is specific to each simulation code. To simplify the implementation of co-processes, a generic co-process has been developed in form of a Python class. It implements all the functionality independent of specific simulation codes (communication, exchange of grid data, quantity operations) and can be used as a template for the derived co-processes, whereby only the methods specific to the analysis code have to be implemented. The class diagram in Figure 3 illustrates this. Currently, co-processes are available for Tau, Ansys and Nastran.

TENT INTEGRATION FRAMEWORK

TENT is a software integration framework developed by DLR. It is currently used and developed in several DLR projects, including IMENS+. TENT provides a user-friendly front-end. Its main features are:

- integrated data management capabilities;
- distributed computing via network boundaries;
- online monitoring and visualization of parameters;
- data access and rights management features.

Integrating applications in TENT

In order to integrate an arbitrary application (e.g. a flow solver like the DLR-own TAU code), a software layer has to be written, which fills the gap between the framework interface and the application interface. We call this layer, which indeed takes most of the time to develop, a software wrapper. As soon as the implementation of code wrappers is finished, they will be added to a TENT starting facility, the component factory. Though the factory may reside on a completely different host, it is directly accessible through the graphical user interface of TENT. Once connected to the factory, the TENT system is ready for creating and configuring a complete workflow. Figure 4 outlines, for the technical-experienced reader, the integration principle and the communications techniques used for integration of IMENS+ components into TENT [2].

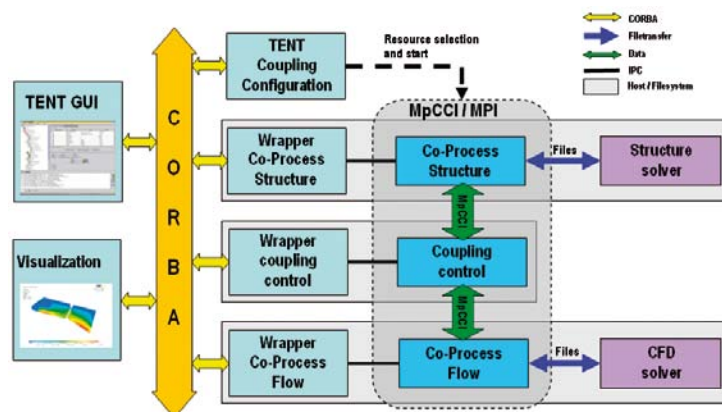


Figure 4: Integration of components in TENT

Working with TENT

Before starting a simulation, the user has to create, configure and optionally store the simulation workflow through the TENT graphical user interface (Figure 6). The procedure is outlined below:

- The user simply has to drag the needed application (in our case Tau, Ansys, Tecplot and some TENT-specific components) from the component tree on the left side of the main window to the centre of the window and drop them above the so called workflow panel;
- Once all components are present in the workflow panel, they have to be connected through special lines, called wires, which ensure the communication between the workflow components;
- After activating the components of a workflow, component-specific panels will appear above the workflow panel. These panels allow setting application-specific parameters;
- Through special steering panels at the bottom of the main window the simulation can now be controlled through mouse interaction (starting, stopping, restart and pause).

Data management with TENT

A typical simulation like the IMENS+ workflow depicted in Figure 6 consists of two kinds of data: the simulation data (mainly in-/output files) itself and meta-data needed for configuring and documenting the simulation. The TENT framework environment comes with extensive capabilities of assisting the user in this process in all of the working steps described above. Using the WebDAV protocol to enable data storage over the internet even through firewall boundaries, TENT uses the following hierarchical data structure to organize simulation data (Figure 5):

- + Projects
 - + Simulations
 - + Components
 - Configurations
 - Data Files

Projects are connected to a meta-schema, which serves as a template for the necessary meta-data for a newly created simulation. Through the meta-data itself a user is able to store all kind of information about his simulation on the data server, like version numbers of the involved codes, date and time information, notes or additional coupling information. Later on TENT offers the possibility to search these meta-data directly on the server, helping the user to find the needed simulation using the information he has specified during creation and storage of the workflow (Figure 6).

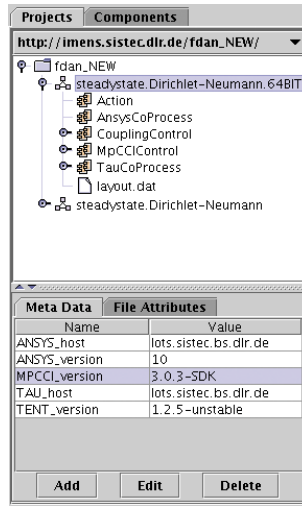


Figure 5: TENT project browser

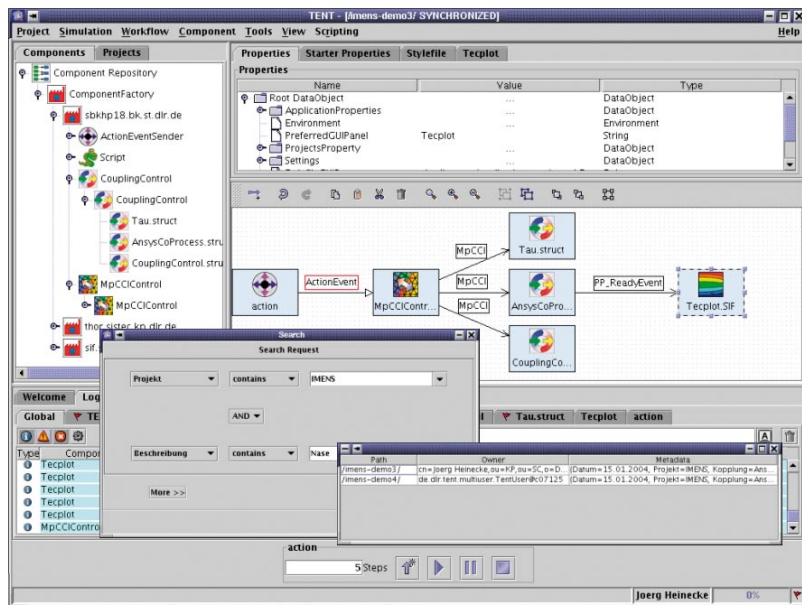


Figure 6: TENT graphical user interface

APPLICATIONS

The focus in the IMENS+ project lies on the simulation of coupled fluid-structure interactions for hypersonic applications (e.g. reentry). The developed simulation environment has been used for a series of coupled fluid-structure analyses [3, 4].

Figure 7 shows a coupled thermo-mechanical simulation with a generic 2D model. The figure shows the temperature distribution in both fluid and structural domains for a transient analysis after 300 seconds. The simulation was performed with Tau as flow solver (laminar Navier-Stokes) and Ansys as structural solver.

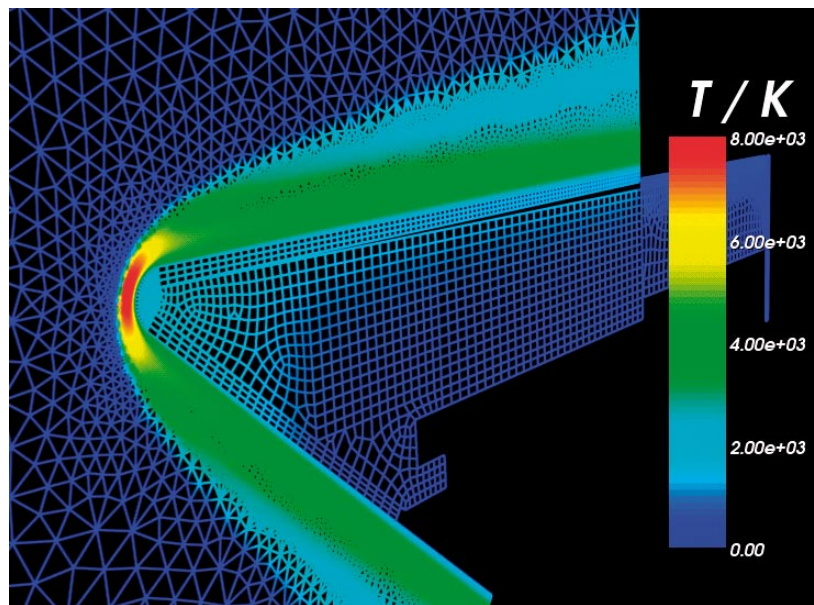


Figure 7: Coupled thermo-mechanical simulation of a generic 2D nose cap model

ACKNOWLEDGEMENTS

The presented research work was partly conducted under the contracts 50JR0121 and 50JR0504 of the German Federal Ministry of Education and Research (BMBF).

REFERENCES

- [1] M. Haupt, R. Niesner, P. Horst: Coupling Techniques for Aero-Thermo-Elasticity; Proc. of Int. Conf. on Computational Methods for Coupled Problems in Science and Engineering, Coupled Problems 2005, Santorin, 2005

- [2] A. Schreiber, T. Metsch, H.-P. Kersken: A problem solving environment for multidisciplinary coupled simulations in computational grids; Future Generation Computer Systems - The International Journal of Grid Computing: Theory, Methods and Applications, Volume 21, Issue 6, S.942-952, 2005
- [3] R. Schäfer, A. Mack, B. Esser, A. Gülhan: Fluid-Structure Interaction of a Generic Model of a Reentry Vehicle Nosecap; Proc. 5th Int. Congress on Thermal Stresses and Related Topics, Blacksburg, VA, WA-1-2-1, 2003
- [4] A. Mack, R. Schäfer: Flowfield topology change due to fluid-structure interaction in hypersonic flow using ANSYS and TAU; In: New Results in Numerical and Experimental Fluid Mechanics IV, vol. 87, Springer, Berlin, 2004

TOWARDS CONSTRUCTION OF A NUMERICAL TESTBED FOR NUCLEAR POWER PLANTS

Osamu Hazama, Dr. Yoshio Suzuki, Hitoshi Matsubara, Rong Tian, Akemi Nishida, Masayuki Tani and Norihiro Nakajima, Center of Computational Science Systems, Japan Atomic Energy Agency

An expectation towards today's computational simulations to accurately forecast the future and provide quantitative predictions is growing. The numerical simulations must be able to reproduce physical phenomena of various complexity, and temporal and spatial scales as well as their interactions. One of the goals of computational science is to help society make important decisions. Safety assessment and performance certification of complex engineering systems such as nuclear power plants is one such important issue to be tackled by numerical simulations since controlled laboratory experiments can be prohibitive, or even impossible, in many ways.

At this moment, no controlled experiments are possible to deal with structural integrity of an entire full-scale nuclear reactor and its cooling systems. This is due to the fact that nuclear power plants are large in scale and functionally very complex structures. Although for safety precautions, they are designed and maintained under very strict layers of fail-safe rules, many of the design parameters are empirically determined, or are determined from limited experimentations.

In order to evaluate safety of nuclear power plants in more deterministic way, many expect virtual experiments by computational science can provide data on an entire facility necessary for the society to make correct decisions. Aging and phenomenon such as earthquakes are some of the factors, which must always be considered when assessing present and future safety of nuclear power plants. In order to maintain safety of nuclear power plants against phenomenon such as extra-large earthquakes and factors such as aging, the Japan Atomic Energy Agency (JAEA) is currently constructing a fully three-dimensional numerical testbed on the ITBL Grid infrastructure.

The numerical simulations of complex structures such as nuclear power plants will inevitably become large in scale, which will require much more effort in many aspects. Various developments have been made in hardware, and numerical simulation software and techniques enabling large-scale simulations. However, as the problem size enlarge, many complications arise in constructing the necessary data sets for and visualizing the results from such large-scale numerical simulations.

In order to solve the problem at this preprocessing phase, which is the construction of a simulation domain model, the authors proposed and implemented a high-performance finite element elastostatic simulation procedures based on component and part-wise assembly. Normally, every part to be included in the simulation is meshed as a single model. However, it is quite difficult to mesh complex and thin nuclear reactor structures as illustrated in Figure 1. Even if the geometric problems can be overcome, meshes in the order of tens and hundreds of million cannot be constructed on a PC due to time/memory limitations. In order to accurately carry out numerical simulations, mesh should be made carefully controlling its size, aspect ratio, etc. This becomes possible only if the meshes are constructed at part-level. Through this approach, the authors were able to construct a finite element model of an experimental high-temperature gas reactor (HTGR) called HTTR, or High Temperature engineering Test Reactor (Figure 1).

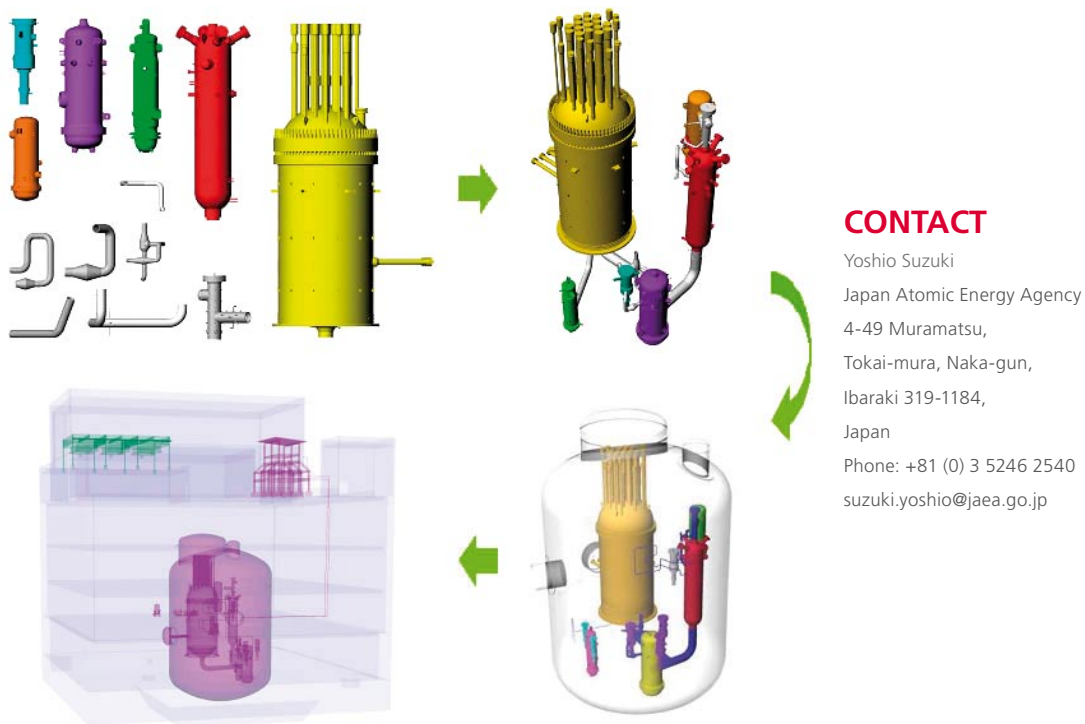


Figure 1: Assembly model of HTTR (High Temperature engineering Test Reactor)

Currently, the discontinuities at the part boundaries are unified by a penalty. Not only are the nodal displacements constrained, but also the displacements, which occur at mesh (overlay) crossings are constrained by penalty and finite element shape functions. This allows more continuous treatment of the discontinuous inter-part discontinuities.

Using the above finite element simulation system, an elastostatic computations were carried out for nuclear reactor structural data depicted in Figure 1. Twenty six parts were considered. The model consists of 33,692,145 1st order tetrahedral mesh and 7,573,604 nodes. Therefore, the number of unknowns (nodal displacements) to be solved is 22,720,812. The SGI Altix supercomputer system at JAEA, ranked 21st in the newest Top 500 list, was used. Approximately, 8 hours were required to solve this problem using 128 PEs. For a smaller problem of the same model consisting of approximately 6 million degrees of freedom, approximately 7633 and 4129 seconds were required to solve this problem using 64 and 128 PEs, respectively. The results acquired, the displacement and von Mises equivalent stress distributions, are illustrated in Figure 2.

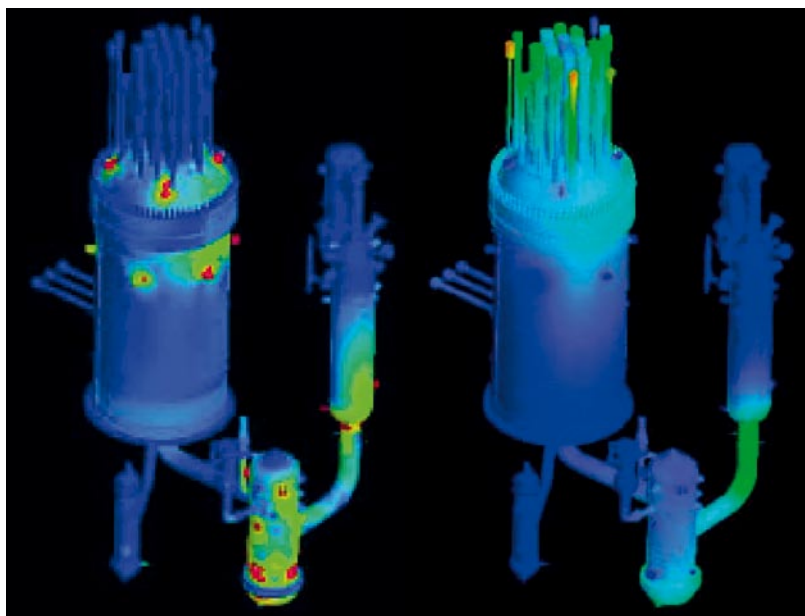


Figure 2: Displacement (left) and von Mises equivalent stress (right) distributions

In order to carry out more detailed simulations, the number of parts will grow to tremendous amount, which will make it impossible to distribute this vast number of parts to an open CPU by human hands. It is believed that Grid infrastructure and its tools can aid this process.

In the recent years, substantial effort has been put into realizing a notion recognized as the Grid, which enables sharing of various resources including computational hardware, software, database, etc. Although there still exists arguments on what exactly the Grid is, it will most likely aid in efficient execution of research activities in various engineering and science fields by organically coupling various resources. In Japan, the Japan Atomic Energy Agency (JAEA) has been taking on a role of developing an infrastructure for realizing a Grid called the ITBL (Information Technology Based Laboratory). This infrastructure aims to construct a virtual laboratory environment which overcomes most difficulties associated with the sharing of computational hardware and software resources, numerical data and results, information. It also provides on-line conferencing system for meetings among members located physically apart from one another. Figure 3 illustrates the current status of the ITBL. Over 20 systems located throughout Japan are connected amounting to over 45 TFLOPS.

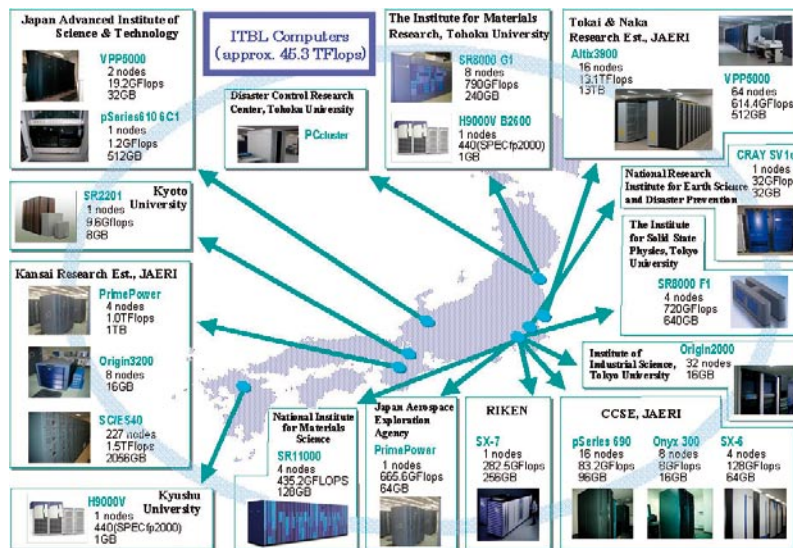


Figure 3: Current status of ITBL (Information Technology Based Laboratory)

The authors have proposed and implemented an assembly modeling and simulation of nuclear reactors, however, a competent system to handle large number of parts and visualization of the results are necessary. Therefore, a project is currently underway to construct a numerical testbed on the ITBL infrastructure for assessing safety of existing nuclear power plants. The image of and partially completed system is illustrated in Figure 4.

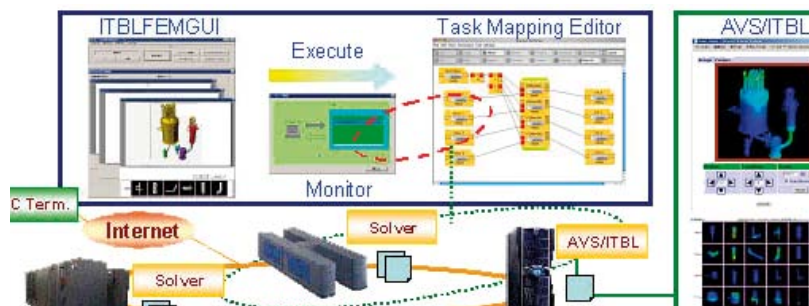


Figure 4: System image (Simulation to visualization) for part-assembly simulation

In the future, transient analysis of structural deformation of nuclear reactor combined with heat transfer and radiation with helium and water coolant flows will need to be solved simultaneously. MpCCI is believed to become a useful tool for this purpose. The coupling mechanism on the ITBL Grid will be developed upon STAMPI and MpCCI. The STAMPI (Seamless Thinking Aid Message Passing Interface) library, developed by JAEA, is a communication library based on the MPI-2 specifications with several unique features. The MpCCI (Mesh-based parallel Code Coupling Interface) library, which is developed by Fraunhofer SCAI, acts to exchange and interpolate the physical values between the simulation codes (meshes and grids). Inclusion of MpCCI into the simulation system in Figure 4 is believed to open up new possibilities for better understanding of unique nuclear related structures and its safety.

FLUID-STRUCTURE INTERACTION IN ABDOMINAL AORTIC ANEURYSMS

Uwe Janoske, University of Cooperative Education Mosbach; Gerhard Silber, Michael Stanull, Günter Benderoth, Fachhochschule Frankfurt am Main, Institut für Materialwissenschaften; Ralf Kröger, FLUENT Deutschland; Thomas Schmitz-Rixen, Gefäß- und Endovascularchirurgie, Thomas J. Vogl, Diagnostische und Interventionelle Radiologie, Klinikum der Johann Wolfgang Goethe-Universität Frankfurt am Main; Rainer Moosdorf, Herz- und Thorakale Gefäßchirurgie, Klinikum der Philipps-Universität Marburg

ABSTRACT

The abdominal aortic aneurysm (AAA) is a frequent illness affecting approximately 15% of all males at the age of 65 or more years. The chance of survival in the case of a rupture of the aneurysm is very limited. Whereas the chances of survival by replacing the aneurysm before a rupture is very high. Diagnostically the discovery by means of CT and NMR is no problem. However, there is an uncertainty in the question, when such an aneurysm has to be operated. A diameter of 55 mm of the aneurysm is a critical value, obtained from two studies. However, this gives only a statistically security of preventing a rupture. In addition, smaller aneurysms can perforate but also larger ones can remain stable for many years, so that the individual risk can not be determined.

By a coupled simulation of the flow and the deformation in the aneurysm it is possible to gain a deeper understanding of the stresses and strains in the aneurysm, which could lead to a rupture of the aneurysm.

The geometry of the aneurysm is determined by computer tomography and was reconstructed as a CAD model using the software Mimics (Materialise, Belgium). For the simulation of the flow the CFD-Code FLUENT is used, whereas the structural mechanical behaviour is described using the FEM-Code ABAQUS. For describing the behaviour of the vascular tissue a strain energy function of Ogden type for weak-compressible material is used. The parameter identification is done on basis of tensile tests with AAA material coming out from patients. The coupling of these two codes can be done by using MpCCI, developed by the Fraunhofer Institut SCAI in Sankt Augustin.

INTRODUCTION

The abdominal aortic aneurysm (AAA) is a frequent illness affecting approximately 15% of all males at the age of 65 or more years. The chance of survival in the case of a rupture of the aneurysm is very limited. Whereas the chances of survival by replacing the aneurysm before a rupture is very high. Diagnostically the discovery by means of CT and NMR is no problem.

However, there is an uncertainty in the question, when such an aneurysm has to be operated. A diameter of 55 mm of the aneurysm is a critical value, obtained from two studies. However, this gives only a statistically security of preventing a rupture. In addition, smaller aneurysms can perforate but also larger ones can remain stable for many years, so that the individual risk can not be determined.

By a coupled simulation of the flow and the deformation in the aneurysm it is possible to gain a deeper understanding of the stresses and strains in the aneurysm, which could lead to a rupture of the aneurysm.

SIMULATION MODEL

In the following sections the simulation model is described in detail. Apart from the geometry, the simulation models for the blood flow and the surrounding structure will be presented separately. Finally the coupling process of the two codes will be explained.

Geometry

Figure 1 shows one of approx. 150 sectional views of an abdominal aortic aneurysm, which originates from a computer tomography and was used as a basis for the reconstruction of the CAD data. Apart from the flow area (light-grey), an area of coagulated blood (thrombus) can be seen inside the aneurysm (dark).

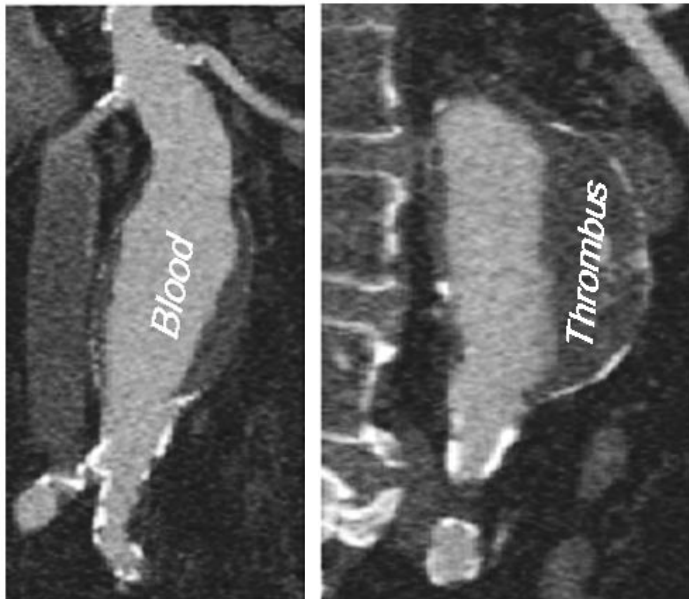


Figure 1: Cross-sections from CT data for an abdominal aortic aneurysm.

CONTACT

Uwe Janoske
University of Cooperative
Education Mosbach
Lohrtalweg 10
74821 Mosbach,
Germany
Phone: +49 (0) 6261 939 478
janoske@ba-mosbach.de

The CT-data was used for the reconstruction of the geometry of the aneurysm using the software Mimics from Materialise. Figure 2 shows the reconstructed geometry with different branches and bifurcations.

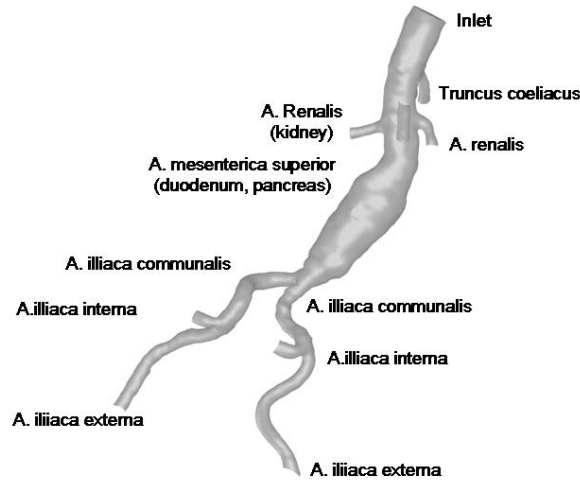


Figure 2: Reconstructed 3D-geometry of the aneurysm with inlet and different outlets.

CFD model

Figure 3 shows the CFD mesh used for the calculation of the blood flow. The flow is assumed to be laminar. The thrombus which is inside the vascular tissue is assumed to be non-porous, so that the thrombus can be treated as a structure (see section 2.3).

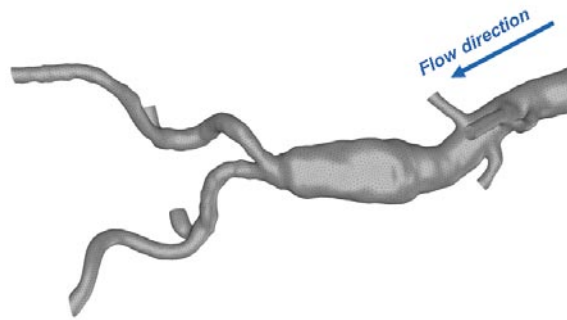


Figure 3: CFD-mesh for the blood flow

The non-Newtonian behaviour of the blood flow is modelled using a Carreau model according to Eq. (1):

$$\mu = \mu_{\infty} + (\mu_0 - \mu_{\infty}) \left[1 + (\dot{\gamma} \lambda e^{T/T_0})^2 \right]^{(n-1)/2} \quad (1)$$

The parameters in Eq. (1) are fitted to experimental data [10] assuming isothermal flow conditions ($T = T_0 = 310\text{ K}$):

$$\begin{aligned}\mu_0 &= 0.44826\text{ Pa s} \\ \mu_\infty &= 0.00293\text{ Pa s} \\ n &= 0.2926599 \\ \lambda &= 6.7474\text{ s}\end{aligned}$$

Figure 4 shows the dynamic viscosity plotted against the shear rate for the fitted values as well as experimental data.

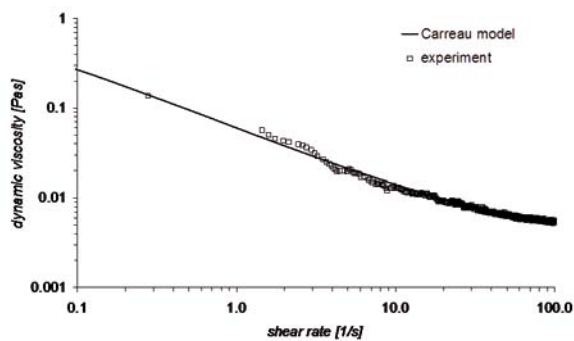


Figure 4: Dynamic viscosity for blood as a function of the shear rate for a constant temperature $T_0=310\text{ K}$

The values for the boundary conditions at the inlet and the outflow are taken from experimental data by Fung [2]. At the inlet a constant velocity is used. The flow rates at the outflow boundaries are:

OUTFLOW	VOLUME FLOW/INLET VOLUME FLOW [%]
Truncus coeliacus	17.53
A. mes. superior	14.43
A. renalis	10.31
A. renalis	10.31
A. iliaca interna	6.19
A. iliaca interna	6.19
Leg 1	17.52
Leg 2	17.52

Structure

The structure, which is shown in Figure 5, consists of the three components: vascular tissue, thrombus as well as the surrounding fat tissue.

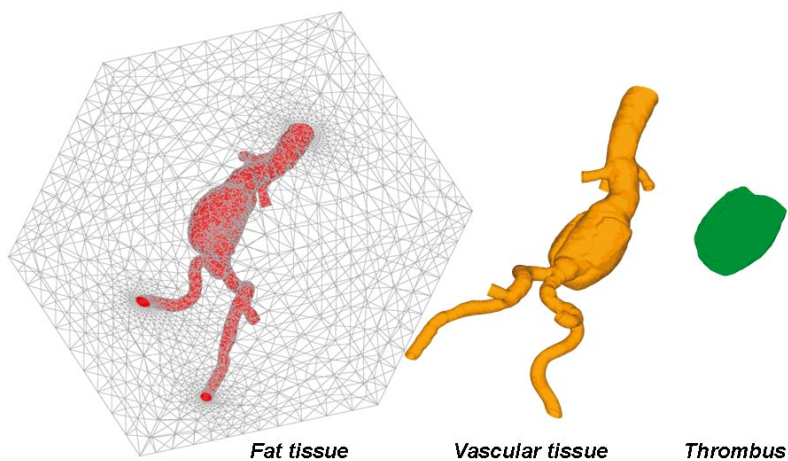


Figure 5: FEM-mesh: fat tissue, thrombus, vascular tissue

The fat tissue was modelled as a rectangular volume and is only used for the implementation of the displacement boundary conditions of the structure which will be fixed at the outer walls of the fat tissue.

The material behaviour of the structure (fat and vascular tissue) is described using a hyperelastic material behaviour after Ogden [5]. Based on measurements of Silber [11] the material parameters can be identified:

HYPER-ELASTIC	ρ [KG/M ³]	μ [PA]	α [-]	D_1 [-]
Vascular tissue	1000	$2.369 \cdot 10^5$	13.695	$8.442 \cdot 10^{-8}$
Fat tissue	900	$7.422 \cdot 10^3$	2.7808	$2.6948 \cdot 10^{-6}$
LINEAR-ELASTIC	ρ [KG/M ³]	E [PA]	ν [-]	
Thrombus	1000	$2.0 \cdot 10^4$	0.45	

The behaviour of the thrombus is assumed to be linear-elastic.

Figure 6 shows the stress plotted against the strain for the three different materials. Beside the measured parameters for the vascular tissue, variations for the coefficient were used (variation 1: $\alpha=14.695$, variation 2: $\alpha=12.695$).

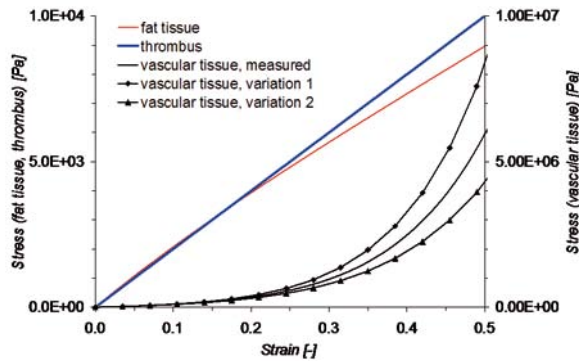


Figure 6: Stress as a function of the strain for the materials used.

Fluid-structure-interaction

For the coupling of fluid and structure MpCCI version 3.0.4 is used, whereby the displacements (from ABAQUS to FLUENT) and relative wall forces (from FLUENT to ABAQUS) are exchanged.

NUMERICAL RESULTS

In the following section, the numerical results are presented for steady-state simulations. The simulations should help the surgeon to decide if a surgery is necessary or not. Therefore, the surgeon needs the information as soon as possible after the CT-analysis. Transient simulations are very time-consuming, so the method of analyzing steady-state results was taken into account.

Steady-state flow conditions

For the characterization of the influence of different parameters, steady-state simulations are used. Beside the volume flow, the material parameters have been varied. Figure 7 shows the displacements and the stress of the vascular tissue.

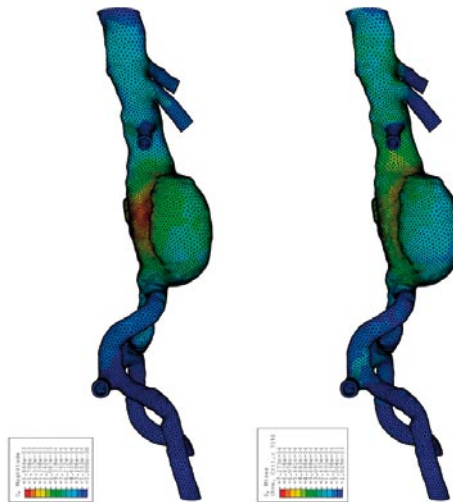


Figure 7: Displacements and stress of the vascular tissue

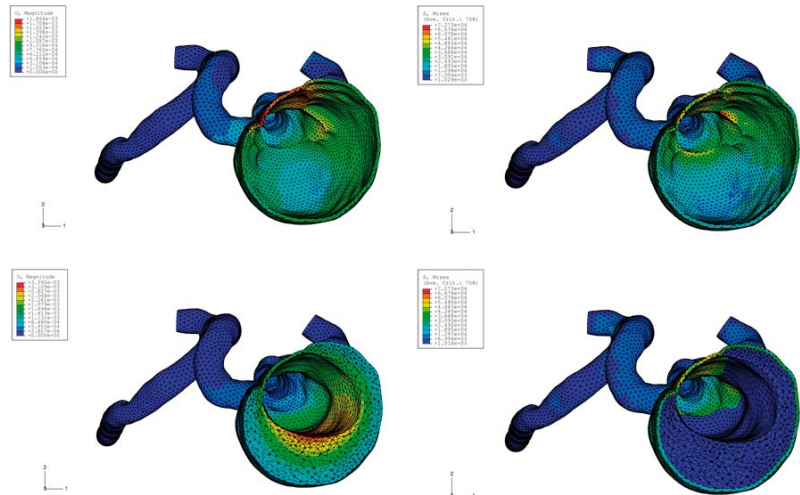


Figure 8: Displacements and stress of the vascular tissue and the thrombus in a cross section
– left: without thrombus, right: with thrombus

The results show the expected behaviour, i.e. higher volume flows lead to higher stress and larger displacements. The variations of the material parameters of the vascular tissue also show the expected behaviour of larger displacements for weaker vascular tissue. The maximum displacement can be found in the middle of the thrombus.

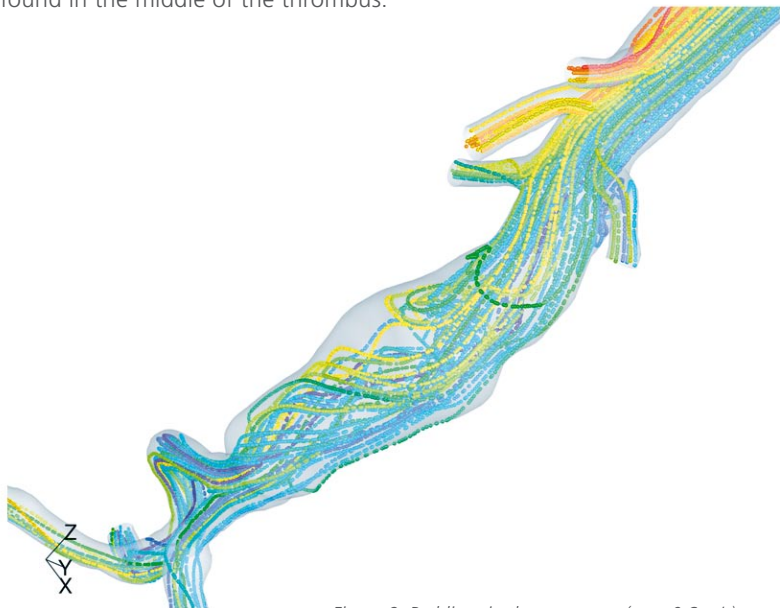


Figure 9: Pathlines in the aneurysm ($v_{inlet} = 0.6 \text{ m/s}$)

Figure 9 shows the pathlines in the aneurysm.

CONCLUSIONS

The fluid-structure interaction in an infrarenal aortic aneurysm using FLUENT and ABAQUS has been shown. Steady-state simulations have been made. The material properties have been determined by various experiments which will be continued to have a larger database also for different patients.

REFERENCES

- [1] D'Audiffret, A., Santilli, S., Tretinyak, A., Roethle, S., Fate of the ectatic infrarenal aorta: expansion rates and outcomes. *Ann Vasc Surg* 2002; 16:534-6.
- [2] Fung, Y. C., *Biomechanics –Mechanical Properties of Living Tissues*, Springer (1993).
- [3] Greenhalgh, R. M., Powell J.T., Screening men for aortic aneurysm. *Bmj* 2002; 325:1123-4.
- [4] Nicholls, S. C., Gardner, J. B., Meissner, M. H., et al, Rupture in Small Abdominal Aortic Aneurysms, *J. Vasc. Surg.* 28:884-888 (1998).
- [5] N.N, ABAQUS Theory Manual.
- [6] N.N, FLUENT Theory Manual.
- [7] Ortega, H. V., Computer Simulation Helps Predict Cerebral Aneurysms, *Journal Articles by Fluent Software Users*, JA071 (1999).
- [8] Raghavan, M. L., Vorp, D. A., Federle, M. P., Makaroun, M. S., Webster, M. W., Wall stress distribution on three-dimensionally reconstructed models of human abdominal aortic aneurysm, *Journal of Vascular Surgery*, Vol. 31, Number 4 (2000).
- [9] Richens, D., Field, M., Neale, M., Oakley, C., The mechanism of injury in blunt traumatic rupture of the aorta, *European Journal of Cardio-Thoracic Surgery* 2 (2002) 288-293.
- [10] Alizadeh, M., Benderoth, G., Kasseckert, M., Rzepka, M., Stanull, M., Vogt, S., Moosdorf, R., Silber, G., Calculation of haemorheological properties for cardiovascular diagnosis based on ultra sound measurements of velocity profiles, *Cardiovascular engineering*, Vol. 10, Number 1 (2005).
- [11] Silber, G., Schrod, M., Benderoth, G., Abolmaali, N., Vogl, T. J., An in vivo-method to determine the mechanical behaviour of human soft tissue, *Proceedings CADFEM Users Meeting, Zürich* (2005).
- [12] Steinman, D. A., Milner, J. S., Norley, C. J., Lownie, S. P., Holdsworth, D. W., Computed Blood Flow Dynamics in an Anatomically Realistic Cerebral Aneurysm, Internet: steinman@irus.rrl.ca, www.irus.rrl.ca/~steinman.

CUSTOMIZATION OF MPCCI FOR USE BY DEVELOPMENT TEAMS: MAGNETO-THERMAL SIMULATIONS

Ian Lyttle, Benjamin Pulido, Ali Zolfaghari, Kevin Parker, Schneider Electric

INTRODUCTION

One of the most attractive features of MpCCI is Fraunhofer's philosophy not to limit the possibilities of the user. However, for the non-expert user, this feature may appear to be an obstacle. The goal of this work is to demonstrate that the openness of the MpCCI program can be used to make specific customizations, hence reducing the effort (beyond the construction of the single-physics simulations) needed to make MpCCI-coupled simulations.

Prior to the commercialization of MpCCI, Schneider Electric had developed internally a code-coupling tool to estimate the temperature rise within electrical distribution equipment [1]. Consequently, there is awareness within Schneider Electric of the requirements and expectations for such coupled analyses. Furthermore, the competencies to construct both the electromagnetics and thermal simulations are well established. From the perspective of the non-expert MpCCI user within Schneider Electric, reducing the additional effort needed to use the MpCCI tool will make the tool more attractive. The goal of this customization is that the effort needed to use MpCCI will comprise less than 5% of the effort needed to construct either of the single-physics simulations.

The type of coupled analysis considered here is called different things by different people: magneto-thermal, electro-thermal, CFD-emag, among others. For this work, it is proposed to use the term magneto-thermal. Although the names may be different, the principle is often the same. An electrical device has alternating current flowing through it, causing a resistive heating (Joule heating). This causes a temperature rise, which increases resistivity of the conductors, increasing the heating.

For the present work, the electromagnetic behavior is calculated using FLUX (developed by Cedrat), the thermal behavior is calculated using ICEPAK (developed by Fluent Inc.), and the coupling is managed using MpCCI. It should be noted that ICEPAK is used as the preprocessor for the thermal simulation; ICEPAK uses FLUENT as the flow solver. The flow of information is shown in Figure 1.

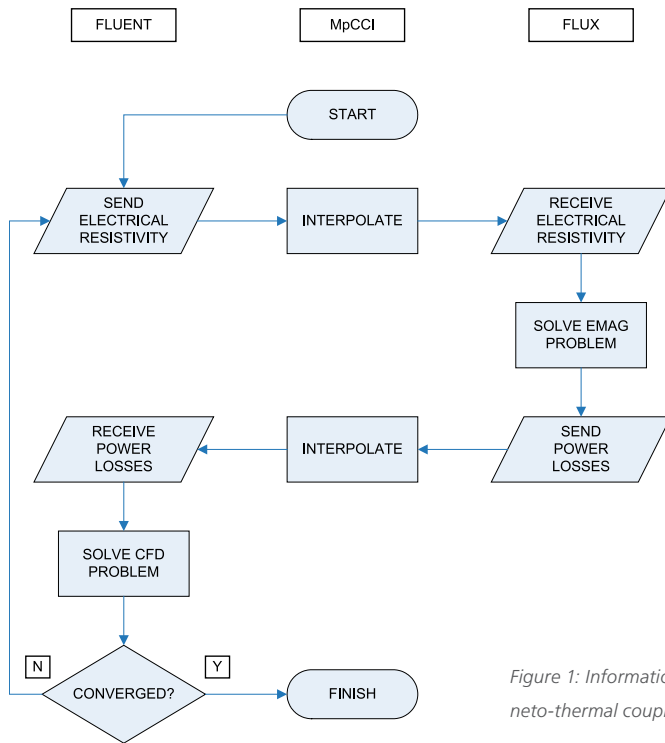


Figure 1: Information flow for magneto-thermal coupled simulation

CONTACT

Ian Lyttle
 Schneider Electric
 3700 6th Street SW
 Cedar Rapids, IA 52404
 USA
 Phone: +1 (319) 368 3033
 ian.lyttle@
 us.schneider-electric.com

ICEPAK is designed such that the user need never know explicitly how to use FLUENT; the solver is kept in the background. The goal for the customization of ICEPAK for MpCCI is the same: the user does not need to know how to use FLUENT, although it is the CFD solver.

The process used by the Schneider Electric end-user for the MpCCI coupling is outlined in Figure 2. For the ICEPAK user and the FLUX user, there are some additional steps which describe the geometric requirements and naming convention for coupled zones. The ICEPAK user and the FLUX user will each save and close their respective projects, so that some additional processing can be done on the project files. This processing is made using scripts developed within Schneider Electric; however, an advanced user of the software and MpCCI can write similar scripts with a modicum of effort.

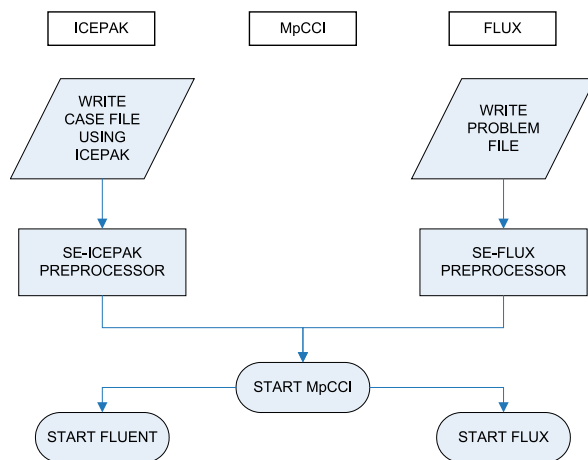


Figure 2: Outline of end-user process for magneto-thermal simulations within Schneider Electric

EXAMPLE: 3D BUSBAR SYSTEM

The example shown here is a busbar system carrying three-phase current. The busbars are made from copper; the RMS-current level is 1600 A. Buoyant air moves around the busbars, cooling the system. Parts of the ICEPAK mesh are shown in Figure 4. The FLUX mesh, although not shown, is similar in scale to the ICEPAK mesh.

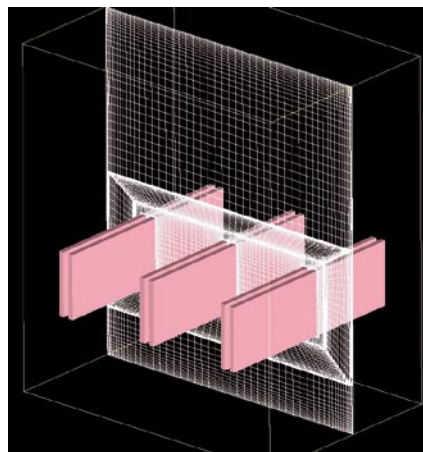


Figure 3: ICEPAK mesh used for coupled simulation of 3D busbar system

Figure 5 shows how the FLUENT and FLUX simulations each move towards agreement with each other. The first result from FLUX

gives a power loss for the system of 41.2 W. For this initial FLUX calculation, ICEPAK provides a maximum temperature in the system of 323 K. It is seen that the coupling takes seven steps, giving a power loss of 44.8 W and a maximum temperature of 324 K. Figure 6 shows the final power-loss density calculated using FLUX. Figure 7 shows the final temperature distribution calculated using ICEPAK.

CONCLUSIONS AND PERSPECTIVES

Within Schneider Electric, we have a need for a coupled magneto-thermal simulation tool. We have everyday users of ICEPAK and of FLUX, but these

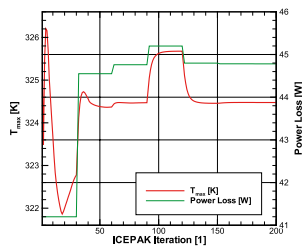


Figure 4: Demonstration of convergence towards agreement for the coupled simulation

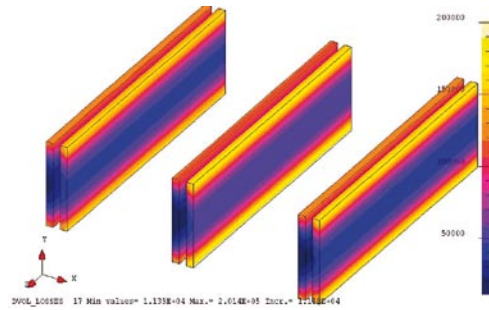


Figure 5: FLUX results: power-loss density [W/m3]

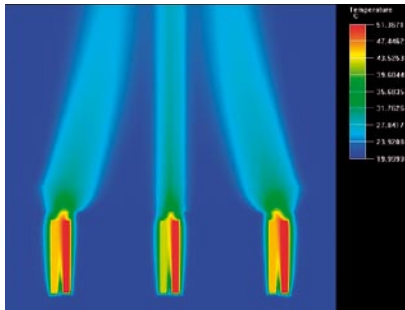


Figure 6: ICEPAK results: temperature distribution [K]

are not necessarily the same people. By customizing the MpCCI interface for use with magneto-thermal simulations using ICEPAK and FLUX, we provide our end users with a coupling tool that adds very little additional effort in building models.

In the introduction, it is noted that one of the most attractive features of MpCCI is its open architecture, allowing for specific customizations. This idea applies equally to the suppliers of the simulation software. Because Fluent Inc. and Cedrat offer open and effective API's for their software, and because these companies have shown enthusiastic support for the MpCCI platform, Schneider Electric is able to use best-in-class software for its coupled simulations.

REFERENCES

- [1]] T. Reed, J. Richter and C. Rodrigues, A Novel Approach for Achieving Coupled Electromagnetic-Thermal Analysis Capability. Proc. of 10th AIAA/ISSMO Multidisciplinary Analysis and Optimization Conference (AIAA-2004-4327)

FLUX FOR ELECTROMAGNETIC DESIGN, EXTENDED TO MULTIPHYSICS USING MPCCI

Sebastien Cadeau Belliard, CEDRAT

INTRODUCTION

CEDRAT Group aims to provide innovating solutions in the electrical and mecatronic fields, from the development of software tools to study, design and manufacture of systems. Well known for FLUX, a leader for the modelling of low frequency electromagnetic phenomena, CEDRAT Group provides a complete range of software solutions in electrical engineering.

FLUX, LEADER FOR ELECTROMAGNETIC SIMULATION AND DESIGN

Backed by nearly 30 years of experience in electromagnetic Finite Element software development, FLUX remains on the cutting edge of the electromagnetic modelling technology to ensure both performance and reliability to its users. A complete range of possibilities makes FLUX a powerful multi-purpose tool for 2D and 3D electromagnetic, electrothermal and electromechanical analysis.

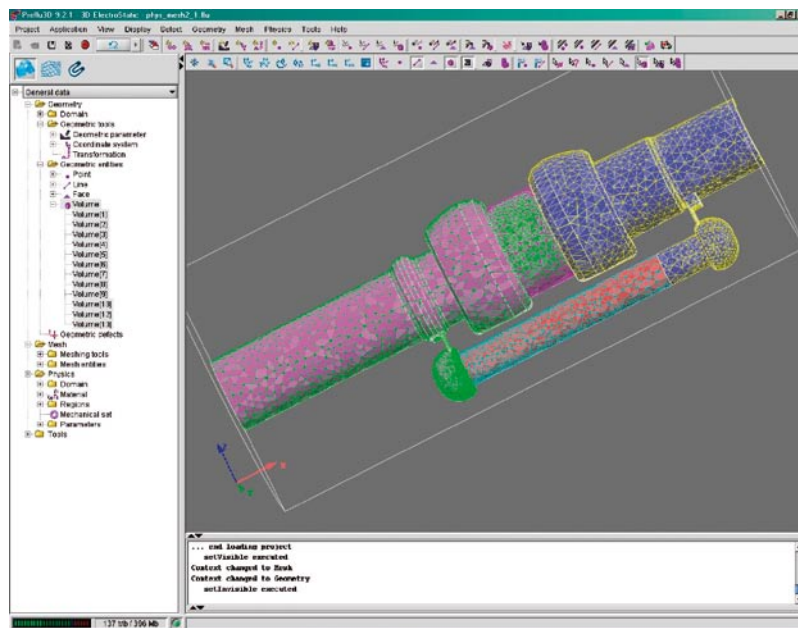


Figure 1: Import and mesh of a PRO/E file in FLUX

FLUX features, among others:

- Multiparametric capabilities,
- Couplings to electrical circuit and motion,
- Advanced import capabilities,
- High level support...

Multiparametric capabilities

For years, FLUX has featured multiparametric capabilities for pre-processing, solving and post-processing.

Any type of value may be changed and varied: geometric quantity (dimension or relative positioning), mesh, materials properties, sources, electrical circuit, boundary conditions, frequency, slip for asynchronous machines, time and many more...

There are no limit to the number and the type of parameters that may vary in a same solving: for example materials, sources and geometry may be modified in the same simulation run to get the optimised configuration of the device or system.

From those multiparametric computations, all valuable results may be obtained as function of any of the parameters (2D, 3D curves, nD table of results, AVI animations, FFT...)

Coupling to electrical circuit and motion

To account for supply and load of the device or system, external electrical circuit may be connected to the simulation. Various components are available in the simulation: switches and diodes, passive components, conductors, sources, motor components (squirrel cage and brush-segment component).

Moreover, FLUX is able also to account for linear and rotating motion in 2D and 3D. It enables to compute both the electromagnetic behaviour and the cinematic values: position, speed, acceleration, force and torque.

Advanced import capabilities

FLUX features advanced import capabilities for CATIA, PRO/Engineer, Inventor, Patran, Nastran as well as import of all main formats (STEP, IGES, SAT, DXF, UNV...). Those import capabilities are accompanied with tools to:

- heal tolerance problems,
- stitch free faces,
- imprint solid assemblies.

CONTACT

Sebastien Cadeau Belliard

CEDRAT SA

15, Chemin de Malacher -
inovallée (ex-ZIRST)

38246 Meylan

France

Phone: +33 (0) 476 90 5045

sebastien.cadeau-belliard@

cedrat.com

High level support

Fast and efficient technical support is one of the key service the user must find to enhance its productivity using a software package. FLUX is accompanied with a complete documentation made of user guides and many use cases for every main application of the software. FLUX technical support teams are composed of electrical engineering PhDs and engineers and provide advanced technical support and trainings to end users.

MULTIPHYSICS CAPABILITIES

Introduction

To enhance its capabilities and run simulation on a system scale, FLUX may already be coupled for a co-simulation with Simulink. This link enables to account for complex command laws and regulation loops keeping a very high accuracy in the magnetic field computation (including eddy currents, skin effect, motion...). In order to extend the capabilities of FLUX to other physical domains, the best solution for the end user is to be able to interact with the best products in their respective application fields. The end user can then seize the advantages of both leading packages to get the best results possible.

Goal of the extension to multiphysics

The multiphysics capabilities of FLUX provide the possibility to couple FLUX to other packages:

- using or not Finite Element method (can be coupled to package dedicated to network simulation, to analytical package)
- dedicated to any physical domain (thermal, mechanical, CFD...)

Two ways to run multiphysics simulation

Two ways have been chosen in FLUX to run a multiphysics simulation:

- FLUX as a software: the exchanges between both packages are made using data files and each package is seen as an executable,
- FLUX as a component of a package: the exchanges between both packages are made using FLUX's API (Application Program Interface). FLUX is then integrated in the other package as a dll.

AN EXAMPLE WITH MPCCI

The links with MPCCI brings a lot to the multiphysics capabilities of FLUX. Its premium interpolation method enables an accurate coupling between FLUX and other packages. It also provides an interface for multiphysics co-simulations, as well as it opens doors to co-simulation with other packages.

An example will be shown during the MPCCI User forum.

CONCLUSION

To complete the capabilities of FLUX to other physical domains, CEDRAT added new features for multiphysics computations. Communicating with MPCCI, FLUX provides to its customers the best connection possible to other premium packages.

Various multiphysics computations can then be run, using the best solutions on the market for their respective physical domain.

ELECTRO-THERMAL ANALYSES OF GAS INSULATED SWITCHGEAR TO PREDICT THE TEMPERATURE RISING

J. S. Ryu, H. Y. Kang, B. B. Hyun, S. W. Lee, Y. G. Kim, Y. J. Shin, LS Industrial System, Korea

In this paper, the tank surface of 3-phase GIS (Gas Insulated Switchgear) is analysed to predict the temperature rising. Usually, because the rating current and the cut-off current of GIS are very high, the high pressure gas (SF6) is used to prevent the breakdown of the insulation and to extinguish the arc generated during cutting off the incident current. Therefore, GIS is assembled in the steel tank.

At the steel tank the eddy current is induced and this becomes the reason of the overheating of the tank more than the reference level. The eddy current is depending on the materials and the structure of the tank.

In this paper, the eddy current distribution is analysed using ANSYS and the thermal distribution is analysed using FLUENT as the sets of MpCCI. The analyses are performed for the several models. And we will suggest a model which is the best one to reduce the temperature rising.

**ONLY ABSTRACTS.
PRESENTATIONS WERE CANCELLED SHORTLY.**

USE OF MPCCI TO PERFORM ELECTRO-THERMAL ANALYSES FOR AIR CIRCUIT BREAKER

H. Y. Kang, J. S. Ryu, B. B. Hyun, S. W. Lee, Y. G. Kim, Y. J. Shin, LS Industrial System, Korea

The purpose of this work was to produce a simulation model of ACB (Air Circuit Breaker) for stationary coupled analysis of current and temperature field using with MpCCI and to determine the materials of the ACB main circuit parts which are overheated.

We changed several major parameters of current-rating and materials affecting on electro-thermal results. Towards this end, interpolation software package called MpCCI is used to Electro-Thermal set of analyses using ANSYS (Electro-MAGnetic) and FLUENT (heat-transfer). Electrical power losses are calculated in the ANSYS and heat source (power losses) is calculated in the FLUENT. The results are satisfied and it got the good results.

The Inverter is the device which converts the D.C. (Direct Current) with the A.C. (Alternating Current) electrically.

The input gets the electricity to be supplied from a common use power supply, it fluctuates a voltage and a frequency, provide at the electric motor and it supplies with the speed of the electric motor uses at efficiency and controls.

In this paper, We analysis the 550kW class inverter inside thermal and temperature distribution due to the heat source of the IGBT, DIODE with 3-D commercial fluid dynamics called ICEPAK.

The heat source of the inverter has many of capacitor problems like the length of life and error of the elements, this lead the heat-sink, fan and duct and it is the a system where become conduction, natural-forced convection. The temperature is decided in inverter by many parameters. The analysis through the experiment is the limited. We can efficient thermal design at fast through the numerical analysis. The size of the inverter with final follows in heat-sink form and it needs to changes the optimization and miniaturization.

The inside structure of the inverter was complicated and when only the lower part (heatsink, heat sources and fan etc.) numerical analysis and when the whole model numerical analysis, there was 15 difference.

For the optimum thermal design of the inverter the frame location and shape change of heat-sink it will be satisfactory and it got the good results.

CONTACT

Jae Seop Ryu
LS Industrial Systems Co.
1 Songjeong-Dong
Huengduk-Gu
Cheongju-City, 361-720
Korea
Phone: +82 (0) 43-261-6535
jsryu2@lisis.biz

Han Young Kang
LS Industrial Systems Co.
1 Songjeong-Dong
Huengduk-Gu
Cheongju-City 361-720
Korea
Phone: +82 (0) 43-261-6535
hykang1@lisis.biz

Fraunhofer Institute for Algorithms
and Scientific Computing SCAI

Klaus Wolf
Schloss Birlinghoven
53754 Sankt Augustin,
Germany

Phone: +49 (0) 2241 / 14 - 2557
klaus.wolf@scai.fraunhofer.de

www.scai.fraunhofer.de
www.mpcci.de

Visual concept: Markus Möritz
Layout: Jennifer Sauerland

ISSN 1860-6296

Copyright © 2006
Fraunhofer Institute SCAI

All rights reserved. No part of this publication may be reproduced, stored in a retrieval system or transmitted in any form or by any means: electronical, electrostatic, magnetic tape, mechanical, photocopy, recording or otherwise, without permission in writing from the publishers.

Only the authors but not the Fraunhofer Institute SCAI can be hold liable for any mistakes made in manuscripts of the conference proceedings.

CONTACT

Fraunhofer Institute SCAI
Schloss Birlinghoven
53754 Sankt Augustin,
Germany
www.scai.fraunhofer.de
www.mpcci.de



Fraunhofer Institute
Algorithms and
Scientific Computing